Isobutene Oligomerization on Heteropolyacids Supported on Silica-Based High Surface Area Supports

by

Elif Kocaman

A Dissertation Submitted to the
Graduate School of Sciences and Engineering
in Partial Fulfillment of the Requirements for
the Degree of

Master of Science
in
Chemical and Biological Engineering

KOÇ
UNIVERSITY

January 12, 2018

Koç University
Graduate School of Sciences and Engineering

This is to certify that I have examined this copy of a master's thesis by

Elif Kocaman

and have found that it is complete and satisfactory in all respects,
and that any and all revisions required by the final
examining committee have been made.

Committee Members:

Assoc. Prof. Dr. Alper Uzun

Assoc. Prof. Dr. Seda Keskin Avcı

Asst. Prof. Dr. Ali Can Kızılkaya

Date: _____

ABSTRACT

Energy consumption of the world depends heavily on fossil fuels. Because the heavy crude oil is accessible at considerably lower prices than their lighter counterparts, the refineries are now motivated to process these heavy feedstocks. The units processing such feedstock produce a significant amount of light olefins as side products. A way of utilizing these low-valued side products is to convert them into more valuable liquid products. Among the alternative processes applied for this purpose, oligomerization offers a great degree of flexibility in terms of product composition. This process requires a solid acid catalyst, such as solid phosphoric acid, zeolites, cation exchange resins, and metal oxides. Because each of these catalysts has their own limitations, there is a strong need for a new type of catalyst. The requirement of a good alternative is having a high density of acid sites with tunable strength to allow controlling the product selectivity. With their unique physiochemical properties, Keggin type heteropolyacids (HPAs) offer a broad potential in this regard. Here, their potential for isobutene oligomerization is explored. For this purpose, first a screening study was performed on tungstophosphoric acid, $H_3PW_{12}O_{40}$ (TPA), tungstosilicic acid, $H_4SiW_{12}O_{40}$ (TSA), and molybdophosphoric acid, $H_3PMo_{12}O_{40}$ (MPA), impregnated on various silica-based high surface area supports, such as MCM-41, SBA-15, and SiO_2, at various loadings. The catalytic performance of more than 28 catalysts were measured under identical conditions to determine the highly performing HPA-support combination. Data indicated that the selectivity towards distillate to gasoline ratio decreased with an increase in HPA loading on TSA/SBA-15 and TPA/MCM-41 catalysts. Because the TPA has the highest thermal stability and the strongest acid strength, the TPA/MCM-41 catalysts were selected for further study to elucidate the structure-performance relationships in more detail. For this purpose, TPA was loaded on MCM-41 at fourteen different loadings ranging from 1 to 90 wt%. Detailed characterization confirmed that the TPA clusters were successfully loaded on the support. The infrared (IR) spectroscopy and X-ray diffraction (XRD) results indicated

the presence of interactions between the TPA clusters and MCM-41, especially at loadings below 50 wt%, where mostly monolayer TPA dispersion was present. These interactions led to the variations in acid site density and their corresponding strength as evidenced by the results of temperature programmed desorption of ammonia measurements. Catalytic performance measurements obtained at 393 K and 15 bar indicated that these TPA/MCM-41 catalysts provide more than 75% isobutene conversion at a weight hourly space velocity (WHSV) of 46 h^{-1}, significantly higher than what the most of the solid acid catalysts provide under comparable conditions. Results further showed that the catalysts were more selective towards distillate range products especially at very low TPA loadings. The relative selectivity of trimers over dimers in the oligomerization product pool was four at a TPA loading of 1 wt% and decreased to 1.5 with increasing loading. Ruling out the presence of any strong correlations between the acid strength and catalytic performance, the data presented a strong dependence of the product selectivity on the availability and vicinity of the acid sites. These results present a broad potential of utilizing HPAs supported on high surface area supports as an alternative family of catalysts for high performance in olefin oligomerization. Ability to adjust the TPA loading in a wide range offers opportunities for tuning the product selectivity.

ÖZET

Dünya enerji tüketimi büyük ölçüde fosil yakıtlara bağlıdır. Ağır ham petrol kaynaklarının hafif kaynaklarından düşük fiyatlarda olması rafinerilerin ağır kaynakları işleme eğilimini arttırmaktadır. Bu kaynakları işleyen üniteler yan ürün olarak önemli miktarlarda doymamış hidrokarbon, olefinleri üretmektedir. Olefinler, daha değerli sıvı ürünlere çevrilerek kullanılabilmektedirler. Bu amaçla başvurulan proseslerden olan oligomerizasyon reaksiyonu elde edilen ürünün komposizyonu açısından geniş bir aralık sunabilmektedir. Oligomerizasyon, katı fosforik asit, zeolit, reçineler ve metal oksitler gibi asit katalizörler varlığında gerçekleşmektedir. Bu katalizörlerin her birinin kendine ait dezavantajları ve limitasyonları bulunduğu için yeni bir çeşit katalizöre ihtiyaç bulunmaktadır. Keggin tipi heteropoliasitler benzersiz fizikokimyasal özellikleri ile bu alanda geniş bir potansiyel sunmaktadırlar. Buradaki çalışmada, heteropoliasitlerin izobüten oligomerizasyonu üzerindeki potansiyeli araştırılmıştır. Bu amaçla, tungstofosforik asit $H_3PW_{12}O_{40}$ (TPA), tungstosilisik asit $H_4SiW_{12}O_{40}$ (TSA) ve molibdofosforik asit $H_3PMo_{12}O_{40}$ (MPA) farklı yükleme oranlarında çeşitli silika bazlı destek malzemeleri (SiO_2, MCM-41 ve SBA-15) üzerine emdirilmiştir. Elde edilen 28'den fazla katalizörün aynı koşullar altında reaksiyon ve karakterizasyon çalışmaları gerçekleştirilmiştir. Buradan elde edilen sonuçlarda, TSA/SBA-15 ve TPA/MCM-41 katalizörleri varlığında heteropoliasit yüklemesinin arttırılması ile distilat/benzin oranının azaldığı görülmüştür. TPA heteropoliasiti en yüksek asitlik kuvvetine ve termal stabiliteye sahip olması sebebi ile izobüten oligomerizasyonu performansı ve katalizörün yapısal özellikleri arasındaki ilişkiyi belirlemek adına detaylı çalışmalar için seçilmiştir. Bu amaçla TPA, MCM-41 destek malzemesi üzerine kütlece %1'den %90'a kadar 14 farklı yüzdede emdirilmiştir. Detaylı karakterizasyonlar TPA'nın MCM-41 yapısına başarılı bir şekilde yüklendiğini göstermektedir. Gerçekleştirilen çalışmalarda, XRD ve IR karakterizasyonları özellikle kütlece %50 TPA yüklemesinin altında (tek katman) TPA ve MCM-41 arasındaki etkileşimlerin yoğun olduğunu

göstermektedir. Gerçekleşen etkileşimlerin asit yoğunlukları ve asit kuvvetleri üzerindeki etkisi NH_3-TPD analizleri tarafından belirlenmiştir. Bu değişimlerin katalitik performansa etkileri izobüten şarjı kullanılarak 393 K 15 bar WHSV: 46 h^{-1} reaksiyon koşullarında (WHSV değeri literatürde karşılaştırılan katalizörlerden oldukça yüksektir) %75 üzeri izobüten dönüşümünde değerlendirilmiştir. Trimer/dimer oranı %1 TPA yüklemesi olan katalizörde 4 iken, bu değer TPA yüklemesinin artması ile 1.5 seviyelerine kadar düşmüştür. Elde edilen sonuçlar, ürün seçiciliğinin asitlik kuvvetinden ziyade asitlik miktarı ve bu asit sitelerinin birbirlerine yakınlığı ile kuvvetli korelasyonlara sahip olduğunu ve düşük miktardaki aktif sitelerin trimer oluşumunu tetiklediğini göstermektedir. Böylelikle, yüksek yüzey alanına emdirilen heteropoliasitlerin olefin oligomerizasyonu için yüksek performansa sahip yeni bir katalizör grubu olabileceği gösterilmiştir. TPA yükleme oranını değiştirerek ürün seçiciliğinin istenilen özelliklere getirilebilmesine olanak sağlanmıştır.

ACKNOWLEDGEMENTS

First I would like to thank my advisor Assoc. Prof. Dr. Alper Uzun for his limitless support, faith, advices during my research and providing to me take part in KUTEM family. He was always with me and he encouraged me get a job while doing my master studies.

I want to express my sincere thanks to my thesis committee members Assoc. Prof. Dr. Seda Keskin and Asst. Prof. Dr. Alican Kızılkaya.

I want to thank Scientific and Technological Council of Turkey (TUBITAK) (Project number: 3140474), Koç University TÜPRAŞ Energy Center (KUTEM) and Turkish Petroleum Refineries Corporation (TÜPRAŞ) for providing support and giving me the opportunity to work on this project. My sincere thanks got to Dr. Serdar Çelebi for always providing help during the project and ongoing business life. I also thank Nur Bağlar and Cem Açıksarı for their supports and motivation.

Special thanks to my co-workers and friends as a Product Development Team at TÜPRAŞ R&D; Emel Başkent Aydemir, Selcen Temel Topallar, Serhat Arca, Ramazan Oğuz Canıaz and Refika Çetintaş for their supports, motivations and collaboration.

My sincere thanks got to Özge Akarçay for her limitless help and numerous goodness. My special thanks go to KUTEM girls, Samira Fatma Kurtoğlu, Melike Babucci, Betül Şeker, Özge Deniz Bozkurt for their supports and friendship. I am really grateful to them. I also want to thank Ahsan Jalal for his patience while we were gossiping and for his real friendship. I want to thank F. Eylül Saraç Öztuna, Navid Solati, Salim Şimşek, Ehsan Sarayloo, Ekin Esen and Volkan Balcı for very good times at KUTEM.

I want to thank my housemate Sevi Zeynep Hasdemir for her encouraging support and coffees.

My special thanks to my METU team Merve Tufan, Deniz Kaya, Berna Sezgin, Zeynep Sümer, Gülçin Çağlayan, Ebru Okur, Onur Yüksel, Gökhan Karabıyık and Ergin Satır for making Ankara sunny and ongoing precious friendship.

I want to thank my childhood friends Burcu Ertürk, Melis Türkmen, Çınar Topaloğlu, and Egemen Yazıcı for being always with me.

I appreciate my confidant, my soul-mate and my beloved Erdem Tan. Thank you for making my face smile even in hardest times. Thank you for encouraging me and being with me always.

Finally, my very special thanks go to my family who make me Elif. Thank you for your inexpressible love, patience and support during my life. Nothing could be same without you.

To my family and Erdem

Table of Contents

LIST OF TABLES

LIST OF FIGURES

Chapter 1

INTRODUCTION

Energy consumption of the world depends heavily on fossil fuels. Because the crude oil reservoirs have been becoming heavier, refineries have been motivated to process these sources [1]. Delayed coking and fluidized cracking technologies are widely used to upgrade heavier feedstocks by thermal and catalytic cracking reactions, respectively. Besides manufacturing valuable products, such as gasoline, kerosene, and diesel, these technologies lead to produce lighter fractions included unsaturated hydrocarbons because of the lack of hydrogen. These undervalued unsaturated hydrocarbons are mostly utilized as liquefied petroleum gas (LPG) fractions. There are recent technologies called the gas-to-liquid technologies to produce more valuable products as gasoline or middle distillate from these lower value light hydrocarbons. Two main processes are applied to produce liquid fuels from gaseous feedstocks, alkylation and oligomerization [2]. The former one is used for producing mostly gasoline range products by processing feedstock containing olefins and paraffins on highly strong acids, such as HF or H_2SO_4 [3]. The latter one, on the other hand, is more flexible in terms of product composition which can be controlled by the level of oligomerization [4]. Another advantage of oligomerization is that this process uses only olefins like ethylene, propylene, linear butenes (1-butene, *cis*-2-butene, *trans*-2-butene), and isobutene produced by cracking processes [5]. During oligomerization, these olefins can be converted into *n*-olefins or isoolefins, which can then be converted to *n*-paraffins and isoparaffins by hydrogenation. Isoparaffins are environmentally friendly, high performance blending components for motor fuels and there are no limitations for their blending ratios [6]. Thus, the blending components can be produced with low sulphur, aromatics, and olefins

content suitable for current European standards [6]. Therefore, product flexibility from gasoline to diesel can be provided greatly to meet the market demand. Apart from production of valuable components of fuels in refineries, oligomerization process can provide synthesis of fine chemicals and intermediates in the petrochemical industry. In order to produce C_9-plasticizers, linear C_8-olefins are desirable intermediates [6].

In industrial scale, the use of oligomerization has begun in 1935 for the conversion of C_3-C_4 alkenes into gasoline over solid phosphoric acid (CatPoly process, UOP). Apart from CatPoly process, there are new industrial processes with the use of zeolites, alumosilicates and ion-exchange resins listed in Table 1) [7].

Table 1. 1. Current commercial processes for the motor fuel components production by the oligomerization of lower alkenes over heterogeneous catalysts [7].

Catalyst	**Process**	**Company**	**Basic Product Application**
Solid Phosphoric Acid	Oligomerization	UOP, HülsAG	Gasoline, jet fuel
	InAlk	UOP	Gasoline
Cation-exchange resins	$Dimer_8$	Snamprogetti, CDTECH	Gasoline
	NExOCTANE	Fortum Oy, Kellogg Brown and Root	Gasoline
Alumosilicate	Polynaphtha	Institut Français du Petrole	Diesel Fuel
	Selectopol	Institut Français du Petrole	Gasoline
	Octol	Hüls, UOP	Gasoline
	Hexall	UOP	Gasoline
	MOGD	ExxonMobil	Gasoline, diesel fuel

Zeolite	EMOGAS	ExxonMobil	Gasoline, diesel/jet fuel
	COD	PetroSA	Diesel Fuel
	OLEOL	OLKAT	Gasoline
	Oligomerization	SAPR-Neftekhim	Gasoline
	Oligomerization	VNIIOSNK	Gasoline

Different solid acid catalysts are used for the oligomerization process, such as solid phosphoric acid [8-10], zeolites [11-17], cation exchange resins [18-21], metal oxides [22], anion-modified metal oxides, nickel compounds immobilized on acidic supports, and acid supported mesoporous materials.

However, although they are used commercially, there are some drawbacks about their usage. For example, SPA has difficulties regarding limited lifetime, disposal, corrosion problems, and producing only gasoline range products [23]. Zeolites, on the other hand, are widely researched catalyst group because of their advantages of being regenerable, being stable over a wide range of temperature, and their shape selective applications [24]. However, they are required to process at high temperatures and pressures compared with other heterogeneous catalysts that lead to form side reactions cracking and aromatization [7]. Ion-exchange resins that are macroporous and strong acids have been mostly used catalyst for both isobutene dimerization and trimerization. However, ion-exchange resins generally have low thermal stability and they cannot be used other type of olefins such as ethylene, propylene, 2-butenes [25].

On the other hand, a very new group of solid acids, called Keggin type heteropolyacids (HPAs) offer unique physiochemical and catalytic properties for oligomerization, because of their high oxidizing capability with strong acidic strength [26-32]. Their redox and acidic properties can be tuned by their chemical composition [26, 29, 33]. HPAs have a general

formula of $H_{8-x}MX_{12}O_{40}$, where M and X are the central- and hetero-atoms, respectively. Typically, M can be either P or Si, and X can be W or Mo [29, 30, 34, 35]. The structure of the heteropoly anion consists of a central tetrahedron XO_4 surrounded by 12 edge- and corner-sharing metal-oxygen octahedral MO_6. Among a wide range of available HPAs, tungstophosphoric acid ($H_3PW_{12}O_{40}$), tungstosilicic acid ($H_4SiW_{12}O_{40}$), molybdo phosphoric acid ($H_3PMo_{12}O_{40}$), and silicomolybdic acid ($H_4SiMo_{12}O_{40}$) are the mostly used ones with a variation of acidic strength in the following order: $H_3PW_{12}O_{40}$ (TPA) > $H_4SiW_{12}O_{40}$ (TSA) > $H_3PMo_{12}O_{40}$ (MPA) > $H_4SiMo_{12}O_{40}$ (MSA) [30,35,36]. Tungsten hetero-atom HPAs are mostly applied for applications requiring acid catalysts because of their strong acidity, high thermal stability and low oxidation capability [34-39]. They are in general more active catalysts than other conventional solid acid catalysts, such as SiO_2-Al_2O_3, H_3PO_4/SiO_2, and zeolites because of their high Brønsted acid capacity and strong acidity. Their high degree of acidity allows operation at mild conditions [34, 40-42]. One of the limitations of HPAs is their low surface areas in the range of <10 m^2/g. Such low surface area limits the availability of the acid sites for surface-type reactions. Therefore, they are usually dispersed on high surface area supports, such as silica, TiO_2, carbon, Al_2O_3, and ZrO_2 [28, 42]. Among these, silica is the mostly used support especially when polar reactants are used because of interacting with Keggin anions weakly preserving the heteropolyacid structure [29,39,43,44].

Mesoporous silicate MCM-41 having hexagonal array of mesoporous is superior to conventional silica supports because of its high specific surface area (800-1000 m^2/g), porosity, high thermal stability, and large adsorption capacity for organic molecules [31, 37, 45, 46]. Thus, MCM-41 can be a promising support for HPAs because of their high specific surface area and regular pore size which enables high dispersion of HPAs and diffusion of reactants and products [47-49]. Although there have already been reports on HPA/MCM-41 systems that requires acidic function to catalyze reactions such as alkylation,

hydrodesulphurization, esterification, and oxidation [30,41,43,44], olefin oligomerization has not been investigated [25].

Acidic properties of HPAs' can be tuned and reaction selectivity can be changed completely. In order to change the acidic properties, one of the most common method is changing the loading of HPAs the on supports [50]. In this thesis study, we applied this knowledge to understand the loading effect on the selectivity of products for isobutene oligomerization. First, a screening study was conducted over three types of heteropolyacids, TSA, TPA, MPA, on various silica-based supports SiO_2, SBA-15, and MCM-41 at different loadings. Then a deeper study was performed on a family of TPA/MCM-41 catalysts with a wide range of TPA loading ranging from 1 to 90 wt %. Incorporating TPA having the highest thermal stability and strength of acid, and MCM-41 having superior properties mentioned above as high surface area, porosity, and high thermal stability offers a huge potential to obtain high performance for isobutene oligomerization at mild reaction conditions.

In order to elucidate the effects of these structural properties on catalytic activities for isobutene oligomerization, we performed detail characterizations on both catalyst and reaction products. X-ray diffraction (XRD), Brunauer Emmett Teller (BET) pore volume, and surface area analysis, temperature programmed desorption with ammonia (NH_3-TPD), thermogravimetric analysis (TGA), and Fourier transform infrared spectroscopy (FTIR) analyses were conducted on the catalysts studied in this study. After detailed characterization, the catalytic performances of the catalysts were measured under identical conditions. Catalytic performance differences were evaluated upon catalyst structures to elucidate the structure-performance relationships of these catalysts for isobutene oligomerization reaction.

Chapter 2 of this thesis includes a detailed literature survey on the olefin oligomerization reaction over different solid acid catalysts with discussions regarding the reaction mechanism.

Chapter 3 introduces the experimental methods for the catalyst preparation, characterization, and catalytic testing that were used in this thesis study.

Chapter 4 reports the results of the catalyst screening study performed under identical reaction conditions on twenty-eight different catalysts prepared by impregnation of three different types of heteropolyacid, TSA, TPA and TPA, on three different types of supports SiO_2, SBA-15, and MCM-41.

Chapter 5 reports the results of a detailed analysis performed on a family of TPA/MCM-41 catalyst prepared at fourteen different TPA loadings ranging from 1 to 90 wt%. This chapter presents the consequences of changing TPA loading on structural characteristics and their catalytic performances determined by detailed characterization and isobutene oligomerization reaction respectively.

References

[1] Association, C.F., *The Economics of Petroleum Refining* 2013.

[2] Bogdan, V.I. and V.B. Kazanskii, *Isobutane alkylation with butenes and the oligomerization of C4 olefins in supercritical reagents.* Kinetics and Catalysis, 2005. **46**(6): p. 834-838.

[3] Eszter Kriván, I.V., Jenő Hancsók *The Oligomerization of Olefin Hydrocarbons in Light FCC Naphtha on Ion Exchange Resin Catalyst.* CHEMICAL ENGINEERING TRANSACTIONS, 2012. **29**: p. 985-990.

[4] Zhang, J., Kanno, M., Zhang, J., Ohnishi, R., Toriyabe, K., Matsuhashi, H., & Kamiya, Y. , *Preferential oligomerization of isobutene in a mixture of isobutene and 1-butene over sodium-modified 12-tungstosilicic acid supported on silica.* Journal of Molecular Catalysis A: Chemical, 2010. **326**(1-2): p. 107-112.

[5] Eszter Kriván, I.V., Jenő Hancsók, *Investigation of Production of Motor Fuel Components on Heterogeneous Catalyst with Oligomerization.* Topics in Catalysis, 2013. **56**(9-10): p. 831-838.

[6] Kriván, E., S. Tomasek, and J. Hancsók, *Application possibilities of zeolite catalysts in oligomerization of light olefins.* Periodica Polytechnica: Chemical Engineering, 2014. **58**(2): p. 149-156.

[7] A. V. Lavrenov, T.R.K., E. A. Buluchevskii, E. N. Bogdanets, *Heterogeneous oligomerization of light alkenes: 80 years in oil refining.* Catalysis in Industry, 2016. **8**(44): p. 316-327.

[8] Coetzee, J.H., et al., *An improved solid phosphoric acid catalyst for alkene oligomerization in a Fischer-Tropsch refinery*.

[9] Prinsloo, N.M., *Solid phosphoric acid oligomerisation: Manipulating diesel selectivity by controlling catalyst hydration.* Fuel Processing Technology, 2006. **87**(5): p. 437-442.

[10] de Klerk, A., D.O. Leckel, and N.M. Prinsloo, *Butene oligomerization by phosphoric acid catalysis: Separating the effects of temperature and catalyst hydration on product selectivity.* Industrial & Engineering Chemistry Research, 2006. **45**(18): p. 6127-6136.

[11] Nkosi, B., F.T.T. Ng, and G.L. Rempel, *The oligomerization of 1-butene using NaY zeolite ion-exchanged with different nickel precursor salts.* Applied Catalysis A: General, 1997. **161**(1-2): p. 153-166.

[12] Bjorgen, M., et al., *1-Butene oligomerization in Bronsted acidic zeolites: mechanistic insights from low-temperature in situ FTIR spectroscopy.* Journal of Physical Chemistry B, 2004. **108**(23): p. 7862-7870.

[13] Villegas, J.I., et al., *A study on the dimerization of 1-butene over Beta zeolite.* Topics in Catalysis, 2007. **45**(1-4): p. 187-190.

[14] Oliveira, P., et al., *Light olefin transformation over ZSM-5 zeolites with different acid strengths - A kinetic model.* Applied Catalysis a-General, 2010. **384**(1-2): p. 177-185.

[15] Yoon, J.W., et al., *Trimerization of isobutene over a zeolite beta catalyst.* Journal of Catalysis, 2007. **245**(1): p. 253-256.

[16] Yoon, J.W., et al., *Trimerization of isobutene over zeolite catalysts: Remarkable performance over a ferrierite zeolite.* Catalysis Communications, 2007. **8**(6): p. 967-970.

[17] Zhang, X., et al., *Catalytic performance and characterization of Ni-doped HZSM-5 catalysts for selective trimerization of n-butene.* Fuel Processing Technology, 2009. **90**(7-8): p. 863-870.

[18] Ji, W.Y., H.J. Sung, and J.S. Chang, *Trimerization of isobutene over solid acid catalysts: Comparison between cation-exchange resin and zeolite catalysts.* Bulletin of the Korean Chemical Society, 2008. **29**(2): p. 339-341.

[19] Hauge, K., et al., *Oligomerization of isobutene over solid acid catalysts.* Catalysis Today, 2005. **100**(3–4): p. 463-466.

[20] Ji, W.Y., et al., *Trimerization of isobutene over solid acid catalysts under wide reaction conditions.* Bulletin of the Korean Chemical Society, 2007. **28**(11): p. 2075-2078.

[21] Jeffrey C.Gee, S.T.W., *Dimerization of linear olefins on Amberlyst® 15: Effects of chain length and double-bond position.* Journal of Catalysis, 2013. **303**: p. 1-8.

[22] Lee, J.S., et al., *Trimerization of isobutene over WOx/ZrO2 catalysts.* Applied Catalysis A: General, 2009. **366**(2): p. 299-303.

[23] Coelho, A., et al., *1-Butene oligomerization over ZSM-5 zeolite: Part 1-Effect of reaction conditions.* Fuel, 2013. **111**: p. 449-460.

[24] Kim, Y.T., et al., *Low-temperature oligomerization of 1-butene with H-ferrierite.* Journal of Catalysis, 2014. **323**: p. 33-44.

[25] Jhung, S.H. and J.S. Chang, *Trimerization of isobutene over solid acid catalysts.* Catalysis Surveys from Asia, 2009. **13**(4): p. 229-236.

[26] Izumi, Y., K. Hisano, and T. Hida, *Acid catalysis of silica-included heteropolyacid in polar reaction media.* Applied Catalysis A: General, 1999. **181**(2): p. 277-282.

[27] Okuhara, T., N. Mizuno, and M. Misono, *Catalysis by heteropoly compounds—recent developments.* Applied Catalysis A: General, 2001. **222**(1–2): p. 63-77.

[28] Kamiya, Y., et al., *Catalytic Chemistry of Supported Heteropolyacids and Their Applications as Solid Acids to Industrial Processes.* Catalysis Surveys from Asia, 2008. **12**(2): p. 101-113.

[29] I.V Kozhevnikova, K.R., ASinnemab, H.WZandbergenc, Hvan Bekkumb, *Study of catalysts comprising heteropoly acid H3PW12O40 supported on MCM-41 molecular sieve and amorphous silica.* Journal of Molecular Catalysis A: Chemical, 1996. **114**(1-3): p. 287-298.

[30] Popa, A., V. Sasca, and J. Halasz, *Catalytic properties of molecular sieves MCM41 type doped with heteropolyacids for ethanol oxidation.* Applied Surface Science, 2008. **255**(5): p. 1830-1835.

[31] Jin, H., et al., *Influence of H4SiW12O40 loading on hydrocracking activity of non-sulfide Ni–H4SiW12O40/SiO2 catalysts.* Fuel, 2010. **89**(8): p. 1953-1960.

[32] Kozhevnikov, I.V., *Heterogeneous acid catalysis by heteropoly acids: Approaches to catalyst deactivation.* Journal of Molecular Catalysis A: Chemical, 2009. **305**(1–2): p. 104-111.

[33] Yue Wu , X.Y., Xiangguang Yang , Xinping Wang , Wenling Chu , and Yucai Hu, *Heterogenization of Heteropolyacids: A General Discussion on the Preparation of Supported Acid Catalysts.* Ind. Eng. Chem. Res. 1, 1996. **35**: p. 2546–2560.

[34] Timofeeva, M.N., *Acid catalysis by heteropoly acids.* Applied Catalysis A: General, 2003. **256**(1–2): p. 19-35.

[35] Pizzio, L.R., C.V. Cáceres, and M.N. Blanco, *Acid catalysts prepared by impregnation of tungstophosphoric acid solutions on different supports.* Applied Catalysis A: General, 1998. **167**(2): p. 283-294.

[36] Yang, W., et al., *H3PW12O40 supported on Cs modified mesoporous silica: catalytic activity in n-butane isomerisation and in situ FTIR study: Comparison with microporous CsxH3−xPW12O40.* Catalysis Today, 2002. **73**(1–2): p. 153-165.

[37] Iglesia, D.G.B.S.L.S.E., *Solid acid catalysts based on supported tungsten oxides.* Topics in Catalysis, 1998. **6**: p. 87-99.

[38] Zhang, J., et al., *Preferential oligomerization of isobutene in mixtures of isobutene and 1-butene over 12-tungstosilicic acid supported on silica.* Applied Catalysis A: General, 2009. **353**(1): p. 68-73.

[39] Madhusudhan Rao, P., et al., *Immobilization of molecular H3PW12O40 heteropolyacid catalyst in alumina-grafted silica-gel and mesostructured SBA-15 silica matrices.* Journal of Catalysis, 2005. **232**(1): p. 210-225.

[40] M.R.HSiddiqui, I.V.S., *Coking and regeneration of H3PW12O40/SiO2 catalysts.* Applied Catalysis A: General, 2001. **214**: p. 47-58.

[41] Blasco, T., et al., *Supported heteropolyacid (HPW) catalysts for the continuous alkylation of isobutane with 2-butene: The benefit of using MCM-41 with larger pore diameters.* Journal of Catalysis, 1998. **177**(2): p. 306-313.

[42] Corma, A., A. Martínez, and C. Martínez, *Acidic Cs+, NH4+, and K+Salts of 12-Tungstophosphoric Acid as Solid Catalysts for Isobutane/2-butene Alkylation.* Journal of Catalysis, 1996. **164**(2): p. 422-432.

[43] Franklin J.Méndeza, A., MarcelEcheverríaa ,N ReynaldoJáureguia, Yanet Villasanaa, Yraida Diaz, Gustavo Liendo-Polancoc, Miguel A.Ramos-Garcíad, TamaraZoltana, Joaquín L.Britoa, and *Mesoporous catalysts based on Keggin-type heteropolyacids supported on MCM-41 and their application in thiophene hydrodesulfurization.* Fuel, 2013. **110**: p. 249-258.

[44] Michel J.Verhoefa, P.J.K., Joop A.Petersa, Hermanvan Bekkuma, *A study on the stability of MCM-41-supported heteropoly acids under liquid- and gas-phase esterification conditions.* Microporous and Mesoporous Materials, 1999. **27**(2-3): p. 365-371.

[45] AfshinGhanbari-Siahkali, A., JohnDwyer, Michael W.Anderson, *The acidity and catalytic activity of heteropoly acid on MCM-41 investigated by MAS NMR, FTIR and catalytic tests.* Applied Catalysis A: General, 2000. **192**(1): p. 57-69.

[46] Varsha Brahmkhatri, A.P., *An efficient green catalyst comprising 12-tungstophosphoric acid and MCM-41: synthesis characterization and*

diesterification of succinic acid, a potential bio-platform molecule. Green Chemistry Letters and Reviews 2012. **5**(2): p. 161-171.

[47] Sayari, A., *Catalysis by Crystalline Mesoporous Molecular Sieves.* Chemistry of Materials, 1996. **8**: p. 1840-1852.

[48] Karen Wilson, J.H.C., *Solid acids and their use as environmentally friendly catalysts in organic synthesis.* Pure and Applied Chemistry, 2009.

[49] Taguchi, A. and F. Schüth, *Ordered mesoporous materials in catalysis.* Microporous and Mesoporous Materials, 2005. **77**(1): p. 1-45.

[50] V. L. Sushkevich, V.V.O.a.I.I.I., *Isoprene synthesis from formaldehyde and isobutene over Keggin-type heteropolyacids supported on silica.* The Royal Society of Chemistry 2016: p. 6354-6364.

Chapter 2

LITERATURE REVIEW ON THE CATALYTIC PROPERTIES AND PERFORMANCE OF THE SOLID ACID CATALYSTS ON OLIGOMERIZATION OF OLEFINS

Oligomerization of light alkenes provides a wide spread of products ranging from motor fuels to plasticizers, resins, additives, and lubricants because of the consecutive reaction mechanism (i.e., monomer → dimers → trimers → tetramers → etc.). Oligomerization products compose of a few monomers ($2<n<100$) on the contrary to polymers ($n>100$). The degree of oligomerization and structure of oligomer (linear or branched) are determined by the operation conditions, stability of olefin feedstock, and catalyst structure.

Chain length and double bond position are two parameters that determine the reactivity of olefinic hydrocarbons. While non-terminal olefins have lower reactivity than terminal ones (α-olefins), short chain α-olefins have more reactivity than heavier ones such that ethylene and propylene are the most reactive α-olefins [1].

Oligomerization is a unimolecular reaction with first order rate dependence the monomer concentration. While the reaction temperature ranges from 423 to 773 K, pressure ranges from 1 to 50 bar. The variety of operation conditions strongly depends on the catalyst and olefin type. Reaction kinetic depends on temperature such that when reaction temperature increases, the rate also kinetically increases [2]. Oligomerization is a highly exothermic reaction (approximately 20 kcal/mol per double bond or 1.046−1.381 kJ/g of reacted olefins) [1]. Since the reaction is highly exothermic, low temperatures favor oligomerization reaction, however kinetic limitation exists for chain growth. High pressure, on the other hand, favors the oligomerization to higher molecular weight oligomers [1]. There are some common results such that diesel selectivity increases with high pressure (above 30 bar, for instance 50 bar) and low temperature (lower than 573 K, typically 473K-493K) [2]. Low pressure and high temperature favors the gasoline range products where

short hydrocarbons and aromatics present [2]. On the other hand, at high temperatures side reactions occur such that cracking reactions above 490 K are not desired [1]. Higher degree of branching occurs when the temperature is high (above 573K) [2]. However, the branching degree can be controlled by shape selective catalysts having ordered pore channels and a narrow pore size distribution [1]. Different fuel products can be desired depending on the branching level and chain length. While an ideal gasoline (high octane number) pools consists of highly branched 8-10 carbon atoms (H/C >2.25), the ideal diesel pool (high cetane number) consists of linear or slightly branched 10-20 carbon atoms paraffins [1]. Furthermore, oligomerization reactions can occur with reactions such as skeletal and double bond isomerization, cracking, and aromatization. Therefore, aromatics and coke are other expected products [1].

In general, reaction rate increases with temperature, pressure, and concentration of reactant. Another important parameter is the space velocity (weight hourly space velocity, WHSV) which ranges from 0.1 to 50 h^{-1}. Studies showed that conversion of alkenes decreased with increasing space velocity over H-ZSM-5 catalyst [2].

Oligomerization of olefins can be performed in fixed bed, moving bed or fluidized bed reactors. Since the reaction is exothermic, heat removal procedures should be considered, such as feed dilution and heat removal through the wall [2].

Olefin oligomerization has a cationic oligomerization path over acids and transition metal catalysts. Mechanism consists of three main steps that are; olefin protonation to form intermediate carbenium ion, chain propagation by reaction of a carbenium ion with an olefin, and deprotonation of carbenium ion with chain growth ending. Intermediate carbenium ion stability and propagation, deprotonation rate constants determine the chain size and reaction operating conditions (temperature and pressure) [1]. Deprotonation (termination) step may be slower than propagation when carbocation is relatively stable meaning that reaction can produce trimer, tetramer, and polymer in the end. For acid catalysts, proton from acid catalyst is transferred to olefin to produce carbenium ion intermediate. The carbenium ion behaves as an electrophile to react with olefin and to form another carbenium ion including two monomers. Reaction mechanism of isobutene oligomerization reaction over Bronsted acid sites are given in Figure 2.1 [3].

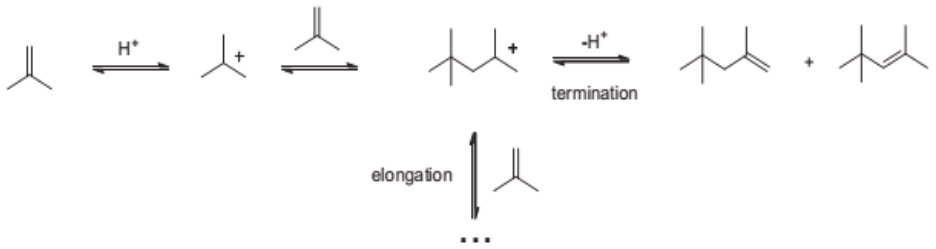

Figure 2.1. Isobutene oligomerization over Bronsted Acid sites [3].

For transition metals, on the other hand, the path of olefin coordination, chain growth, and termination are followed to produce primary product. Figure 2.2 indicated propylene oligomerization over nickel based Lewis acid catalyst [3].

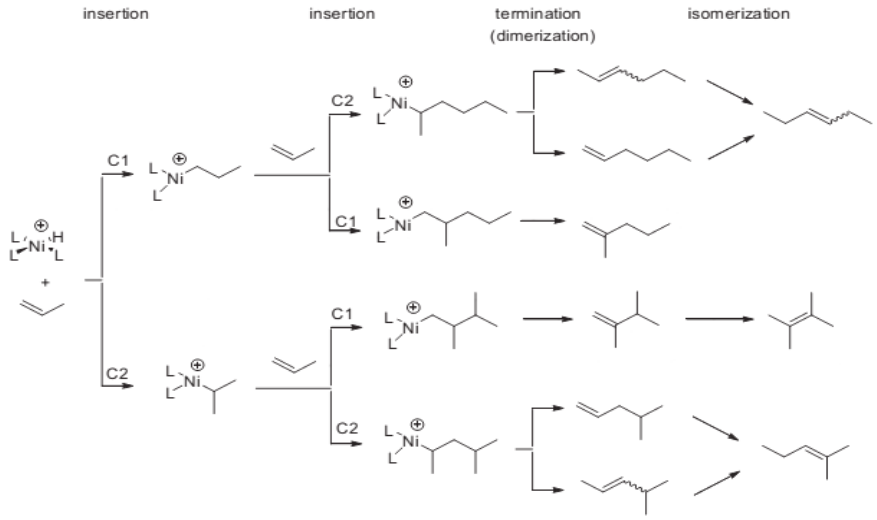

Figure 2.2. Propylene oligomerization over Lewis Acid sites [3].

In the following paragraphs, recent developments on oligomerization by different solid acids is summarized.

2.1 Zeolites

Zeolite catalysts are mostly favored because of their advantages of being regenerable and their stability over a wide range of temperature compared with commonly used homogeneous catalysts. Mostly used ones are ZSM-5, Mordenite, Zeolite Y, Zeolite Beta, and Ferrierite catalysts. Zeolites

can process mixture of olefins because of applicable operating conditions at wide range of temperature and pressures [4].

Zeolites are applied in industrial scales, such that Mobil olefin to gasoline and distillate (MOGD) process is one of the most referenced ones using the ZSM-5 zeolite to convert light olefins (C_2-C_4) to gasoline or diesel fuels developed by the Mobil Research and Development Company [5]. MOGD process operates at 558-648 K and 300 bar in a fluidized bed reactor. Gasoline selectivity can change from 27 to 57 wt % as 94 wt % of the products is olefin while 2 wt% is aromatic, and the product has a RON number 92. Medium distillates' cetane number increases from 33 to 52 after hydrogenation. Another process developed by ExxonMobil is Exxon Mobil Olefins to Gasoline (EMOGAS) using C_3-C_4 as a feedstock on HZSM-22 or HZSM-57 catalysts where diesel/gasoline ratio depends on two different configurations of the unit. In a chamber type of reactor, 35-55 bar pressure and 450-477 K temperature range are the operating conditions and providing a catalyst life time of 2-4 months. Tubular operates at 55-75 bar pressure and 477 K, with a catalyst life time of 2-8 months. Olefin conversion is 95-97%. Conversion of olefins to distillate (COD) process operates with COD-9 catalyst (Süd-Chemie) based on ZSM-5 zeolite. Reaction conditions are 473-573 K and 45 bar. Catalyst life is 20-80 days. Process is selective to diesel fraction with a cetane number of 52-54 after hydrogenation of products. However, produced gasoline has low octane number as 81-85 RON [6]. This is because of shape selective ZSM-5 catalyst which is more selective to produce linear molecule by its one-dimensional pore structure and pore size [6].

Zeolites are classified according to their microporous pore structure. Moreover, every zeolite types can have different Si/Al ratio. In order to provide different acidity and acid strength on zeolite catalyst, their Si/Al ratio can be changed, or they can be modified with alkali metals. The activity and selectivity of zeolite catalysts are affected by Si/Al ratio, decationation degree, added cations properties and molecular sieve effect [6]. These statements mean that product distribution can be controlled by determining zeolite type, modification method and operational conditions for each type of olefins [4]. Moreover, because of their microporous structure, some zeolites can be shape selective. In order to produce desired molecular formula, shape selectivity has a significant role.

For example, to produce diesel fractions with zeolite catalysts, it is important to suppress the isomerization reactions (branching) depending on the pore size and channel system that can be 3-dimensional or 1-dimensional. ZSM-5 (0.55-0.56 nm pore size, 10 membered rings, 3-dimensional) typical medium pore size zeolite is reported as catalyst to restrict branching as COD process mentioned above [2]. Kinetic diameter of short alkane, such as *n*-heptane is 0.43 nm, on the other hand, a monobranched alkanes, such as 2-methyl hexan have 0.5 nm and dibranched one 2,3 dimethyl pentane is approximately 0.56 nm. Other medium pore zeolites, such as ZSM-11 (MEL) and ZSM-12 (MTW) and different frameworks, such as FER, ERI, MFS, NES, and EUO, are reported for diesel production. It is reported that, branching increases with pores size in ethylene oligomerization [2].

On the other hand, chain branching can be minimized with 1-dimensional channel systems, such as ZSM-22 and ZSM-23 [4]. However, 1-dimensional pore structures suffer from pore-mouth poisoning (blocking of the channels) [2]. There are several studies to improve structural properties of 1-dimensional zeolites, such as creating mesopores. For example, alkaline treatment with different concentrations of NaOH was used to develop mesoporous ZSM-12 zeolite. While catalyst activity is improved, shape selectivity of catalyst is suppressed because of mesoporous structures [2].

Zeolites are required to process reactions at high temperature and pressures compared with other heterogeneous catalysts [6]. It is known that Bronsted acid sites in zeolites catalyze oligomerization by carbenium ion mechanism. Product distribution shifts to higher molecular weight olefins at moderate temperature (473-573K) and pressure (30-100 bar) [4]. However, while high temperature and pressure favors the oligomerization reaction on zeolites, side reactions such as cracking and aromatization occur also. All these side reactions lead to accumulation of heavy hydrocarbons (coke) in zeolite pores and catalyst deactivation [6]. Studies show that solvents that can solve heavy oligomers and coke precursors can be used to stabilize catalyst performance by desorbing them from catalyst pore. Solvent molecules having smaller volume than pores can be able to remove similar molecular weight oligomers from pores. For example, co-feeding ethylene with *n*-heptane showed higher activity compared with *n*-octane, *n*-decane, toluene or cyclohexane at 423 K and 35 bar [4]. On the other and, in another study over large-pore USY zeolite, octane

and dodecane solvents showed higher activity and stability for 1-hexene oligomerization at 473K and 50 bar [4].

However, deactivation can occur even at low temperatures. In the study conducted by Hauge et al., catalyst suffered from deactivation at 303-343 K for isobutene oligomerization. Deactivation is directly related with catalyst size that larger sizes lead to higher deactivation. Smaller pore hinders the severe coke formation. Thus, deactivation can be classified into two ways; deposition of cokes at the active sites due to reaction conditions and deposition at the pore mouth (pore plugging) because of size [2].

In order to both improve the lifetime of zeolites and alter their acidic properties; many modification methods are used. For example, exchanging with metal cations (K, Ca, Ni, Zn, Cr) and silicon-containing compounds or steam pre-activation (dealumination) methods are widely used [6]. Nkosi et al. studied over NaY catalyst modified with alkali and alkaline-earth cations (M) followed by nickel promotion (NiMNaY). Catalyst deactivation increased and dimerization decreased with an increase in acidity (electronegativity). Increasing alkali cationic radius resulted in increased dimerization and decreased catalyst deactivation. High activity, high selectivity and decreased deactivation were provided by Cesium exchanged catalyst [7].

On the other hand, it is known that diesel fractions can be produced with shape selective zeolite catalysts. However, the pore shape selectivity is valid when the oligomerization takes place inside. Otherwise oligomerization can also occur on the surface acid sites, and selectivity to branch molecule increases [2]. Thus, partially deactivation of zeolite surface acid centers is another modification method used to change product selectivity to diesel fraction also. Treating with amines (collidine), ammonium borate and dealumination with oxalic acid are methods of partially deactivation. Large molecules, kinetic diameter is higher than zeolites pore size, are used [6]. 2,4,6- trimethylpyridine (0.74 nm) is another molecule having a kinetic diameter as 0.74 nm higher than shape selective ZSM-5 zeolite (0.55-0.56nm) [2].

Acidity (Brønsted or Lewis) has a crucial role on the product selectivity and reaction performance. It is reported that, while Brønsted acid sites favor oligomerization, stronger Lewis acid sites may initiate side reactions, such as polymerization, aromatization, and coking. Si/Al ratio

of zeolites determines the acidity and acidic strength of the catalyst. The higher is the Si/Al ratio, the stronger is the acidic strength and the lower is the acid site density. Mlinar et al. reported that, low Si/Al ratio leads to poor activity of H-ZSM-5 and high selectivity to shorter growth of molecule (dimerization). The amount of acid sites on external surface and Lewis/Brønsted (L/B) ratio of the zeolite catalysts affect the catalytic performance on butene trimerization [8]. Nkosi et al. studied modification of Y-zeolites with cations and found that lower acidity favors the dimer production. Dimer selectivity increased with cation size too. Schmidt et al. studied on a model mixture of olefin and refinery C_5 fraction over Mordenite and ZSM-5 catalyst. It was found that higher Si/Al ratio results in higher conversion of olefins and dimer selectivity (Mordenite, isopentane conversion: 95%, linear pentene conversion: 25-45%, dimer selectivity: 92-95 wt%). The catalyst showed steadily activation during 600 h of reaction [2]. Yoon et al. studied the isobutene oligomerization on different zeolite catalysts, such as Beta, USY, mordenite and ferrierite. They found that Beta zeolite is more suitable for oligomerization. Because of their relatively small pore and rapid deactivation by high molecular weight oligomers, most of the zeolite catalysts are not suitable for trimerization reactions. Performance and stability were found very poor over typical zeolites like Mordenite, USY, ZSM-5, and dimers were found to be the main product rather than trimers and tetramers. Since the oligomerization of isobutene is a consecutive reaction (monomer> dimer > trimer > tetramer), dimer selectivity increases with decreasing conversion irrespective of the catalyst type. However, beta (BEA) zeolite shows high conversion and high trimer selectivity contrary to other zeolites [9].

The L/B ratio of zeolites are increased by dealumination of H-Zeolite with steam treatment at high temperature or addition of typical Lewis acids like $AlCl_3$ or $FeCl_3$. However, steam treatment at very high temperatures, 973 K, results in porosity decrease and structure destruction that lead to very rapid deactivation [9]. Higher L/B ratio results in higher degree of oligomerization [9]. In the studies of Beta (BEA) and Ferrierite (FER) catalyst, high L/B ratio results in stable isobutene conversion and high trimer selectivity. However, because of larger pore size compared with FER, BEA has higher tetramer selectivity too [9]. Table 2.1, 2.2, and 2.3 shows catalytic performances of selected zeolites and modified zeolites in oligomerization of olefins at optimized reaction conditions respectively.

Table 2. 1. Catalytic performances of selected zeolites in oligomerization with optimized conditions [2, 10].

Zeolite	Pore Size [a]	Si/Al	Feed	T (K)	P (bar)	WHSV (h^{-1})	X (%)	Selectivity [b] (%)
Theta-1	M	25	60:40 propene/propane molar mixture	473	40	5.88	92	77
ZSM-22	M	30	2-butene (16 wt%), propane (78wt%), and pentane (6 wt%)	423	60		82	37.9
Ferrierite	M	66	1-butene	463	46	2.03	99.9	66.9
Ferrierite	M	6	2-butene (16 wt%), propane (78wt%), and pentane (6 wt%)	413	60		66	21.4
Mordenite	L	30	1-butene	503	44	2.01	99.8	62.9
Offretite	L	9	1-butene	523	47	0.55	99.9	68.3
ZSM-12	L	100	1-butene	473	41	3.05	99.9	74.8
ZSM-5	M	30	1-butene	483	42	1.50	100	71.8
ZSM-5	M	15	60:40 propene/propane molar mixture	473	40	5.88	82	75
ZSM-5	M	15	60:40 1-pentene/heptane molar mixture	473	40	5.88	97	55

[a] Pore size for 10- and 12- membered rings are can be classified as medium (M) for 10-MR and large (L) for 12-MR. [b] Selectivity to oligomers or diesel range products.

Table 2. 2. Catalytic performances of modified zeolites in oligomerization with optimized conditions [11].

Catalyst Type[a]	Si/Al	Catalyst Preparation[b]	X %	Selectivity[c] wt%
HM	5.8	Calcination at 573 K for 24h	60	Dimer; 71 Trimer; 23 Tetramer; 6
HM	5.8	Calcination at 673 K for 24h	55	Dimer; 68 Trimer; 25 Tetramer; 6
HM	5.8	Calcination at 773 K for10.5h	45	Dimer; 76 Trimer; 21 Tetramer; 3
HM	5.8	Calcination at 873 K for 10h	30	Dimer; 79 Trimer; 18 Tetramer; 3
NaM	6.0	11% calcined at 773K for 27h	9	Dimer; 73 Trimer; 23 Tetramer; 4
NaM	6.0	33% calcined at 773K for 12h	31	Dimer; 79 Trimer; 18 Tetramer; 3
NaM	6.0	52% calcined at 573K for 24 h	20	Dimer; 71 Trimer; 23 Tetramer; 5
NaM	6.0	52% calcined at 673K for 24 h	61	Dimer; 69 Trimer; 23 Tetramer; 6
NaM	6.0	52% calcined at 773K for 4 h	69	Dimer; 61 Trimer; 28 Tetramer; 11
NaM	6.0	52% calcined at 873K for 8 h	36	Dimer; 74 Trimer; 21 Tetramer; 5
NaM	6.0	64% calcined at 773K for 10.5h	70	Dimer; 62 Trimer; 28 Tetramer; 10
NaM	6.0	86% calcined at 773K for 13.5h	75	Dimer; 60 Trimer; 29 Tetramer; 11
NaM	6.0	97% calcined at 573K for 25h	24	Dimer; 77 Trimer; 20 Tetramer; 3
NaM	6.0	97% calcined at 673K for 25h	82	Dimer; 59 Trimer; 29 Tetramer; 10
NaM	6.0	97% calcined at 773K for 8h	74	Dimer; 62 Trimer; 29 Tetramer; 10
NaM	6.0	97% calcined at 873K for 12h	50	Dimer; 71 Trimer; 22 Tetramer; 7

[a]HM: Hydrogen Mordenite , NaM: Sodium Mordenite, [b]Ion exchanged with NH_4Cl, 11% means that replaced 11% of sodium ions with ammonium, [c]Feedstock ; 1-butene (65% wt), n-butane (11% wt), Isobutene (9% wt), Trans-2-butene (4% wt), Cis-2-butene (4% wt), Isobutane (3%wt), Propene (2% wt), Propane (2% wt), 373 K 51 bar WHSV:3.5h^{-1}

Table 2. 3. Catalytic performances of modified zeolites in oligomerization with optimized conditions [12, 13].

Catalyst Type[a]	Ion Exchange	Catalyst Preparation[b]	Selectivity[c] %
NaY	$NiCl_2$	Ni(4.85)/NaY	Dimer; 70.22 (30min), 69.51 (120min)
NaY	$Ni(NH_3)_6Cl_2$	Ni(4.25)/NaY	Dimer; 59.81 (30min), 61.24 (120min)
NaY	$NiSO_4$	Ni(5.20)/NaY	Dimer; 68.52 (30min), 73.26 (120min)
NaY	$Ni(NO_3)_2$	Ni(5.95)/NaY	Dimers; 66.99 (30min), 62.82 (120min)
NaY	$Ni(Acet.)_2$	Ni(5.45)/NaY	Dimers; 71.88 (30min), 76.85 (120min)
NaY	0.5 M LiCl followed by 0.2 M $NiCI_2$	Ni(1.87)Na(3.26)Li(0.47)Y	Dimer; 73.51 (120min)
NaY	0.5 M LiCl followed by 0.5 M $NiCI_2$	Ni(4.96)Na(1.41)Li(0.58)Y	Dimer;73.51 (120min)
NaY	0.1 M $NiCI_2$	Ni(0.71)Na(7.19)Y	Dimer; 89.36 (120min)
NaY	0.2 M $NiCI_2$	Ni(1.89)Na(6.29)Y	Dimer; 79.22 (120min)
NaY	0.3 M $NiCI_2$	Ni(2.65)Na(3.65)Y	Dimer; 77.29 (120min)
NaY	0.5 M $NiCI_2$	Ni(4.85)Na(2.23)Y	Dimer; 69.51 (120min)
NaY	0.5 M KCl followed by 0.5 M $NiCI_2$	Ni(2.60)K(3.94)Na(1.82)Y	Dimer; 82.77 (120min)
NaY	0.5 M RbCl followed by 0.5 M $NiCI_2$	Ni(2.66)Rb(6.67)Na(2.19)Y	Dimer; 89.42 (120min),
NaY	0.5 M CsCl followed by 0.5 M $NiCI_2$	Ni(1.50)Cs(10.12)Na(2.50)Y	Dimer; 98.20 (120min)

[a]NaY: Sodium Zeolite Y, [b]Ion exchanged followed by calcination at 773K for 12h for former five and , by drying at 373K for 2h than calcination at 773K for 16h for latters. [c]Feedstock ; 1-butene (27% wt), iso-pentane (73%wt), 383 K 41 bar, Autoclave

Table 2. 4. Catalytic performances of modified zeolites in oligomerization with optimized conditions [14].

Catalyst Type[a]	Catalyst Treatment[b]	X %	Selectivity[c] wt%
NH_4Y	Calcination at 823K to obtain HY	83.1	Dimer;32.5 Trimer; 57.1 Tetramer; 10.4
NH_4Y	Calcination at 823K to obtain HY followed by dealumination at 773K	91.0	Dimer; 26.3 Trimer; 53.8 Tetramer; 19.9
NH_4Y	Calcination at 823K to obtain HY followed by dealumination at 873K	98.4	Dimer; 16.0 Trimer; 52.4 Tetramer; 31.7
NH_4Y	Calcination at 823K to obtain HY followed by dealumination at 973K	74.1	Dimer; 50.6 Trimer; 36.1 Tetramer;13.4

[a]NH_4Y: Ammonium form of Zeolite Y (Si/Al:2.75) [b]Dealumination was performed under nitrogen saturated with water for 12h [c] Feedstock: Isobutene and n-butane,343 K 15 bar, WHSV(isobutene): 10 h^{-1}

2.2 Ion Exchange Resins

Ion exchange resins, especially macroporous resins, are widely researched to produce petrochemicals and solvents for last decades because of replacement of sulfonic acids with acids such as H_2SO_4 and HCl (separation problem, corrosion risk) [1,15]. For C_4 olefins oligomerization, while Amberlyst resins used to produce gasoline or diesel range, Nafion type one is used to produce intermediates of lubricant production [1].

Properties of resins are affected by monomers, polymerization, and crosslinking (e.g divinylbenzene) degree and specific function groups incorporated with polymeric matrix that provides catalytic activity. The function group can be acidic, basic, redox or metallic complexes (transition metals) according to applications. Furthermore, halogens like bromine and chlorine can also be a functional group that improves their thermal stability. Acidity, surface area, porosity, and pore size distribution affect the catalytic performance of resins [1].

Amberlyst-15 is an example of a sulfonic polystyrene co-divinylbenzene macroporous resin while Nafion is an example of a sulfonic perfluorinated resin. Nafion because of both high acidity and thermal stability (to operate higher temperetures) has received more attention. Although weaker carboxylic, phosphonic, phosphinic, and arsenic acids containing resins are prepared, sulfonic ones have more industrial applications. Etherification, esterification, hydration, hydrolysis, alkylation and oligomerization are widely applied reactions. However, resins have low thermal stability compared with other solid catalysts (zeolites, metal oxides etc). Their operation temperatures are limited to 423 K and that prevents regeneration at high temperatures. Although, resins can be regenerated by washing with solvent (e.g *n*-butane), regenerated catalysts have lower activity and rapid deactivation compared with fresh ones [1, 9, 16].

Resins with their different types were able to use on oligomerization of olefins according to their acidity, pore size, surface area, pore size distribution, and thermal stability [1]. Table 2.2 shows Amberlyst and Purolite catalysts properties that are mostly used for oligomerization reaction.

Table 2. 5. Physical and structural properties of different Amberlyst (A) and Purolite (P) Resins [1, 17-19].

Resin	Crosslinking degree[a] or %DVB	Sulfonation type [b]	Acid capacity (meq H^+ g^{-1})	BET area[c] (m^2 g^{-1})	Pore Volume[d] (cm^3g^{-1})	Particle diameter[e] (mm)	Pore diameter (Å)	Maximum operating temperature[f] (K)
A-15	H	C	4.8	42	0.28	0.74	343	393
A-16	M	C	5.32	1.69	0.013	0.6-0.8	304	403
A-35	H	O	5.4	29	0.21	0.51	329	423
A-36	M	O	5	21	0.143	0.63	240	423
A-70	L	C	3.01	31	0.48	0.57	195	463
P-CT175	H	O	4.98	29	0.22	0.94	662	418
P-CT252	M	O	5.4	22	0.42	0.775	394	403
P-CT275	H	O	5.2	28	0.42	0.72	601	418
P-CT276	M/H		5.2	23	0.21	0.775	357	408

[a] H — high; M — medium; L — low; M/H — medium-high; VH — very high.

[b] C — conventionally sulfonated; O — oversulfonated; B — bi-sulfonated; SS — surface-sulfonated.

[c] BET (Brunauer Emmett Teller) method.

d Adsorption–desorption of N_2 at 77 K.

e Obtained by sieving.

f From manufacturer.

For oligomerization reactions, it was stated that minimum acidity is required [20], thus weak acids (functionalized with carboxylic acid group) are not suitable, whereas stronger acids (sulfonic acids) are appropriate. Amberlyst-15, -35, and -36, Purolite-CT275, Nafion and Indion-125, and -130 are preferred ones [21-23]. Oligomerization reaction over sulfonic acid resins follows carbenium ion mechanism. $–SO_3H$ groups acts as both proton donors and acceptors meaning that push-and-pull mechanism like in case of other solid acid catalysts (e.g zeolites) [1].

In propylene oligomerization, although solid phosphoric acid is a first commercial solid acid catalyst, Nafion resins have been proven to give high conversions at lower temperatures. In a fixed-bed reactor with 5 g of catalyst and 55 cm^3/min of propylene gas feed at 8 bar 423K, Nafion-NR50 showed 95 % conversion while SPA had 6 % conversion. However, after that temperature (e.g 473K) Nafion is no more appropriate for the reaction because of its thermal stability. On the other hand, at lower temperature, it was shown that propylene oligomerization cannot proceed (2-8 % conversion) because of thermodynamic stability of propylene molecules (e.g 373K) [1, 22].

In butenes oligomerization, Amberlyst-15, Amberlyst-1010 and Duolite-C26 type resins were studied. Amberlyst 15 (D_{pore} 20–30 nm, surface area 53 m^2/g, acidity 4.7 meq H^+/g) was compared with XN-1010 (D_{pore} 5 nm, surface area 540 m^2/g, acidity 3.3 meq H^+/g dry) under reaction conditions of 373 K, 15 bar and WHSV = 1.7 h^{-1}. Results showed that, Amberlyst 15 performed better results on liquid production and produced mainly dimers (74 wt %), trimers (20 wt %), and tetramers (5 wt %). Amberlyst-1010, on the other hand, resulted in lower liquid production and products (50 wt % dimers, 40 wt % trimers and 9 wt % tetramers). Another study conducted on Amberlyst-15 with different particle sizes resulted that liquid production decreased when the particle size increases. The recommended particle size is smaller than 44 μm [1].

O' Connor et al. studied the effect of degree of functionalization ($–SO_3H$ group concentration) for Duolite-C26 resin. $–SO_3H$ group concentration was changed in the range of 1.9 to 5.0 meq H^+ g^{-1} dry resin. According to their studies, they did not found acidity effect

on product distribution, however, non-linear relationship between conversion and acidity was found. Reaction rate is first order for low acidity concentrations (<2.9 meq H^+ g^-1). For high concentrations (>4 meq H^+ g^{-1}) reaction order increases [1].

Liquid phase 1-butene oligomerization was studied at 393 K, WHSV: 8 h^{-1} and 3.5 MPa pressure using down-flow reactor over Amberlyst-1010 and Nafion. Deactivation was more for Amberlyst-1010, conversion reached a maximum value of 45 % at a time-on-stream value of 8 h and decreased slowly. Conversion over Nafion reached to 70 % at a time-on-stream value of 18 h before deactivation began. On the other hand, when the dimer selectivity is desired, Amberlyst-1010 is preferred. Higher acidity of Nafion leads to form trimers and heavier oligomers [1]. In order to obtain high conversions for 1-butene oligomerization, higher operating temperatures (423K) are required because of inactivity of 1-butene compared to isobutene. However, catalyst deactivation and thermal degradation occurs even at 423 K [1].

Isobutene is more active than the other C_4 fractions, and oligomerization reaction can be used to separate isobutene from C_4 fractions at low temperatures. Isobutene is processed to obtain dimers, trimer, tetramers etc. In order to obtain an alternative to methyl tert-butyl ether (MTBE), dimers are preferred because of their high-octane number. For example, 100% isobutene conversion and 66% di-isobutene selectivity were obtained after 4 h of reaction at 348 K over macroporous acidic resins Indion-125 or Indion-130. Di-isobutylene selectivity can be increased by using polar components. These components lead to spreading of resin structures and an improvement in the accessibility of active centers although the activity lowered. Macroporous sulfonic acid resin Lewatit K-2631 was studied in the presence/absence of polar component as methanol at 313–353 K and 16 bar. It was stated that, absence of polar components results in more trimer and tetramer selectivity, whereas in the presence of them dimer selectivity increased. Table 2.3 illustrated commercial technologies that uses ion exchange resins with selectivity enhancer to produce di-isobutenes.

Table 2.6. Commercial technologies for di-isobutene production by using selectivity enhancers [1, 24].

Company	**Technology**	**Catalyst**	**Additive**
Neste Oil Kellogg Brown & Root	NexOCTANE	Acid Resin	Water /TBA
CDTECH Snamprogetti	CDIsoether	Acid Resin	Awater/TBA
UOP	InAlk	SPA or acid resin	MeOH/MTBE
Lyondell	Alkylate 100	Acid Resin	Water /TBA

Studies reported that, higher alcohols (ethanol, isopropanol) decreased conversion but increased selectivity to di-isobutenes compared with methanol. Overall, tertiary butyl alcohol (TBA) is the mostly preferred one, because small amounts are enough to obtain desired selectivity and no ethers form with isobutene (because of steric hindrance). If TBA dehydrates as a side reaction, then products isobutene and water also enhance the selectivity. Thus, TBA, water or both are applied as selectivity enhancers [1].

The effect of polar components is stated such that $MeOH^{2+}$ which has lower acid strength then H^+ is formed by methanol adsorption on active sites. Therefore, acid strength and rate of oligomerization decreased. Methanol can react isobutene also to form MTBE that decreases available isobutenes. Isobutene conversion decreases, but dimer selectivity increases. Etherification reaction is less favored by heavier alcohols (ethanol, iso-propanol), thus alcohol availability increases results in decreasing acidic strength of catalysts more [1].

Acidity effect was studied by using Amberlyst-15 modified with NaOH that deactivates the active sites of the catalyst. Decreasing acidity resulted in cctivity and dimer selectivity. Sodium ions strongly adsorb on active sites hindering the mobility of protons and resin swelling [1]. Another modification is sulfonic acid protons exchange with metal ions by introducing both Lewis and Brønsted acid sites. While several metal ions as alkali metals, alkaline earth metals, and rare earth ions are used, alkali metal ions are mostly preferred. Ambelyst-15 exchanged with Na^+ showed remarkable dimerization performance for isobutene oligomerization.

On the other hand, isobutene trimerization products are other type of desired additives to kerosene, diesel pools and raw materials to lubricants. According to studies conducted by Yoon et al, acidity, porosity and space velocity effects on isobutene conversion and trimer selectivity were investigated. Amberlyst 15 and 35 showed the best results (90% conversion) were followed by Amberlyst-DT (70% conversion). Because of diffusional limitations, Amberlyst-31 was ineffective although having strong acidity. On the other hand, Diaion WK-40 showed very low performance (1% conversion) because of its weak acidity. To conclude, both macroporous structure and strength of acids are important for isobutene trimerization. Sulfonic acid resins superior to strong solid acids such as beta and ferrierite zeolites because of a higher trimer selectivity and low tendency to deactivation by pore blockage. However, they have lower thermal stabilities.

Another study showed that diluted isobutene concentration, low space velocity, and high amount of acid sites favor both conversion and trimer selectivity on sulfonic acid macroporous resins (Amberlyst 15-35 at 343 K 15 bar). Dilution of feed and control of reaction temperature can be provided by C_2-C_{10} paraffins to hinder the thermal catalyst degradation and to promote trimer selectivity. Dimerization is favored by low temperature while tetramerization is favored by high temperatures. Moreover, it was stated that in order to obtain trimer selectivity more than 50 wt% isobutene conversion should be higher than 60%. In the study that used isobutene (diluted with n-butane at a 1:1 wt ratio) as feed at a WHSV of 10 h^{-1} (isobutene) and at 343K, conversion was measured as 99.4 wt% with a trimer selectivity of 75.5 wt % and selectivities for low dimers and tetramer as 9.4 wt% and 15.1 wt%, respectively [1].

2.3 Solid Phosphoric Acid (SPA)

SPA has been used commercially since 1930s (Catpoly process developed by Universal Oil Products Company (UOP)) to produce high-octane olefinic motor gasoline by the oligomerization of C_2-C_5 olefins [5, 25, 26]. Especially, SPA is used for upgrading Fischer-Tropsch derived propene and butenes to high quality hydrogenated gasoline. Manufacturing

of SPA only requires natural substances (kieselguhr and phosphoric acid) followed by extrusion and calcination at high temperature [25-27]. There are also studies that are trying to use catalyst without a binder [27]. However, despite their commercial application, catalyst has some drawbacks such as short catalyst life time, together with disposal and corrosion problems. There is no way to reuse the spent catalyst. Additionally, catalyst produces nearly exclusively gasoline fractions products [5].

One of the requirement of SPA catalyst is that feed contains a small amount of water to maintain the catalytic activity. Catalyst hydration state determines not only the catalytic activity, but also the selectivity for oligomerization reaction [25]. Water effect on SPA is related to phosphoric acid species (H_3PO_4, $H_4P_2O_7$, and polyphosporic acid) composition and distribution on catalyst surface [27]. Phosphoric acid is composed of catalytically active phosphoric acid species mixtures on a mixture of silica and different silicon phosphates which act as the support [27]. These phosphoric acid species are formed by the dehydration of monomer unit orthophosphoric acid (H_3PO_4). Since different phosphoric acid species has different acid strength, the water content affects the reactivity and selectivity of the catalyst [28]. Prinsloo et al. studied propylene oligomerization on solid phosphoric acid catalysts and investigated the diesel selectivity relationship with hydration level. According to results, acid strength increased with decreasing hydration level and diesel selectivity increased with acidic strength [26]. Another study conducted by Klerk et al. also stated similar results. “Cold and wet” mode (lower reaction temperature and high hydration level) of catalyst provides the highest yield of high quality motor gasoline. A “cold and dry” or a “hot and dry” mode of operation can be applied for more distillate production [29].

Crushing strength of catalyst particles related to structural distortions within unit operations is another important parameter for SPA catalysts (that are not using binder) from commercial viewpoint [27]. Amounts of silicon ortho- and pyrophosphate phases were found related with crushing strength. The ratio of silicon ortho- and pyrophosphate phases was also reported as relate with the H_3PO_4 concentration, impregnation temperature, calcination temperature, and water addition. Catalyst crushing strength increased with increasing silicon

pyrophosphate phases. Higher acid concentration results in higher crushing strength. Impregnation temperature has positive effect on increasing silicon pyrophosphate phase, thus catalyst strength. However, temperatures above 473 K has no effect on improving the catalyst crushing strength. Additionally, more of the acid was converted into silicon phosphates at higher calcination temperatures (548-748 K). On the other hand, silicon pyrophosphate phases decreased with water addition (0-60 wt %) during calcination step. However, for all parameters, total acid as H_3PO_4 amount decreased with converting phosphoric acid to silicon phosphates. That may decrease the catalytic activity since it was reported that only the phosphoric acid species are active catalytically [27].

2.4 Metal Oxides

In isobutene oligomerization, several oxides such as sulfated titania, and zirconia have also been used. Mantila et al. studied the isobutene oligomerization over sulfated TiO_2 and showed a stable conversion even at room temperatures. They also indicated that a high Lewis Acid/Brønsted Acid (L/B) ratio promotes the catalyst stability. NiO-W_2O_3/Al_2O_3 is another catalyst for gasoline production from isobutene (WHSV 9.0 h^{-1}; 40:60 isobutane/isobutene wt/wt% 323-423K) [30]. While conversion decreased with increasing temperature because of the deactivation by the side reactions (high oligomers) over W_2O_3/Al_2O_3 catalyst, the opposite behavior was observed over NiO-W_2O_3/Al_2O_3 catalyst. The presence of Ni^{2+} leads to high selectivity of dimers (100 wt%). If the olefins adsorbed strongly on the acid sites, the reaction continue, and consequently C_8-olefin selectivity decreases [30].

In another study, sulfated zirconia and nickel zirconia sulfated catalysts were investigated for isobutene oligomerization (301 K, atmospheric pressure and GHSV:16 h^{-1}) [16]. Results showed that while Lewis and Brønsted acids were formed in sulfated zirconia, only Lewis sites were formed in nickel zirconia catalyst. The results showed that lower acidity promoted higher activity for isobutene oligomerization. Ni^{2+} presence again diminished the deactivation rate by coordinating the p-allyl electrons of olefins instead of isobutenes [31].

On the other hand, WO_x/ZrO_2 catalyst is a well-known acid catalyst used for isobutene trimerization also (443 K and 15 bar, 99 % isobutene, WHSV: 5-20 h^{-1}). The tetragonal phase of ZrO_2 was reported as having high stability, conversion and selectivity to trimers for isobutene oligomerization while monoclinic zirconia is an inefficient catalyst. It was reported that when the calcination temperature increased the monoclinic phase appeared. Moreover, the amorphous WO_x/ZrO_2 catalyst showed a very poor performance although its porosity and concentration of acid sites were high. Interestingly, for WO_x/ZrO_2 catalyst performance, the phase of zirconia was found more important than the acid type. However, there were limited information about types of acids (Lewis or Brønsted) promoting the reaction. The performance of WO_x/ZrO_2 formed by calcination at 973 K was reported as catalyst is superior or equal to acid resins, zeolites and sulfated titania in stability, selectivity and regenerability [9, 32].

Oligomerization of isobutene has been performed over nickel compounds supported on oxides or different zeolites for many years. Catalytic activity of such catalysts were related to the surface acidic properties and the chemical nature of the nickel ions. Although thermally activated alumina did not show strong Brønsted acid sites on surface, Lewis acid sites appeared with addition of sulfate ions [33]. For $NiSO_4/\gamma\text{-}Al_2O_3$ catalyst, increasing anion content (SO_4^{-2}) resulted in an increase in the strength and acidity of metal Lewis acid sites (Al^{3+} and/or Ni^{2+}), thus in catalytic activity. For example, for propene dimerization, 1 wt % nickel addition to sulfated γ-alumina improved catalytic activity and dimer selectivity. It was reported that the acid centers attached with SO_4^{-2} groups were responsible for the adsorption of isobutene and reaction intermediates [33].

Brückner et al. worked on an industrial 20 wt% $NiO/SiO_2–Al_2O_3$ catalyst prepared by impregnation of two acidic $SiO_2–Al_2O_3$ supports with bis-cyclopentadienyl nickel ($Ni(Cp)_2$) or bis-cyclooctadienyl nickel ($Ni(COD)_2$) and tried to investigate both Ni^+ and Ni^0 sites and their effects on butene oligomerization. They found that active and selective sites for linear C_8 olefins were Ni^{n+} species (n = 1 and/or 2). Brønsted acid sites had important role for the stability of Ni single sites and these sites were initially active to rise cationic mechanism

leading to branched olefins formation. This Ni^{n+} formation led to change from an acid-catalyzed carbenium ion mechanism to a metal-catalyzed coordinative mechanism which was able to shift the product distrubution from branched olefins to linear ones. For example, while highly acidic catalysts containing low Ni/Al ratio produced undesired branched products such as dimehtylhexenes, for catalysts having lower acidity meaning higher Ni/Al ratio, the products such as n-octenes and methylheptenes were obtained with high selectivity [34].

Jeon et al. worked on Ni/Al_2O_3 catalyst for C_4 oligomerization by investigating the 1, 3 butadiene and phosphorous promoters effects on the reactivity of catalyst. The reaction temperature and pressure were 343 K and 50 bar, respectively. In order to investigate the 1,3-butadiene effect, there were three types of feeds such as C_4, C_4 mixture after selective hydrogenation, and pure 1-butene. C_4 feedstock contains 73.7 wt% butenes, 26.2 wt% butanes, and 0.15 wt% 1,3-butadiene, while feedstock of C_4 mixture after hydrogenation contains 71.8 wt% butenes, 28.2 wt% butanes and 0.004 wt % 1,3-butadiene. According to their results, performance of the catalyst was reduced in the presence of 1,3-butadiene because of irreversible complexing of 1-3 butadiene with active nickel sites and this effect can be eliminated by the hydrogenation of the feed [35]. On the other hand, branched products on Ni–P–triphenyl phosphine oxide/Al_2O_3 catalyst was higher, that was desirable to produce octenes. When TPPO (Triphenylphosphine oxide) was added to the Ni–P/Al_2O_3, higher octene selectivity was obtained than on TPPO-free Ni/Al_2O_3 despite of low butene conversion. When TPPO-free catalyst was used, it was observed that primary products remain partially adsorbed leading to occur secondary reactions such as trimerization and consequently, higher oligomers production. Selectivity for dimerization may be provided by TPPO that may allow an easier desorption of octenes [35].

2.5 Heteropolyacids (HPAs)

There are very few studies that are using supported heteropolyacids over the oligomerization reactions. On the other hand, heteropolyacids, such as $H_3PW_{12}O_{40}$ and $H_4SiW_{12}O_{40}$ have exceptionally strong acidity encouraging their applications for a wide

variety of acid catalyzed reactions. However, because of their low surface area, heteropolyacids must be supported on carriers, such as SiO_2 to use them in catalytic applications efficiently.

One of the methods of separating the isobutene from C_4 feeds is selective oligomerization. Although selective oligomerization is provided by SiO_2/Al_2O_3 catalysts commercially, low selectivity resulting in loss of linear butenes and low catalytic activity are the main problems. Therefore, there is a need for catalysts that are highly active and selective for the isobutene oligomerization in a mixture of butenes. Cation exchange resins, sulfated zirconia, SiO_2/Al_2O_3, solid phosphoric acid and zeolites are catalysts that are used for butene oligomerization. However, these studies are generally conducted only by pure isobutene or linear butene [36]. Zhang et al. studied the preferential oligomerization of isobutene in a 1-butene and isobutene mixture (1:1 mole) over $H_4SiW_{12}O_{40}/SiO_2$ with different $H_4SiW_{12}O_{40}$ loadings and compared the catalytic performance with that of H-Beta, SiO_2/A

l_2O_3, and SO_4^{2-}/ZrO_2. While $H_4SiW_{12}O_{40}/SiO_2$ has higher activity and selectivity compared to other catalysts, the activity was dependent on the $H_4SiW_{12}O_{40}$ loading on SiO_2. Conversion reached a highest level with maximum amount of acid sites obtained at 40 wt% loading. On the other hand, the selectivity for isobutene oligomerization was also dependent on the $H_4SiW_{12}O_{40}$ loading such that the highest selectivity (95 wt%) was achieved on 10 wt% $H_4SiW_{12}O_{40}/SiO_2$ at 293 K. This high performance was inferred to be because of the absence of strong acid sites on the outermost surface. Among the other solid acid catalysts, sulfated zirconia SO_4^{2-}/ZrO_2 showed higher selectivity for isobutene oligomerization, however conversion of isobutene was moderate. However, at 333K for 10 wt % $H_4SiW_{12}O_{40}/SiO_2$, the conversions of linear butene and isobutene were 4 and 84%, respectively, and the selectivity for isobutene oligomerization was obtained high as 96 wt%, that is comparable to that obtained using $SO4^{2-}/ZrO_2$. When temperature effect was evaluated, C_8 (dimer) were main product at all reaction temperatures and the amounts of C_{12} (trimer), C_{16} (tetramer), and C_{20+} increased at higher reaction temperatures suggesting that high temperatures provides reaction of C_8 with butenes [36].

Reaction time generally increases the conversion of isobutene indicating that direct oligomerization of isobutene occurs. However, conversion of linear butenes over $H_4SiW_{12}O_{40}/SiO_2$ with low $H_4SiW_{12}O_{40}$ loadings, such as 10 wt% occurs in the existence of induction period. They suggested possible reasons for formation of induction period such as transforming linear butenes to more active isobutene initially, or forming and/or accumulating active intermediates derived by butenes on the surface in order to activate linear butenes, or competitive adsorption between isobutene and linear butenes on the acid sites. However, former two explanations were not acceptable because 293 K is not enough to process skeletal isomerization of linear butene to isobutene on 10 wt% $H_4SiW_{12}O_{40}/SiO_2$, and the conversion of isobutene like linear butenes should accelerate as the reaction proceed if the second explanation was valid. Therefore, third explanation was acceptable because tertiary carbenium ions formed from isobutene are more stable than secondary carbenium ions formed from linear butenes [36].

Studies continued to increase the selectivity and to decrease loss of linear butenes. Zhang et al. studied on the preferential oligomerization of isobutene in a mixture of isobutene and 1-butene (1:1 mole) on 15 wt% $H_4SiW_{12}O_{40}/SiO_2$ modified with Na^+ ions at 333K. Higher selectivity for isobutene oligomerization was obtained by Na^+ modified $H_4SiW_{12}O_{40}/SiO_2$ and Na^+ ion content increased the selectivity. While $Na_3HSiW_{12}O_{40}/SiO_2$ provided the highest isobutene oligomerization selectivity (~97 wt %), increase in the Na^+ ion content decreased activity because of the lack of strong acid sites by modification of alkaline metal cations. Unmodified $H_4SiW_{12}O_{40}/SiO_2$ had different acid strengths as medium and strong acid sites. They also concluded that $Li_3HSiW_{12}O_{40}/SiO_2$ and $K_3HSiW_{12}O_{40}/SiO_2$ also showed high selectivity for isobutene oligomerization and high activities that are comparable with $Na_3HSiW_{12}O_{40}/SiO_2$. It was suggested that the amount of acid sites and strength of acid sites on the outermost surface affect the catalytic performance of $Na_xH_{4-x}SiW_{12}O_{40}/SiO_2$. Zhang et al. suggested that since oligomerizations of isobutene and linear butenes did not show activity on $Na_4SiW_{12}O_{40}/SiO_2$, the reactions did not occur on Na^+ ion and only Brønsted acid sites over the sodium-modified catalysts (x = 0, 1, 2, and 3) provided activity. Because the

reactions occured on the Brønsted acid sites, isobutene and linear butenes oligomerization took place through tertiary and secondary carbenium ions respectively. Because the secondary carbenium ions are energetically unfavorable compared with the tertiary carbenium ions, stronger acid sites were required for the oligomerization of linear butenes than that of isobutene. At the same reaction conditions, isobutene reactivity were higher than linear butenes such that conversion of linear butenes over $Na_3HSiW_{12}O_{40}/SiO_2$ (x = 3) at 24 h was only 0.8 %, while that of isobutene was 41%. It was concluded that the number of medium surface acid sites were decreased with an increase Na^+ content, while the strong surface acid sites almost disappeared. Since strong surface acid sites were decreased more than medium strong acid sites with modification, the linear butenes oligomerization decreased more than isobutene oligomerization at the same conditions [37].

Chen et al. worked on a series of silica-supported $H_4SiW_{12}O_{40}$ catalysts modified with various loadings of teflon ($H_4SiW_{12}O_{40}/SiO_2$-Teflon), which were prepared by an impregnation method used for isobutene oligomerization. Modification with teflon provided not only surface hydrophobicity but also lipophobicity and led to higher C_8 selectivity and longer lifetime than that of $H_4SiW_{12}O_{40}/SiO_2$ in isobutene oligomerization probably because of decrease in the interactions between coke precursors with the aid of surface-appropriate lipophobicity. Here, while hydrophobicity indicates ability to repel water and lipophobicity indicates ability to repel oil. However, by using the more hydrophobic compounds the poisoning from water could be lowered [38].

References

[1] Bruno M. Antunes, A.E.R., Zhi Lin, Inês Portugal, Carlos M. Silva *Alkenes oligomerization with resin catalysts.* Fuel Processing Technology, 2015: p. 86-99.

[2] Muraza, O., *Maximizing Diesel Production through Oligomerization: A Landmark Opportunity for Zeolite Research.* Industrial & Engineering Chemistry Research, 2015. **54**: p. 781-789.

[3] Csaba Fehér, E.K., Zoltán Eller, Jenő Hancsók and Rita Skoda-Földes, *The Use of Ionic Liquids in the Oligomerization of Alkenes.*

[4] Kim, Y.T., et al., *Low-temperature oligomerization of 1-butene with H-ferrierite.* Journal of Catalysis, 2014. **323**: p. 33-44.

[5] Coelho, A., et al., *1-Butene oligomerization over ZSM-5 zeolite: Part 1-Effect of reaction conditions.* Fuel, 2013. **111**: p. 449-460.

[6] A. V. Lavrenov, T.R.K., E. A. Buluchevskii, E. N. Bogdanets, *Heterogeneous oligomerization of light alkenes: 80 years in oil refining.* Catalysis in Industry, 2016. **8**(44): p. 316-327.

[7] Nkosi, B., F.T.T. Ng, and G.L. Rempel, *The oligomerization of butenes with partially alkali exchanged NiNaY zeolite catalysts.* Applied Catalysis A: General, 1997. **158**(1-2): p. 225-241.

[8] Zhang, X., et al., *Trimerization of Butene over Ni-doped Zeolite Catalyst: Effect of Textural and Acidic Properties.* Catalysis Letters, 2008. **126**(3-4): p. 388-395.

[9] Jhung, S.H. and J.S. Chang, *Trimerization of isobutene over solid acid catalysts.* Catalysis Surveys from Asia, 2009. **13**(4): p. 229-236.

[10]. Coelho, A., et al., *1-Butene oligomerization over ZSM-5 zeolite: Part 1 - Effect of reaction conditions.* Fuel, 2013. **111**: p. 449-460.

[11] Kojima, M., M.W. Rautenbach, and C.T. O'Connor, *Butene oligomerization over ion-exchanged mordenite.* Industrial and Engineering Chemistry Research, 1988. **27**(2): p. 248-252.

[12] Nkosi, B., F.T.T. Ng, and G.L. Rempel, *The oligomerization of 1-butene using NaY zeolite ion-exchanged with different nickel precursor salts.* Applied Catalysis A: General, 1997. **161**(1-2): p. 153-166.

[13] Nkosi, B., F.T.T. Ng, and G.L. Rempel, *Oligomerization of butenes with partially alkaline-earth exchanged NiNaY zeolites*. Zeolites: A Refined Tool for Designing Catalytic Sites, ed. L. Bonneviot and S. Kaliaguine. Vol. 97. 1995. 385-392.

[14] Yoon, J.W., et al., *Oligomerization of isobutene over dealuminated Y zeolite catalysts.* Applied Catalysis a-General, 2008. **337**(1): p. 73-77.

[15] Gates, B.C., *Handbook of Heterogeneous Catalysis*

2008: Wiley-VCH.

[16] Ji, W.Y., H.J. Sung, and J.S. Chang, *Trimerization of isobutene over solid acid catalysts: Comparison between cation-exchange resin and zeolite catalysts.* Bulletin of the Korean Chemical Society, 2008. **29**(2): p. 339-341.

[17] Cadenas, M., et al., *Liquid-phase oligomerization of 1-hexene catalyzed by macroporous ion-exchange resins.* Topics in Catalysis, 2011. **54**(13-15): p. 998-1008.

[18] Honkela, M.L., et al., *Comparison of ion-exchange resin catalysts in the dimerisation of isobutene.* Applied Catalysis A: General, 2005. **295**(2): p. 216-223.

[19] Marchionna, M., M. Di Girolamo, and R. Patrini, *Light olefins dimerization to high quality gasoline components*.

[20] Beckman, R.A., Nierlich, M.F., Peters, M.U., Buschken, H.A.S.W., Kerker, D.L., Maschmeyer, R.D., Rottger, R.D., *Oligomerization of Isobutene in N-butenic Hydrocarbon Streams*, 2007: United States Patent.

[21] Alcántara, R., et al., *Trimerization of isobutene over Amberlyst-15 catalyst.* Reactive and Functional Polymers, 2000. **45**(1): p. 19-27.

[22] Harmer, M.A. and Q. Sun, *Solid acid catalysis using ion-exchange resins.* Applied Catalysis A: General, 2001. **221**(1-2): p. 45-62.

[23] Cruz, V.J., et al., *Acid ion-exchange resins catalysts for the liquid-phase dimerization/etherification of isoamylenes in methanol or ethanol presence.* Reactive and Functional Polymers, 2005. **65**(1-2): p. 149-160.

[24] Schmidt, R., M.B. Welch, and B.B. Randolph, *Oligomerization of C-5 olefins in light catalytic naphtha.* Energy & Fuels, 2008. **22**(2): p. 1148-1155.

[25] Bekker, R. and N.M. Prinsloo, *Butene Oligomerization over Phosphoric Acid: Structural Characterization of Products.* Industrial & Engineering Chemistry Research, 2009. **48**(22): p. 10156-10162.

[26] Prinsloo, N.M., *Solid phosphoric acid oligomerisation: Manipulating diesel selectivity by controlling catalyst hydration.* Fuel Processing Technology, 2006. **87**(5): p. 437-442.

[27] Coetzee, J.H., et al., *An improved solid phosphoric acid catalyst for alkene oligomerization in a Fischer-Tropsch refinery*.

[28] Mashapa, T.N. and A. de Klerk, *Solid phosphoric acid catalysed conversion of oxygenate containing Fischer-Tropsch naphtha.* Applied Catalysis A: General, 2007. **332**(2): p. 200-208.

[29] de Klerk, A., D.O. Leckel, and N.M. Prinsloo, *Butene oligomerization by phosphoric acid catalysis: Separating the effects of temperature and catalyst hydration on product selectivity*. Industrial & Engineering Chemistry Research, 2006. **45**(18): p. 6127-6136.

[30] Tzompantzi, F., et al., *Improved selectivity to C8-Olefins for isobutene oligomerization on NiO-W2O3/Al2O3 catalysts.* Chemical Engineering Communications, 2009. **196**(10): p. 1198-1205.

[31] Tzornpantzi, F.J., et al., *One pot preparation of NiO/ZrO(2) sulfated catalysts and its evaluation for the isobutene oligomerization.* Catalysis Today, 2008. **133**: p. 154-159.

[32] Lee, J.S., et al., *Trimerization of isobutene over WOx/ZrO2 catalysts.* Applied Catalysis A: General, 2009. **366**(2): p. 299-303.

[33] Sarkar, A., et al., *Active sites of a NiSO4/γ-Al2O3 catalyst for the oligomerization of isobutene.* Topics in Catalysis, 2014. **57**(6-9): p. 730-740.

[34] Brückner, A., et al., *The role of different Ni sites in supported nickel catalysts for butene dimerization under industry-like conditions.* Journal of Catalysis, 2009. **266**(1): p. 120-128.

[35] Jeon, J.K., S.K. Park, and Y.K. Park, *Effects of phosphorous promoters on catalytic performance for oligomerization of butene over Ni-based catalysts.* Catalysis Today, 2004. **93-5**: p. 467-470.

[36] Zhang, J., et al., *Preferential oligomerization of isobutene in mixtures of isobutene and 1-butene over 12-tungstosilicic acid supported on silica.* Applied Catalysis A: General, 2009. **353**(1): p. 68-73.

[37] Zhang, J., Kanno, M., Zhang, J., Ohnishi, R., Toriyabe, K., Matsuhashi, H., & Kamiya, Y. , *Preferential oligomerization of isobutene in a mixture of isobutene and 1-butene over sodium-modified 12-tungstosilicic acid supported on silica.* Journal of Molecular Catalysis A: Chemical, 2010. **326**(1-2): p. 107-112.

[38] Chen, G., et al., *Surface-appropriate lipophobicity - Application in isobutene oligomerization over Teflon-modified silica-supported 12-silicotungstic acid.* Applied Catalysis a-General, 2006. **310**: p. 16-23.

Chapter 3

MATERIALS AND METHODS

3.1 Catalyst Preparation

$H_3PW_{12}O_{40}$ (TPA), $H_4SiW_{12}O_{40}$ (TSA), and $H_3PMo_{12}O_{40}$ (MPA) were purchased from Sigma Aldrich. SBA-15 (> 900 m^2/g), MCM-41 (A grade, > 850 m^2/g) and SiO_2 were purchased from ACS Materials and Sigma Aldrich respectively. Isobutene (99.9 vol%) and N_2 (99.9 vol%) were purchased from Handels GmbH and Linde gas company, respectively. Supports were calcined at 793 K for 5 h. Heteropolyacids (HPAs) were dried at 363 K under vacuum for 3 h. HPAs were supported on calcined supports by using a wet impregnation method. The HPA loading amounts of catalysts were ranged from 1 to 90 wt% and water was used as a solvent. For example, for 1 wt% TPA loading, TPA/MCM-41 (1 wt%), 0.01 g of TPA was dissolved in 3 g of water and was mixed on a magnetic stirrer at 100 rpm at room temperature for 15 min. After mixing process, 0.99 g of MCM-41 was added into solution. Total solution was mixed for 24 h by identical mixing procedure. After drying prepared catalyst at 383 K for 5 h, calcination in static air was performed at 523 K for 4h. The identical procedure was applied to prepare catalysts at certain loadings.

3.2 Catalyst Characterization

3.2.1 Fourier Transform Infrared (FTIR) Spectroscopy

All molecules have bonds which are continuously vibrating and moving around. These bonds can vibrate with stretching or bending modes. Stretching can occurs as symmetric or asymmetric. A molecule having three or more atoms can also vibrate with bend motions where there is an angle between atoms [1]. IR spectroscopy is used to analyze the structure of organic compounds by using a beam of infrared light. Not all covalent bonds have band in IR spectrum. Only bonds having dipole moment are IR active. Infrared radiation is a form of electromagnetic radiation that interacts with a covalent bond having electrical dipole [2]. IR radiation is passed through a sample. Some of the infrared radiation is absorbed by the sample while some of it is passed through (transmitted). The obtained spectrum represents the molecular absorption and transmission, and creates a molecular fingerprint of the sample [3]. IR radiation should absorb any vibration causing a change in dipole of the molecule. Symmetric stretch does not alter the overall dipole moment of the molecule as it vibrates, so does not absorb IR [2]. IR provides information about specific functional groups and molecular fingerprint that can be used for comparison of samples. Molecular formula or structure cannot be inferenced from IR data [3]. Bond vibrations create absorption bands and the intensity of absorption bands related to dipole moment change of bond and number of specific bonds exist [1]. Bond length and charge difference of two atoms are two parameters that determine the bond dipole. The bigger electronegativity difference means the more intense absorption [1].

The spectrometer includes a source, beamsplitter, two mirrors, a laser and a detector; the beamsplitter and mirrors are collectively called as interferometer [5]. The FTIR is the most common type of IR spectroscopy and is a sensitive technique to identify organic chemicals as a whole and some of inorganics. FTIR is the most preferred one because of its three unique

advantages. First, FTIR can complete many scans and can average in a shorter time than one scan on most dispersive instruments. Additionally, more energy reaches to sample and detector than dispersive spectrometer because FTIR does not limit the amount of light that reaches to detector using a slit. The slit dispersive instrument that comes more limited as the increased spectral resolution is desired. Thus, higher signal results in higher signal to noise ratio meaning that more sensitive analysis for small absorptions and clearer spectrum. Lastly, FTIR laser is also used as reference signal to provide reference for precision and accuracy of spectrometer. Spectra obtained by FTIR can be compared the spectra collected five minutes or five years with confidence. This is not available on a dispersive infrared, or any system that needs external calibration standards [5].

For the FTIR measurements performed in this study, a Bruker Vertex 80v IR spectrometer was used with a platinum diamond attenuated total reflection (ATR) instrument. Spectra in a range of 600-3000 cm^{-1} were obtained at a spectral resolution of 2 cm^{-1} in air at room temperature. Before sample scan, background signal was collected and averaged by 64 scans. Approximately 10mg of each sample was loaded into the ATR cell. 256 scans were collected and averaged for each sample. Background subtracted spectra for pristine catalysts were deconvoluted by using Fityk program in a Voigt function mode.

3.2.2 Brunauer-Emmett-Teller (BET) Surface Area Analysis

BET theory depends on the physical adsorption of gas molecules on a solid surface to measure the specific surface area of material. The concept of theory is the extended version of Langmuir theory monolayer molecular adsorption to multilayer adsorption by following hypotheses; infinitely physical adsorption of gas molecules, no interaction between adsorption layers, and application of Langmuir theory for each layer. Adsorption should not be confused with absorption in which fluid permeates a solid. However, adsorption is adhesion of atoms or molecules to surface depending on not only on surface area but also

temperature, gas pressure and strength of interaction between sample and gas. Gas molecules and solid surfaces interaction is usually weak. Because of that, surface is cooled with nitrogen because of its strong interaction with most solids and its high purity to obtain detectable adsorptions. Known amount of nitrogen are released to sample cell. After saturation pressure, no more adsorption occurs unless pressure is increased. After layers are formed, sample is removed from nitrogen and heated to release adsorbed nitrogen and to quantify. BET isotherms show amount of adsorbed gas as a function of relative pressure [4].

In this study, BET surface area measurements were performed on a Micromeritics ASAP 2020 – Physisorption Analyzer. Approximately 300 mg of samples was used. Samples were degassed at 523 K for 4 h. N_2 adsorption was applied at 77 K using t-method between 0.091 and 0.4 P/P0 to determine surface areas.

3.2.3 Thermogravimetric Analysis (TGA)

Thermogravimetric analysis is used to determine the sample stability by weight changes of sample in relation to change in temperature under a defined condition with respect to heating rate, gas atmosphere, gas flow rate and crucible type. One can analyze sample under constant temperature also. The gases are generally nitrogen, helium and air. The sample is loaded on pan which is made of aluminum or platinum, and is placed in furnace. The furnace temperature can be increased linearly or stepwise by waiting for a certain time at certain temperature. Furnace temperatures generally increases up to 1000 °C. Apart from the weight change as a function of temperature, a derivative weight loss curve can also be used to see the point where most mass loss occurred [5].

TGA analyses were performed by TA Instruments TGA Q500 model instrument, in this study. Platinum pans were used and tared before sample loading. TGA analyses of approximately 15 mg of each samples was performed under N_2 flow (60 ml/min). For fresh catalysts, a heating rate of 10 K was applied up to 373 K and isothermal treatment was

followed for 4 h at that temperature. Temperature was then increased up to 973 K by a heating rate of 2 K/min.

3.2.4 X-Ray Diffraction (XRD)

X-ray powder diffraction (XRD) is used to identify phase of crystalline material and to provide information on unit cell dimensions. X-rays are formed by a cathode ray tube and filtered to produce monochromatic radiation. The interaction between incident rays and sample forms constructive interference and diffracted ray providing Bragg's Law ($n\lambda = 2d \sin \theta$). Bragg's law relates the wavelength of electromagnetic radiation to diffraction angle and lattice spacing in sample. Θ is the angle between crystal surface and radiation beam, n is an integer, d is the interplanar distance of the crystal and λ is the wavelength of the incident wave. If the angle of incidence does not satisfy the Bragg's Law, destructive interference occurs at all other angles. XRD pattern provides a unique fingerprint of the crystals exist in sample [6].

In this study, XRD analyses were performed using a Bruker D8 Discover X-Ray Diffraction having a Cu Kα1 radiation source with wavelength of 1.5418 Å. A Vantec-1 detector with a slit-size of 1 mm was used. The power rating of X-ray generator was set to 40 kV and 40 mA. The 2θ range of the measurements was in between 1–70° with a step size of 0.00985°. Approximately 10 mg of sample was loaded on a double-sided tape on a glass slide. Then, the glass slide was placed on a sample holder. Background signal generated by the tape was subtracted. ICDD PDF-4 2014 database was used for phase identification.

3.2.5 Temperature Programmed Desorption (TPD)

Temperature programmed desorption is a common technique to explore the influence of adsorbate phase behavior on the kinetics of surface process. TPD is also called as temperature programmed reaction. A gas or gas mixture is adsorbed on sample, then sample is heated

with a certain temperature program. Some of the reaction products desorb from surface by heating and these products are monitored by mass spectrometer [7]. Corresponding to desorption of each reaction products, there are peak series in the TPD spectrum. Each peak related to different kinetic process. The process having low activation barrier has low peak temperature, vice versa [7]. NH_3-TPD is a widely used technique to determine the number of acid sites and acidic strength of catalysis quantitatively.

In this study, temperature programmed desorption of ammonia (NH_3-TPD) was carried out by a MKS Cirrus 2 mass spectrometer connected to a Micrometrics AutoChem II 2920 instrument equipped with a thermal conductivity detector. Catalysts were pretreated at 523 K for 2 h in a flow of Helium (50 cm^3 /min), then were exposed to NH_3 at 313 K for 1 h (50 cm^3/min). Excess NH_3 was removed in a He flow at 373K for 1 h. The temperature of the sample was increased at a rate of 3 K/min to 973 K and TCD signal of the exit gas was monitored. The spectrum of NH_3-TPD was deconvoluted by using an Origin Lab program. Area under peak curves were calculated by OriginLab program. NH_3 calibration by TCD Signal vs Time was used to calculate acid amounts quantitatively. Peak position temperatures were recorded to analyze the acidic strength of supported HPAs.

3.3 Oligomerization of Isobutene over Supported Heteropolyacid Catalysts

Oligomerization of isobutene (Handels GmbH) over supported HPA catalysts were performed in a ½”-stainless steel tubular fixed bed continuous flow reactor. For each run approximately 0.3 g catalyst was loaded into a reactor in which it was supported on a bed made of glass-wool. The catalyst was activated in situ with flowing N_2 (99.9%, 20 ml/min^{-1}) at 473K for 3h. TGA data cited in Appendix, A1 showed that catalyst decomposition temperature was higher than 473 K. After cooling to reaction temperature 393 K in N_2 flow, the reactor was pressurized to 15 bar using nitrogen. Isobutene (99.9%) was fed to reactor at a rate of 0.388 ml/min^{-1}. The analysis of liquid products was performed by GC-Simdis (CNS

Simdis, Analytical Controls by PAC). Conversion of isobutene was calculated from the weight ratio of liquid product and gaseous feedstock, selectivity was calculated according to boiling point curves obtained from GC-Simdis as weight percentages of C_5-C_8 (309-380 K), C_9-C_{12} (380-398 K), C_{13}-C_{16} (398-463 K) and C_{16+} (>463 K) hydrocarbons. All runs were performed for 5 h, longer-term studies were also performed on some of the samples to confirm catalytic stability for up to 48 h. Selectivity and conversion values were determined as the average of a time-on-stream period of from 2 to 5 h.

References

[1] *Infrared Spectroscopy*. Available from: http://www.chem.ucla.edu/~harding/notes/notes_14C_IR.pdf.

[2] D.A. Skoog, F.J.H., and S.R. Crouch, *Principles of Instrumental Analysis*. 6th ed2007, Thomson Higher Education.

[3] *INFRARED SPECTROSCOPY (IR) Theory and Interpretation of IR spectra.*

[4] Nina Hwang, A.R.B., *BET Surface Area Analysis of Nanoparticles.*

[5] *Thermogravimetric Analysis (TGA) & Differential Scanning Calorimetry (DSC)*. Available from: http://www.enfp.umd.edu/sites/default/files/documents/LMD-TGA-DSC.pdf.

[6] *Principles of X-ray Diffraction.*

[7] *Temperature-Programmed Desorption (TPD) Thermal Desorption Spectroscopy (TDS)* Available from: http://www.uhv.es/sites/marte/includes/doc/tds.pdf

Chapter 4

THE SCREENING STUDY

This chapter presents the results of the screening study performed on isobutene oligomerization to compare the catalytic performance of different heteropolyacids (HPAs) supported on different silica-based supports at different loadings. The supports used for this study were SiO_2, SBA-15, and MCM-41; and the HPAs were TPA, TSA, and MPA loaded at different loadings (5-20-50-75 wt%). The reaction conditions were identical set at 393 K and 15 bar and the WHSV was 46 h^{-1}. A total of twenty-eight different catalysts were prepared and tested for isobutene oligomerization. The following section summarizes these results with complementary data provided in the Appendix of this Chapter (Appendix A1).

4.1 Results and Discussion

Oligomerization of isobutene (Handels GmbH, 99.9 vol%) over supported HPA catalysts was performed in a fixed bed continuous flow reactor, 0.3 g catalyst was plugged with glass-wool and activated *in-situ* in flowing N_2 (Messer, 99.9%, 20 ml/min^{-1}) at 473K for 3 h. After cooling down to the reaction temperature, the reactor was pressurized to 15 bar with N_2. Isobutene (99.9%) was fed to reactor at a rate of 0.388 ml/min^{-1}. Analysis of the liquid products was performed by using a GC-Simdis (CNS Simdis, Analytical Controls by PAC) analyzer. Conversion of isobutene was calculated from the weight ratios of the liquid products to gaseous feedstock. Products boiling below 309 K were not counted as product as as the reactant's boiling point is close to this temperature. However, these hydrocarbons can be dissolved in liquid products. Thus, the conversion was calculated by extracting the mass

percentages boiling below 309 K. Selectivity was calculated according to the boiling point curves obtained from GC-Simdis as weight percentages of C_5-C_8 (between boiling temperature 309-387 K), C_9-C_{12} (between boiling temperature 387-458 K), C_{12+} (boiling temperature higher than 458 K) hydrocarbons. Additionally, apart from these detailed selectivity criterion, products were also analyzed as gasoline and distillate range according to the corresponding boiling point ranges of the gasoline and distillate pools. The gasoline range was determined as $309 < T < 448$ K, while the distillate range was $T > 448$ K. All runs were performed for 5 h. The conversion and product selectivities were determined as the average of product samples collected every half hour during a time-on-stream of 3 to 5 h. Figure 4.1 shows the liquid product analyses according to boiling point curve obtained by GC-Simdis.

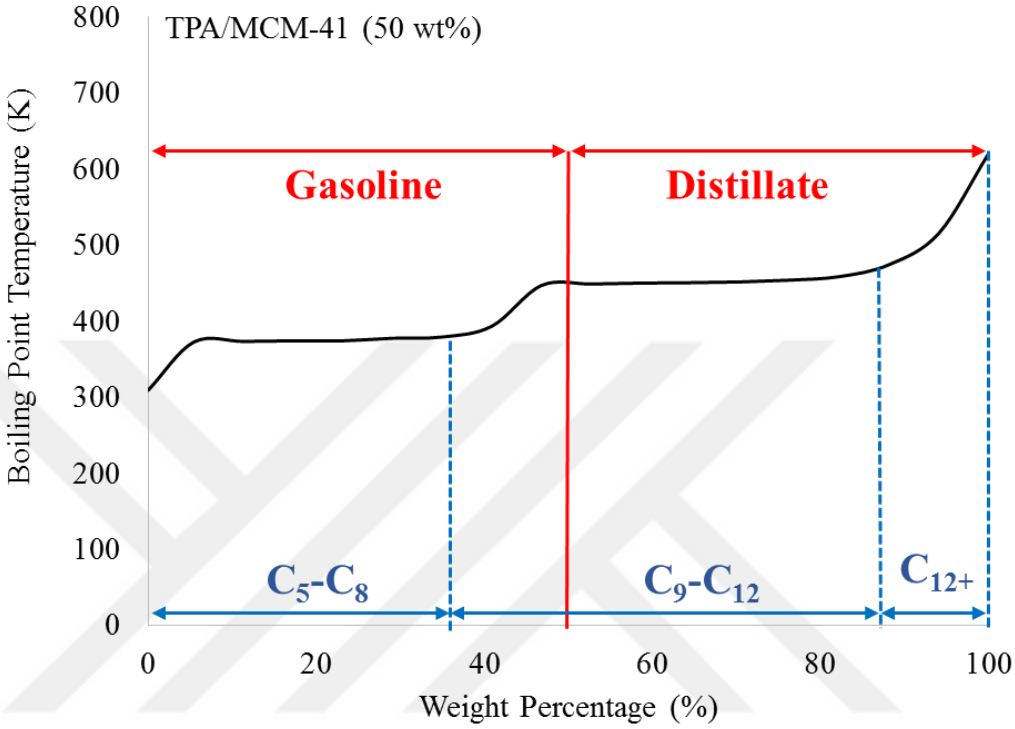

Figure 4.1 Liquid product analysis from the GC-Simdis analyzer.

All runs were performed under identical conditions and the corresponding conversion values were higher than 75 wt% for most of the catalysts. Figure 4.2 shows the catalytic performance for isobutene oligomerization for all of the catalysts related to according to C_5-C_8, C_9-C_{12}, and C_{12+} hydrocarbons with conversion values. The columns in Figure 4.2 represents the C_5-C_8 selectivity (wt%) for each catalyst, while the dots presenting the selectivities for C_9-C_{12} and C_{12+} (wt%), respectively. Conversion values (%) were given with dots. Moreover, Figure 4.3 shows the catalyst performance as the ratio of gasoline to distillate products as distillate/gasoline (D/G) ratio. In Figure 4.3, the columns represent the gasoline ratios (wt %), and D/G values were given with dots.

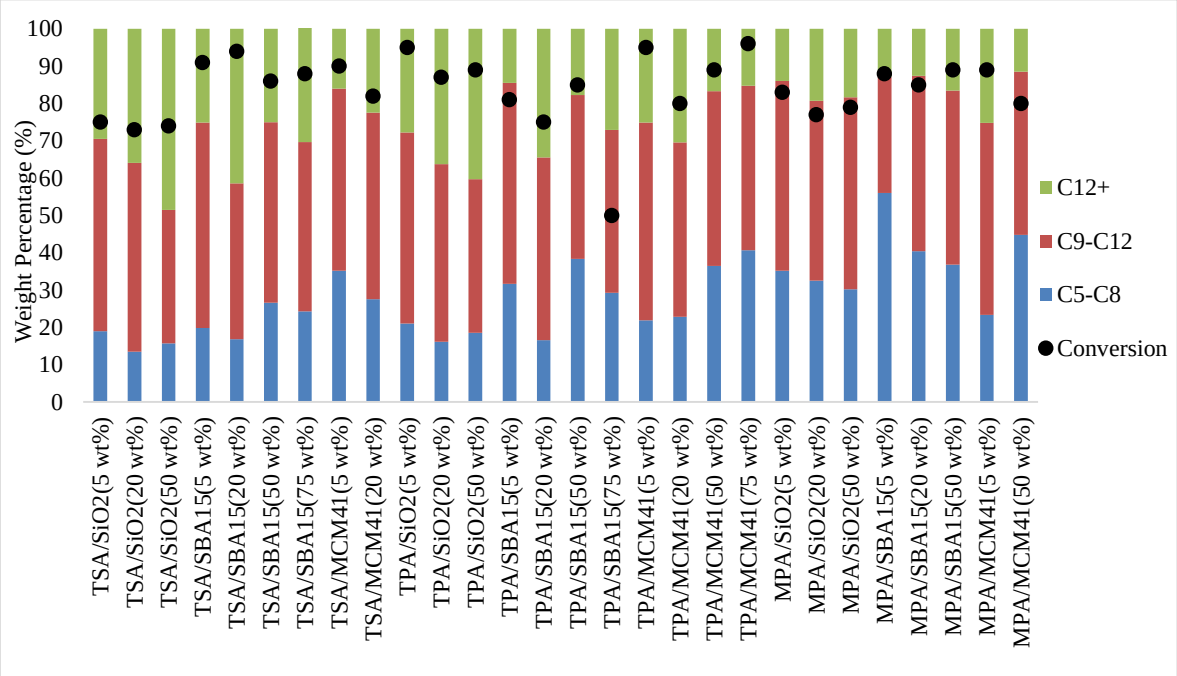

Figure 4.2 Isobutene Oligomerization Performances on Different Catalysts (C_5-C_8, C_9-C_{12}, and C_{12+} selectivities).

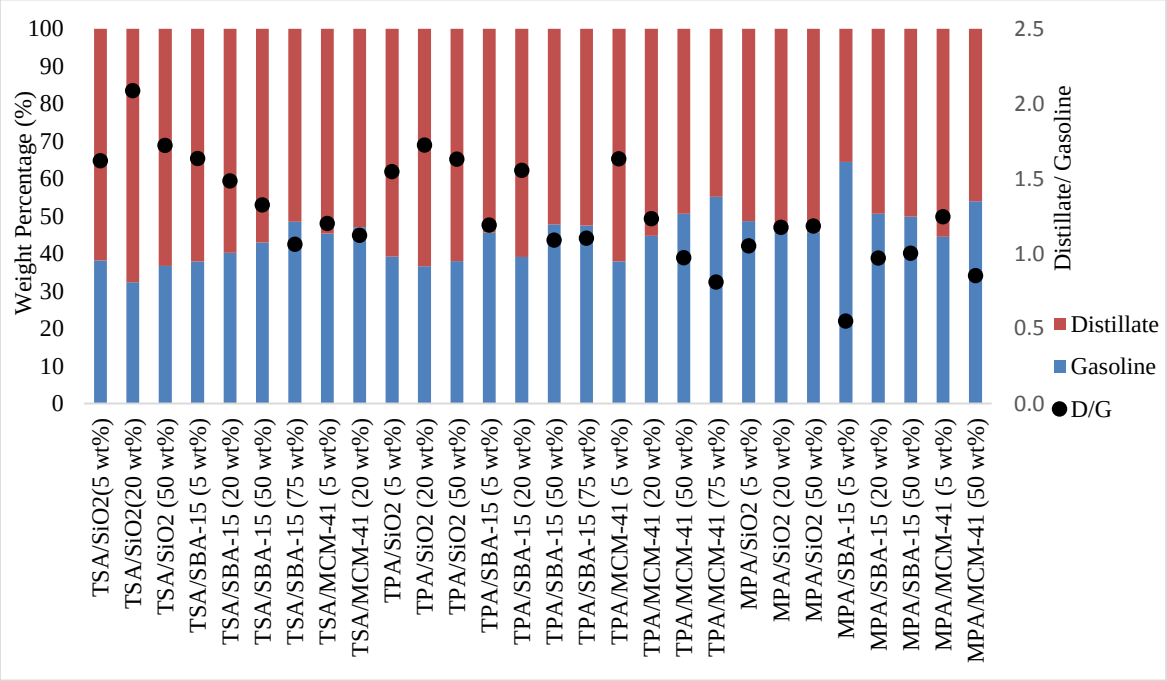

Figure 4.3 Isobutene Oligomerization Performances on Different Catalysts (Gasoline and Distillate Selectivity).

Reaction results conducted at identical operation conditions illustrate that the product selectivity can be tuned by using different HPAs, supports and HPA loadings. C_5-C_8 selectivity changed from 13 to 56 wt%, C_9-C_{12} selectivity varied from 30 to 55 wt%, and C_{12+} selectivity ranged from 32 to 65 wt%. All conversion values were above 75% except for the TPA/SBA-15 (75 wt%) catalyst. Gasoline fraction showed a change from 32 to 65 wt%, and the D/G ratio changed in between 0.6 to 2.1. Detailed discussion on the effect of HPA and support type, and the HPA loading on both the structural properties of the catalysts and the corresponding catalytic performance for isobutene oligomerization are provide in the Appendix A1.

Based on the results of this screening study, TPA/MCM-41 and TSA/SBA-15 catalysts were found to present a good variation of product selectivity with varying HPA loading.

Since TPA has highest thermal stability and highest acid strength, this class of catalysts were chosen for a deeper analysis focusing on elucidating the structure-performance relationships in detail [1-3]. These results are presented in Chapter 5.

References

[1] Chen, G., et al., *Surface-appropriate lipophobicity—Application in isobutene oligomerization over Teflon-modified silica-supported 12-silicotungstic acid.* Applied Catalysis A: General, 2006. **310**: p. 16-23.

[2] Zhang, J., et al., *Preferential oligomerization of isobutene in a mixture of isobutene and 1-butene over sodium-modified 12-tungstosilicic acid supported on silica.* Journal of Molecular Catalysis A: Chemical, 2010. **326**(1-2): p. 107-112.

[3] Zhang, J., et al., *Preferential oligomerization of isobutene in mixtures of isobutene and 1-butene over 12-tungstosilicic acid supported on silica.* Applied Catalysis A: General, 2009. **353**(1): p. 68-73.

Chapter 5

ISOBUTENE OLIGOMERIZATION ON MCM-41 SUPPORTED TUNGSTOPHOSPHORIC ACID[1]

5.1 Introduction

The refineries are now forced to process heavier crude oil as they are relatively cheaper compared to their lighter counterparts [1]. Technologies, such as delayed coking and fluid catalytic cracking, are widely used to upgrade these heavier feedstocks. These technologies produce lots of valuable products ranging from gasoline to diesel fuel components along with gaseous products containing a significant amount of olefins. However, the market demand for these gaseous unsaturated hydrocarbons is mostly limited with the utilization in LPG fractions and petrochemicals. A recent trend is to convert these undervalued light olefins into more valuable liquid hydrocarbons that are more suitable for gasoline and diesel pool, or for middle distillate. This approach is also needed for the utilization of shale gas components. The conversion can be done by several different technologies, such as alkylation and oligomerization [2]. Among these technologies, alkylation is used to produce mostly gasoline range products by using very strong acids, such as HF or H_2SO_4, to process a feedstock containing isobutene with isobutene [2]. Oligomerization, on the other hand, is more flexible in terms of both feed (C_2-C_4 range olefins) and product composition [3, 4]. This technology requires a solid acid catalyst [5], such as solid phosphoric acid [6-8], zeolites [9-15], cation

[1]Contents presented in this chapter has been submitted to *Applied Catalysis A* by authors, Kocaman, E., Akarçay Ö., Çelebi S., Bağlar N. and Uzun, A. The original manuscript has been reformatted to conform to the format requirements of this thesis.

exchange resins [16-19], and metal oxides with acidic function [20]. The structure, location, and the strength of active sites in these catalysts determine the product selectivity. For instance, the solid phosphoric acid has been used commercially since 1930s (Catpoly process developed by Universal Oil Products Company (UOP)) for the production of high-octane olefinic motor gasoline by the oligomerization of C_2-C_5 olefins [7, 21, 22]. Zeolites, on the other hand, are a widely studied group of catalysts offering various advantages, such as high degree of regenerability, thermal stability, and shape selectivity [23]. They are also applied in industrial applications. For instance, the COD-9 catalyst (Süd-Chemie), mostly based on ZSM-5, provides 95-97 % olefin conversion in a commercial process called "Conversion of Olefins to Distillate" (COD) operating at 473-573 K and 45 bar. This process is highly selective to diesel fraction because of the shape selectivity of ZSM-5 catalyst [24]. Ion-exchange resins, on the other hand, have macroporous structures with strong acidity and high acid capacity offering long lifetime (low tendency to pore blockage deactivation) and high trimer selectivity for C_4 olefins [25]. For instance, Nafion-NR50 provides 95% conversion for propene oligomerization at 423 K and 8 bar at a space velocity of 10 h^{-1}, while SPA offering only 6% conversion under the identical conditions [25].

Although all of these catalysts can be used commercially, there are some drawbacks regarding their utilization. For instance, SPA catalysts produce only gasoline range products, and they have a limited catalytic lifetime. Besides, they generate corrosion problems, and are difficult to dispose [21]. Zeolites require higher operating temperatures and pressures compared to other solid acid catalysts; and this requirement leads to some side reactions, such as cracking and aromatization, directly influencing the product quality [24]. Ion-exchange resins cannot be regenerated because of their low thermal stability [26]. These limitations in solid acid catalysts suggest a strong need for a new type of catalysts. A good alternative in this respect is the Keggin type heteropolyacids (HPAs). These relatively new class of catalysts offer unique physiochemical and catalytic properties suitable for various

reactions including oligomerization of light olefins [3, 27-32]. One of the main advantages of these catalysts is that their redox and acidic properties can be tuned by varying their chemical composition [27, 30, 33]. These materials have a general formula of $H_{8-x}MX_{12}O_{40}$, where M and X are the central- and hetero-atoms, respectively. Typically, M can be either P or Si, and X can be W or Mo [30, 31, 34, 35]. The structure of the heteropoly anion consists of a central tetrahedron XO_4 surrounded by 12 edge- and corner-sharing metal-oxygen octahedral MO_6. Among a wide range of available HPAs, tungstophosphoric acid ($H_3PW_{12}O_{40}$), silicotungstic acid ($H_4SiW_{12}O_{40}$), phosphomolybdic acid ($H_3PMo_{12}O_{40}$), and silicomolybdic acid ($H_4SiMo_{12}O_{40}$) are the most commonly used ones with a variation of acid strength in the following order: $H_3PW_{12}O_{40}$ (TPA) > $H_4SiW_{12}O_{40}$ (TSA) > $H_3PMo_{12}O_{40}$ (MPA) > $H_4SiMo_{12}O_{40}$ (MSA) [32,37,38]. Because of this variation in acid strength, the HPAs with a tungsten hetero-atom are usually the choice of material for various reactions requiring strong acidity, high thermal stability, and low oxidation capability [34-39]. These materials are, in general, more active catalysts than other conventional solid acid catalysts because of their strong Brønsted acidity. Their strong acidity allows operation at mild conditions [34, 40-42]. However, these materials offer a very low surface area, generally in the range of <10 m^2/g. Such low surface area limits the availability of the acid sites for surface-type reactions. Therefore, they are usually dispersed on high surface area supports, such as silica, titania, and carbon [29, 42]. Among these, silica is the most widely used support because it interacts weakly with Keggin anions preserving the heteropolyacid structure [30, 39, 43, 44]. The acidic properties of HPAs on these supports can be varied simply by changing the corresponding HPA loading. For instance, Sushkevich et al. tested the effect of HPA loading on the selectivity of amorphous silica-supported TPA for isoprene synthesis from formaldeyde and isobutene. Their results illustrated that a catalyst with 20 wt% TPA loading provides the best performance with an isoprene yield of 48%. The effect of HPA loading on the catalytic performance was inferred to be associated with the high

content of weak Brønsted acid sites [45]. Zhang et al. studied the relation between the changes in surface acidity and loadings for SiO_2-supported TSA. They performed temperature-programmed desorption of benzonitrile (BN-TPD) complemented by an infrared (IR) spectroscopy investigation on BN- and pyridine-adsorbed catalyst. Their results illustrated that the formation of medium strength Brønsted acid sites occurred until the surface of SiO_2 covered with a single layer of TSA and reached a maximum at an HPA loading of 30 wt%. The formation of sites with different acid strength was accompanied by the direct interactions between the TSA and SiO_2 [46].

Applications of HPAs for light olefin oligomerization is quite limited [5]. One of the few studies on this reaction was reported by Zhang et al. on the selective oligomerization of isobutene in the presence of 1-butene (with a molar ratio = 1:1 in the feed). They illustrated that 40 wt% TSA loading on SiO_2 provides the highest activity for isobutene oligomerization, while the selectivity to isobutene oligomerization reaches a maximum of 95 wt% on a TSA/SiO_2 catalyst with a TSA loading of 10 wt% [38]. Here, we extend this approach to a family of another HPA catalyst supported on a support with a significantly high surface area. For this purpose, TPA was selected as the HPA because of its higher acid strength than that of TSA. And as a support, we used a mesoporous silica, MCM-41. This support has hexagonal mesoporous arrays, thus it is superior to the conventional silica supports because of its high surface area (in the range of 800-1000 m^2/g), porosity, and high thermal stability [3, 37, 47]. With these properties, MCM-41 is a promising support for HPAs because it enables high dispersion of HPAs and ease of diffusion for the reactants and products [48-50]. There have been reports on HPA/MCM-41 systems on various reactions, such as alkylation, hydrodesulphurization, esterification, and oxidation [31, 41, 43, 44]. However, to the best of our knowledge, MCM-41-supported HPA catalysts have not been studied for olefin oligomerization [26]. This report illustrates their potential for this reaction.

5.2 Results and Discussion

5.2.1 Catalyst Characterization

Detailed characterization of the TPA/MCM-41 catalysts prepared at fourteen different TPA loadings, ranging from 1 to 90 wt%, was performed to (i) verify successful incorporation of TPA in MCM-41; (ii) confirm the structural integrity of TPA in MCM-41; (iii) elucidate any interactions between TPA and MCM-41; (iv) reveal the effect of TPA loading on catalytic properties, such as on acid strength. Results obtained from BET analyses showed that the surface area and pore volume decreased from 865 m^2/g and 0.72 cm^3/g to 17 m^2/g and 0.02 cm^3/g with an increase in TPA loading from 1 to 90 wt%. Data given in Figure 5.1 indicate that these changes in surface area and pore volume are strongly correlated with the loading amount up to 75 wt%, after which a slight deviation was present.

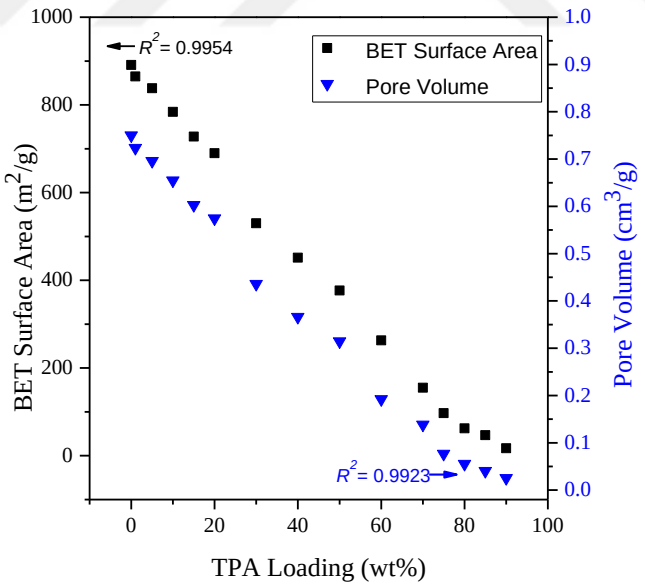

Figure 5.1. Variation of surface area (■) and pore volume (▼) of the TPA/MCM-41 catalysts with the corresponding TPA loading.

Average thickness of the TPA layer was estimated from the difference between the pore volume of MCM-41 and that of the supported catalysts divided by the surface area of the corresponding TPA/MCM-41 (Equation A1, in A2). Accordingly, as given in Figure A2.2, (in Appendix A2), the average thickness of TPA layer was less than 1.15 nm for TPA loadings of less than 50 wt%. However, this thickness value increases exponentially to 42 nm when the TPA loading exceeds 50 wt%, indicating the formation of multilayers at such high TPA loadings. This result indicates the presence of a monolayer TPA on MCM-41 surface up to a loading of 50 wt% [51].

Figure 5.2 presents the XRD patterns of TPA/MCM-41 catalysts from $2\Theta = 10$ to 90°. The bulk TPA has the following features at $2\Theta = 24$, 35, 38, 53, and 60° [52]. The data also include a sharp peak at approximately $2\Theta = 2°$ with weak peaks at $2\Theta = 3$ to 5° associated with MCM-41. These relatively high intensity peaks are not shown in Figure 5.2 for the sake of highlighting the features of HPA related peaks, which have significantly low intensities compared to those of MCM-41 at low angles. The complete range of XRD results can be found in Figure A2.3, in A2.

The XRD of TPA/MCM-41 samples prepared at varying TPA loadings illustrate that the features belonging to TPA are not detectable or shift to different positions at loadings below 30 wt%. These results show that the TPA clusters have a very high degree of dispersion at loadings below 30 wt% with some distortions present in their structure [51]. At higher loadings, on the other hand, TPA features start to appear with some variations in the intensities. These variations in intensities indicate possible changes in electronic environment and/or orientations of the planes, originated from the direct interactions between TPA and MCM-41. These interactions were investigated by means of IR spectroscopy.

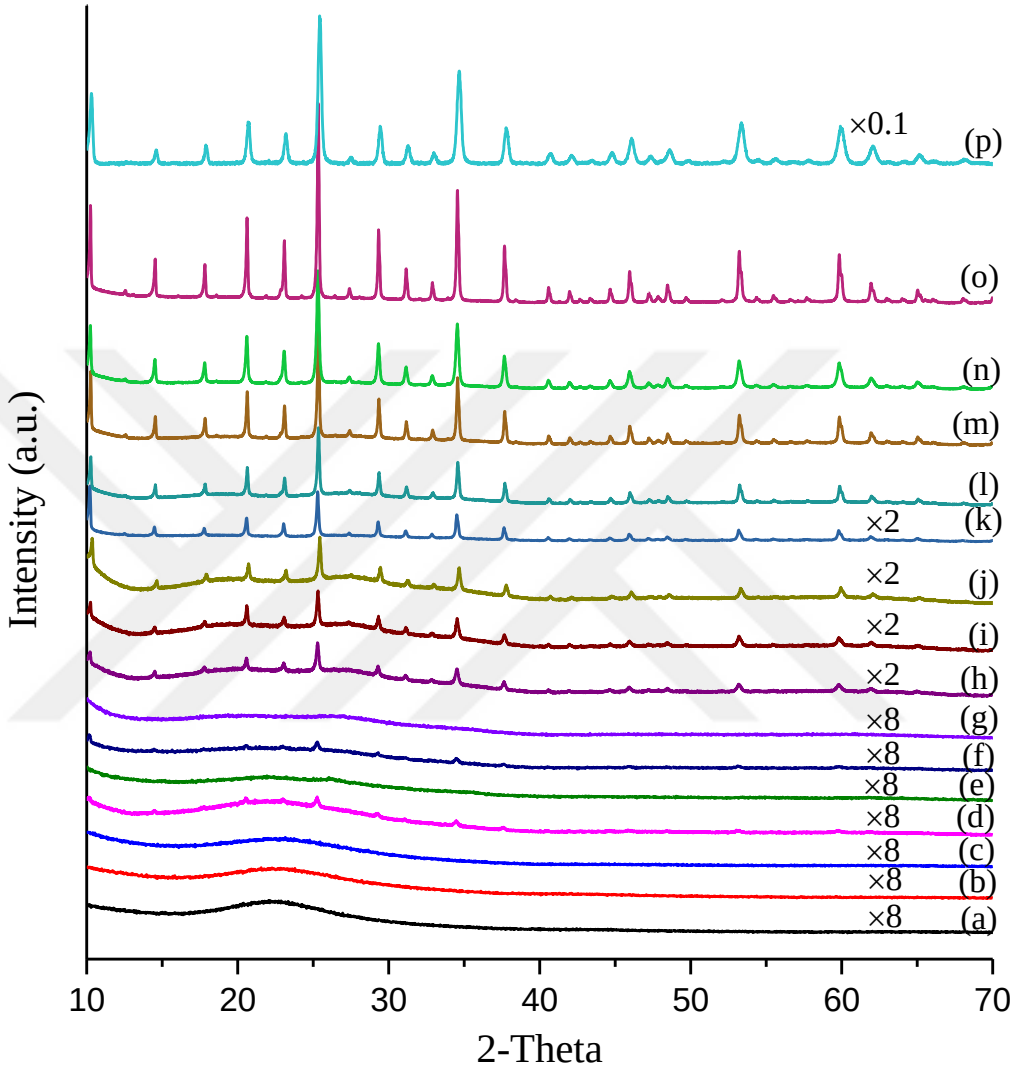

Figure 5.2. XRD patterns of (a) pure MCM-41, (b) 1 wt%-; (c) 5 wt%-; (d) 10 wt%-; (e) 15 wt%-; (f) 20 wt%-; (g) 30 wt%-; (h) 40 wt%-; (i) 50 wt%-; (j) 60 wt%-; (k) 70 wt%-; (l) 75 wt%-; (m) 80 wt%-; (n) 85 wt%-; (o) 90 wt%-TPA loaded on MCM-41; and (p) bulk TPA.

Figure 5.3 illustrates the IR spectra of pristine and MCM-41 supported TPA samples in comparison with that of the pristine MCM-41 in 700-1400 cm^{-1} region. The raw data in complete IR region are provided in Figure A2.4, in A2; and the difference spectra obtained

by subtracting the spectrum of MCM-41 from that of all catalysts are also given in Figure A2.5, in A2. In the IR spectrum of bulk TPA given in Figure 5.3, the bands at, are 770, 881, 965, and 1076 can be assigned as antisymmetrical stretching vibrations of $\nu_{as}(W–O_c–W)$, $\nu_{as}(W–O_b–W)$, $\nu_{as}(W=O_d)$ and $\nu_{as}(P–O_a)$, respectively [53]. When these features are compared with their corresponding positions in TPA/MCM-41 samples, it is observed that they (except for $\nu(P–O)$) shift to higher wavenumbers (blue shift) upon the incorporation of TPA into MCM-41. Data presented in Figure 5.4 illustrate that the corresponding band positions approach to their bulk counterparts with an increase in TPA loading. Accordingly, the changes in TPA structure, and thus, the interactions between the TPA and MCM-41, are more significant at especially low loadings [23]. When the loading was below 30 wt%, the IR features were significantly different than their bulk counterparts and were not detectable indicating a strong distortion of the TPA cluster. These distortions in TPA structure originate from the presence of strong interactions with the MCM-41 surface. The IR spectra of the samples are consistent with the XRD results presented in Figure 5.2 confirming the presence of these distortions in the TPA structure at loadings lower than 30 wt%, as discussed above. Such changes in the structure of Keggin clusters upon interaction with SiO_2 at low loadings were also illustrated by Zhang et al. [46] and Berry et al. [54] using IR and X-ray photoemission spectroscopies, respectively.

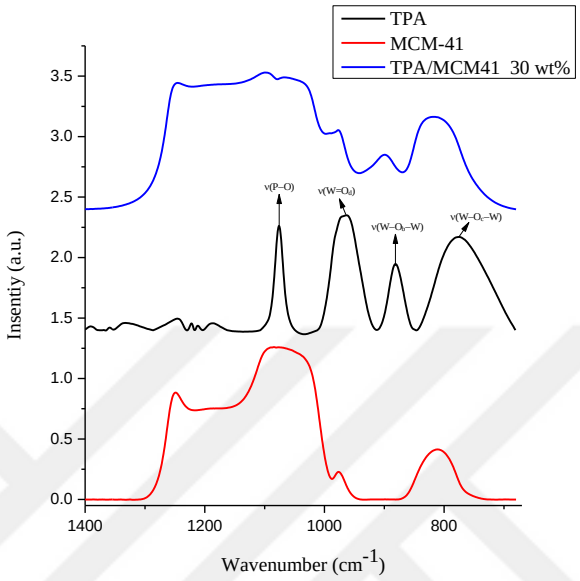

Figure 5.3. Infrared Spectra of Keggin Structure region: pristine TPA, pristine MCM-41, and TPA/MCM-41(30 wt%) catalyst.

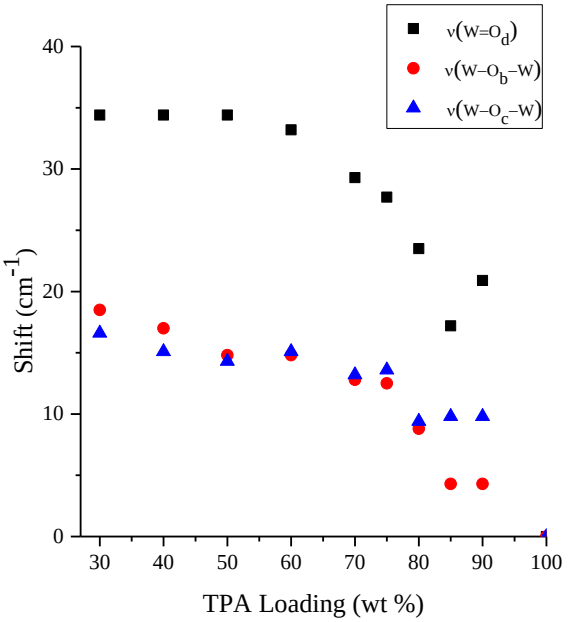

Figure 5.4. Effect of TPA loading in TPA/MCM-41 catalysts on the IR features of TPA ($\nu(W{=}O_d)$, ■; $\nu(W{-}O_b{-}W)$, ●; $\nu(W{-}O_c{-}W)$, ▼). The degree of blue shifts were calculated with respect to the corresponding positions in the pristine TPA using the difference spectra obtained by subtracting the MCM-41 spectrum from the spectrum of the corresponding TPA/MCM-41 catalysts.

The presence of these interactions between the TPA and MCM-41 especially for the loadings where monolayers present is expected to influence the acid properties of the catalysts. Aiming at quantifying the changes on acid strength, we performed NH_3-TPD measurements (summarized in Table A2.1, in A2). Figure S6, in SI shows a representative data set of NH_3-TPD profile on a representative TPA/MCM-41 catalyst and related calculations. NH_3-TPD profile of bulk TPA (Figure 5.5) presents a small broad peak at 461 K followed by another peak at 602 K and a very sharp one at 878 K. TGA data obtained for TPA in flowing N_2 indicate that the TPA starts to decompose at 738 K (Figure A2.7 in A2 [32]). Thus, the third peak was considered as the thermal decomposition products of the TPA. Pinto et al. also reported the third sharp desorption peak as an indication of the TPA (in the form of ammonium salt) decomposition [55]. Thus, the remaining low temperature peaks at 461 and 602 K correspond to low- and medium-strength Brønsted acidic sites (LT and MT), respectively.

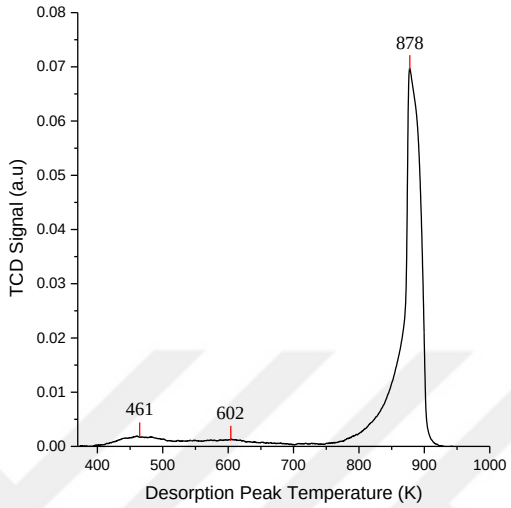

Figure 5.5. NH_3-TPD profile of the pristine TPA obtained under a He flow of 50 cm^3 /min with a temperature ramp rate of 3 K/min from 373 to 973 K using 100 mg of catalyst.

When the TPA loading was 5 wt%, the NH_3-TPD measurements show that LT and MT desorption peaks shift to 417 and 602 K, respectively, indicating a decrease in acid strength. Figure 5.6 illustrates the variation of these LT desorption peak positions on each catalyst with the corresponding TPA loading. Accordingly, the LT desorption peaks show an increasing trend with increasing TPA loading with an R^2 of 0.95 (when excluding loadings lower than 30 wt%). This increasing trend indicates that the acid strength increases with an increase in TPA loading. Here, we note that the data obtained on catalysts with TPA loadings lower than 30 wt% did not show any correlation with the LT positions. As discussed before, this different behavior is originated from the distortions in the structure or form of the TPA because of the presence of strong interactions with the support at low loadings consistent with the XRD results presented in Figure 5.2. We also note that the MT desorption peak temperatures do not show any noticeable trend with TPA loading (Figure A2.8, in A2). These results are broadly consistent with the results of Sushkevich et al. [45] illustrating that the

acid strength measured by NH_3-TPD increases and approaches to that of bulk TPA upon an increase in TSA loading on SiO_2.

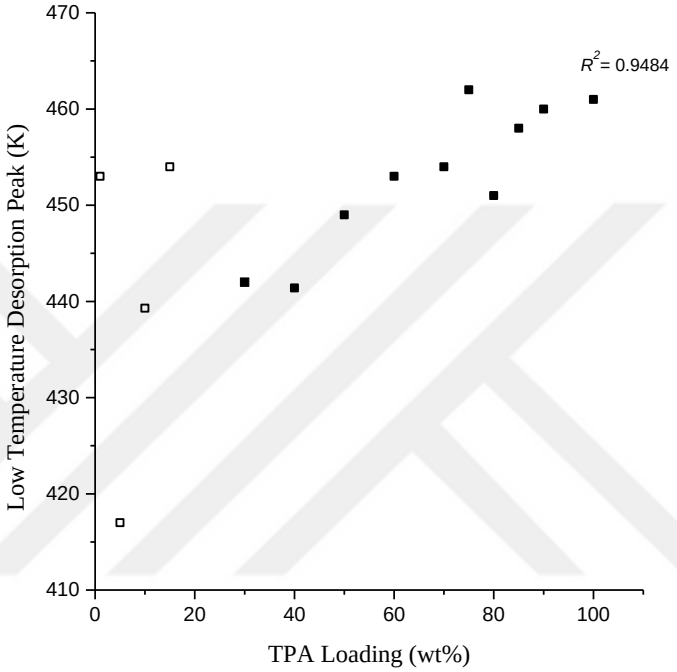

Figure 5.6. Variation of the LT desorption peak positions with the corresponding TPA loading. Catalysts with TPA loadings lower than 30 wt% presenting strong distortions shown with open symbols (□) were excluded from the correlation coefficient calculations.

NH_3-TPD results also provide information on the changes in the concentrations of acid sites. Sarazen et al. stated that SiO_2 supported HPAs with tungsten-addenda atoms include various acid strength [56]. As shown in Figures A2.9 and A2.10 in A2, the amount of low and medium strength sites associated with desorption temperatures of 417 and 602 K, respectively, present a volcano-shape plot with an increase in TPA loading (given) reaching a maximum at approximately 50 wt% loading. These results are consistent with the BN-TPD results reported by Zhang et al. [46] on TSA/SiO_2 catalysts with a TSA loading ranging from

5 to 70 wt% reported. They reported for TSA that the strong Brønsted acid sites formed in the second layer, and acid sites were covered with the excess TSA leading to a decrease in the amount of strong acids. Consistently, we infer that the number of acid sites increases until covering the whole support surface with TPA, and then the formation of multilayer blocks some of these sites and leads to a decrease in the number of acid sites. These results indicate changes on the relative concentrations and strengths of the acid sites with changing HPA loading, suggesting a change on catalytic activity.

5.2.2 Catalytic Performance

Several different solid acid catalysts were considered in the literature for the oligomerization of isobutene. In most of these studies, the weight hourly space velocity (WHSV) was varied in between 0.5 to 10 h^{-1} at various temperature and pressure conditions. Table 1 summarizes the catalytic performance of some of these catalysts in comparison with the results of catalytic performance tests performed on our catalysts. Accordingly, the MCM-41-supported TPA catalysts presented in this study provide similar, stable conversions at significantly higher space velocities (46 h^{-1}) under comparable reaction conditions. Thus, we infer that having a large surface area on the MCM-41 provides a high degree of dispersion of the TPA so that their availability increases to provide such significantly high activity.

Table 5.1. Operating conditions, catalytic properties and performance of some of the solid acid catalysts on isobutene oligomerization with a comparison of the corresponding values of the catalysts presented in this study.

Catalyst	Temperature, K	Pressure, bar	WHSV, h^{-1}	Surface Area, m^2/g	Conversion, %	Dimer Selectivity, %	Trimer Selectivity, %	Ref.
WOx/ZrO_2[a,b]	343	15	5	68	100	5	80	[20]
Ferrierite (20)[c]	343	15	10	400	100	28	60	[14]
USY (60)[a,c]	343	15	10	750	85	60	33	[57]
Al/USY (60)[a,c]	343	15	10	745	99	21	48	[57]
HY (2.75)[a,c]	343	15	10	722	83	33	57	[58]
HY500[d] (2.75)[a,c]	343	15	10	660	91	26	54	[58]
HY600[d] (2.75)[a,c]	343	15	10	617	98	16	52	[58]
HY700[d] (2.75)[a,c]	343	15	10	382	74	51	36	[58]
Amberlyst-35[a]	343	15	50		91	22	66	[59]
Amberlyst-15	373	1	2.5		98	8	82	[60]
Sulfated Titania	413	40	2.5		100	38	60	[61]
TSA/SiO_2 (50 wt%)[d]	393	1	14		57	90		[62]
$NiO\text{-}W_2O_3/Al_2O_3$	423	1	9	227	14.8	82	18	[63]
TPA/MCM-41 (1 wt%)[d,e]	393	15	46	865	75	18	66	This work
TPA/MCM-41 (50 wt%)[d,e]	393	15	46	376	81	35	47	This work
TPA/MCM-41 (90 wt%)[d,e]	393	15	46	17	83	37	52	This work

a. n-butane diluent by 50 wt%.
b. Calcined at 700 °C
c. Si/Al ratio is given in parentheses
d. Heteropolyacid loading is given in parentheses
e. Detailed results are provided in SI

As illustrated above and as shown in Table A2.1 in A2, the variation of TPA loading presents a strong influence not only on the concentration but also on the acid strength. Figures 5.7 and 5.8 show the consequences of these changes on the product selectivities (at 393 K, 15 bar, WHSV: 46 h^{-1}) at relatively high isobutene conversion exceeding 75 % on each of the catalyst. Accordingly, the catalysts provide a product distribution of olefins ranging from C_5 to C_{17+} (as provided in Table A2.2, in A2). These products were grouped according to the degree of oligomerization required to form them. The corresponding product groups are as follows: C_5-C_8 (mostly dimers, C_8, with cracking products in the range of C_5-C_7, this group represents gasoline fractions), C_9-C_{12} (mostly trimers, C_{12}, with cracking products in the range of C_9-C_{11}, this group represents middle distillate fractions), C_{13}-C_{16} (mostly tetramers, C_{16}, with cracking products in the range of C_{13}-C_{15} range) and C_{17+} (detailed results are tabulated in Table A2.2). Moreover, the true oligomer selectivities were also considered separately (C_8, C_{12}, and C_{16} products for dimers, trimers, and tetramers, respectively). Data provided in Figure 5.7A for true oligomer selectivities illustrate that C_8 selectivity increases from 15 to 30 wt% up to a TPA loading of 50 wt% and then remains almost constant. C_{12} selectivity shows a volcano type variation such that its selectivity decreases from 50 to 30 wt% up to a TPA loading of 30 wt%, and then it increases to 50 wt% as the loading increases to 90 wt%. C_{16} selectivity, on the other hand, presents an almost constant selectivity independent of TPA loading. Data presented in Figure 5.7B further show that the selectivity towards C_5-C_8 products increases from approximately 18 to 35 wt% with an increase in TPA loading from 1 to approximately 50 wt% and then remains almost constant. The selectivity for C_9-C_{12}, on the other hand, presents an opposite trend and decreases from approximately 70 to 45 wt% with an increase in TPA loading up to 50 wt% and subsequently increases to approximately 55 wt% upon an additional increase in TPA loading to 90 wt%. Selectivities for C_{13}-C_{16} and C_{17+} range products present decrease from approximately 15 to less than 8 wt% and from approximately 5 to 3 %, respectively, with increasing TPA loading. Furthermore, Figure 5.7 also represent the relative selectivities of C_{12}/C_8 (Figure 5.7C) and C_9-C_{12}/C_5-C_8 (Figure 5.7D) indicating the relative selectivities of trimers over dimers (middle distillate over gasoline). Data indicate that the catalysts become much more selective towards trimer formation, approximately four-times, as the loading decreases to 1 wt%. This result might be associated with the fact that the TPA structure becomes highly distorted at these very low loadings as discussed above.

Additionally, the lowest selectivity for C_9-C_{12} selectivity is obtained at 50 wt% loading of TPA where transition to multilayer from monolayer occurs. The true oligomer selectivities for C_8 and C_{12} are also related with TPA thickness such that monolayer produces more C_{12} fraction. Furthermore, relative selectivity of trimers over dimers decreases to an almost constant value of 1.5 as the multilayer forms. These results suggest that the TPA/MCM-41 catalyst is always more selective for trimers over dimers independent of TPA loading, and this selectivity increases as the loading decreases.

The vicinity of the active sites is an important parameter in oligomerization as shown by Bernauer et al. on propene oligomerization. Their results illustrated that turnover rates per Al(H^+) of close protons is 2-10 times higher over H-ZSM-5 catalysts. However, olefin adsorption, proton transfer, and propagation of oligomeric alkoxides are prohibited by close protons of a distance 5.0–5.5 Å and charged intermediates in void volume. On the other hand, while adsorption and intrinsic growth rate of oligomeric alkoxides are lower over close protons, instability of oligomeric alkoxides and H-bonded olefins because of the arrangement of close protons results in rapid desorption of products and shorter C–C bond formation [64]. Consistent with these results, the TPA/MCM-41 catalysts presented here also show a similar trend.

However, the decrease in TPA loading can also lead to various changes on the strength of acid sites as discussed above. Moreover, as our IR data show the TPA seems to undergo some strong structural distortions when monolayers present, especially below 30 wt% (Figure 5.4). Thus, we infer that not only an increase in the distance in between two neighboring TPA cluster at low loadings, but also the structural variations together with a change in the acid strength might be responsible for the high trimer selectivity at low loadings. Sarazen et al. studied the effects of confinement and acid strength on oligomerization performance over Brønsted acid sites. They concluded that higher reactivity of alkene chain growth is obtained in the presence of stronger acids for a given confinement because of carbenium ion stability while smaller voids promote shorter C–C bond formation [56, 65, 66].

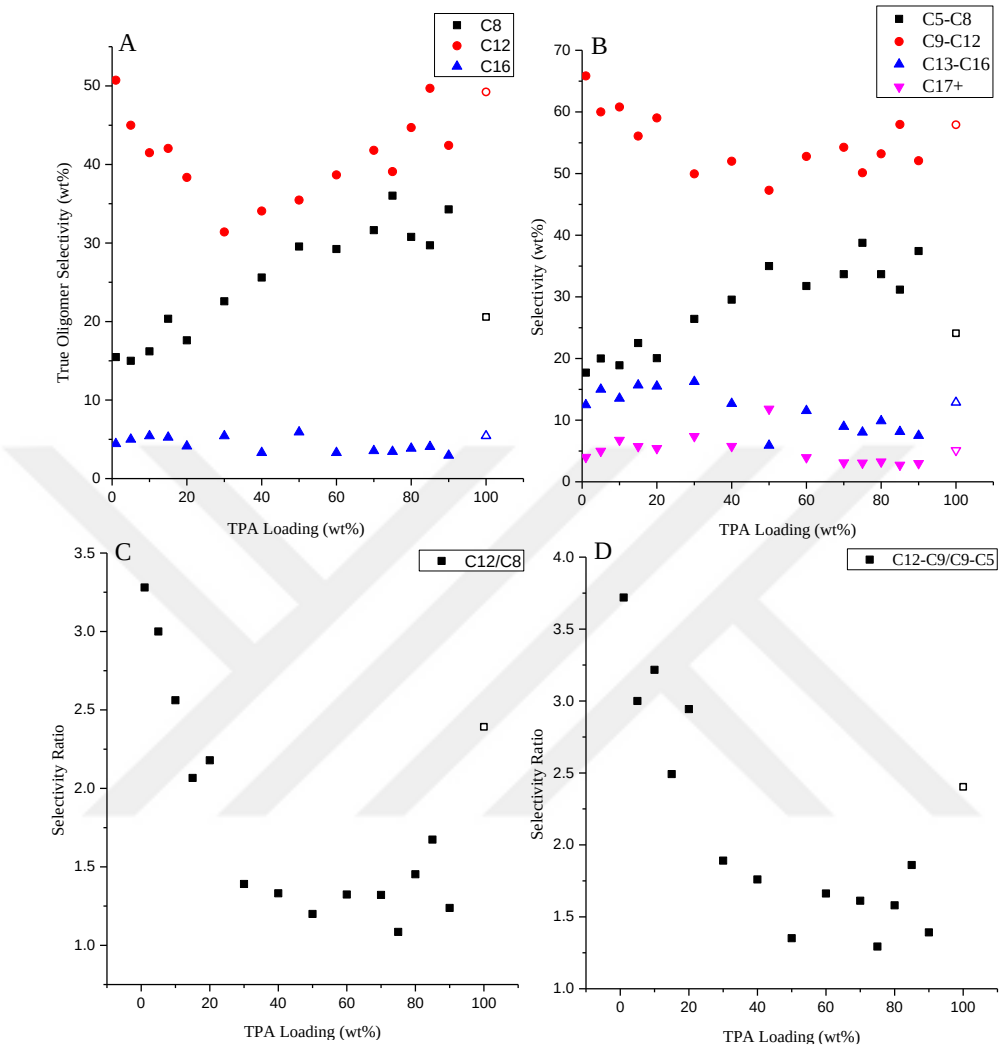

Figure 5.7. The variation of product selectivities with TPA loading: A) True oligomer selectivity; B) Overall selectivity; C) Relative selectivity of true oligomers, C_{12}/C_8; D) Relative selectivity for trimers over dimers, C_9-C_{12}/C_5-C_8. Data belonging to bulk TPA are shown in open symbols.

Aiming at elucidating the links between the acid characteristics of these catalysts and the corresponding selectivities, we considered the variation of the total product selectivities and true oligomer selectivities as well as the relative trimer selectivity with respect to dimers with changing acid strength and concentration.

For this purpose, we focused on variations of total and true oligomer selectivities with the amount of acid sites on LT and MT desorption region. Figure 5.8 illustrates that C_5-C_8 selectivity increases from 18 to 35 wt% almost linearly with the amount of acid sites calculated

from the area under the LT desorption peak (The area under the MT desorption peak for each catalyst do not provide any trend as shown in Figure A2.9). C_9-C_{12} selectivity presents an opposite trend such that its selectivity decreases from 70 to 45 wt% with an increase in the amount of LT acid sites. C_{13}-C_{16} and C_{17+} selectivities show a decrease from 15 to 8 wt% and from 5 to 3 wt% with an increase in the amount of acid sites, respectively. Similar to the case in Figures 5.7C and 5.7D, the relative selectivity of trimers over dimers represents a decreasing trend with increasing acid site density as shown in Figures 5.8C and 5.8D. These results confirm our conclusions regarding the dependency of the product selectivities on the acid site density. In order to rule out the presence of any effect of acid strength on the selectivities, we consider the variation of selectivities with LT desorption peak positions. Results presented in Figures 5.8E and 5.8F indicate that even though there is slight a variation in individual product selectivities with increasing LT peak positions, the trend is not strong enough to indicate a profound effect of acid strength on the selectivity. Here, we note that even though the acid strengths of the samples prepared by varying the TPA loading from 1 to 90 wt% are different from each other with a variation presented in Figure 5.6, the difference is not that significant to merit a strong influence on the product selectivity. Thus, we infer that for these TPA/MCM-41 samples the product selectivity is mainly determined by the vicinity of active sites, for which the catalysts become more selective towards distillate with an increase in the available space for each of the active center. These results are broadly consistent with the results of Bernauer et al. on propene oligomerization over H-ZSM-5 [66].

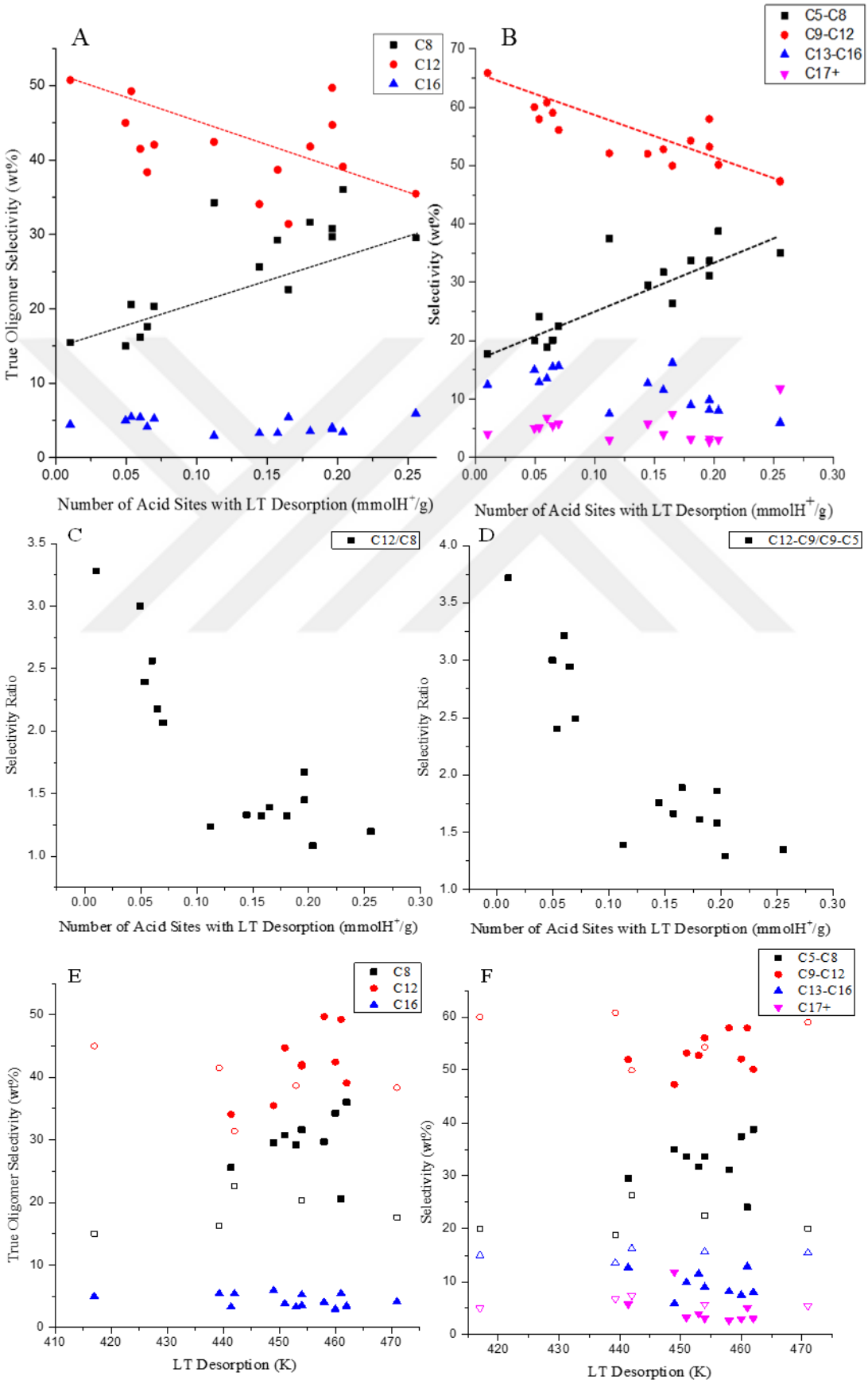
A
C8
C12
C16
True Oligomer Selectivity (wt%)
Number of Acid Sites with LT Desorption (mmolH+/g)
B
C5-C8
C9-C12
C13-C16
C17+
Selectivity (wt%)
Number of Acid Sites with LT Desorption (mmolH+/g)
C
C12/C8
Selectivity Ratio
Number of Acid Sites with LT Desorption (mmolH+/g)
D
C12-C9/C9-C5
Selectivity Ratio
Number of Acid Sites with LT Desorption (mmolH+/g)
E
C8
C12
C16
True Oligomer Selectivity (wt%)
LT Desorption (K)
F
C5-C8
C9-C12
C13-C16
C17+
Selectivity (wt%)
LT Desorption (K)

Figure 5.8. The variation of product selectivities by number of acid sites with LT desorption: A) True oligomer selectivity; B) Overall selectivity; C) Relative selectivity of true oligomers, C_{12}/C_8; D) Relative selectivity for trimers over dimers, C_9-C_{12}/C_5-C_8. The variation of product selectivities with LT desorption: E) True oligomer selectivity; F) Overall selectivity. Data belonging to LT positions that are not correlated with TPA loading are shown in open symbols. Data belonging to bulk TPA are shown in open symbols too.

5.1 Conclusion

Changes in structural properties of TPA/MCM-41 catalysts with the corresponding TPA loading from 1 to 90 wt% and their effects on isobutene oligomerization performance were investigated. The catalysts were characterized in detail by combining various techniques, BET, XRD, FTIR, and NH_3-TPD. IR results indicated that the TPA features shift to higher energies when the TPA is supported on MCM-41. This shift becomes more significant as the degree of dispersion increases, and thus, the interactions of the TPA clusters with the support become more significant, with a decrease in TPA loading. The consequences of these interactions on acid properties were investigated by NH_3-TPD analyses. Results illustrated that the acid strength of TPA varies significantly with a change in its loading amount on MCM-41. When the loading is fairly low, the data indicate a decrease in acid strength. Amount of acid sites, on the other hand, show a volcano type variation, such that acid capacity of supported catalysts increases until reaching monolayer coverage and then decreases. Consequences of these changes on the catalytic performance were investigated focusing on the oligomerization of isobutene in a once-through flow reactor. Results show that the TPA/MCM-41 catalyst provides an exceptional isobutene conversion rate. Data also present a strong dependence of the distillate/gasoline ratio in the product stream on the acid site density illustrating a significant advantage of MCM-41 support in the way of offering a high degree of dispersion thanks to its significantly high surface area.

References

[1] Sahu, R., et al., *A review of recent advances in catalytic hydrocracking of heavy residues.* Journal of Industrial and Engineering Chemistry, 2015. **27**: p. 12-24.

[2] Bogdan, V.I. and V.B. Kazanskii, *Isobutane Alkylation with Butenes and the Oligomerization of C4 Olefins in Supercritical Reagents.* Kinetics and Catalysis, 2005. **46**(6): p. 834-838.

[3] Zhang, J., et al., *Preferential oligomerization of isobutene in a mixture of isobutene and 1-butene over sodium-modified 12-tungstosilicic acid supported on silica.* Journal of Molecular Catalysis A: Chemical, 2010. **326**(1-2): p. 107-112.

[4] Kriván, E., I. Valkai, and J. Hancsók, *Investigation of Production of Motor Fuel Components on Heterogeneous Catalyst with Oligomerization.* Topics in Catalysis, 2013. **56**(9-10): p. 831-838.

[5] Nicholas, C.P., *Applications of light olefin oligomerization to the production of fuels and chemicals.* Applied Catalysis A: General, 2017. **543**: p. 82-97.

[6] Coetzee, J.H., et al., *An improved solid phosphoric acid catalyst for alkene oligomerization in a Fischer–Tropsch refinery.* Applied Catalysis A: General, 2006. **308**: p. 204-209.

[7] Prinsloo, N.M., *Solid phosphoric acid oligomerisation: Manipulating diesel selectivity by controlling catalyst hydration.* Fuel Processing Technology, 2006. **87**(5): p. 437-442.

[8] de Klerk, A., D.O. Leckel, and N.M. Prinsloo, *Butene Oligomerization by Phosphoric Acid Catalysis: Separating the Effects of Temperature and Catalyst Hydration on Product Selectivity.* Industrial & Engineering Chemistry Research, 2006. **45**(18): p. 6127-6136.

[9] Nkosi, B., F.T.T. Ng, and G.L. Rempel, *The oligomerization of 1-butene using NaY zeolite ion-exchanged with different nickel precursor salts.* Applied Catalysis A: General, 1997. **161**(1-2): p. 153-166.

[10] Bjørgen, M., et al., *1-Butene Oligomerization in Brönsted Acidic Zeolites: Mechanistic Insights from Low-Temperature in Situ FTIR Spectroscopy.* The Journal of Physical Chemistry B, 2004. **108**(23): p. 7862-7870.

[11] Villegas, J.I., et al., *A study on the dimerization of 1-butene over Beta zeolite.* Topics in Catalysis, 2007. **45**(1-4): p. 187-190.

[12] Oliveira, P., et al., *Light olefin transformation over ZSM-5 zeolites with different acid strengths – A kinetic model.* Applied Catalysis A: General, 2010. **384**(1-2): p. 177-185.

[13] Yoon, J., et al., *Trimerization of isobutene over a zeolite beta catalyst.* Journal of Catalysis, 2007. **245**(1): p. 253-256.

[14] Yoon, J.W., et al., *Trimerization of isobutene over zeolite catalysts: Remarkable performance over a ferrierite zeolite.* Catalysis Communications, 2007. **8**(6): p. 967-970.

[15] Zhang, X., et al., *Catalytic performance and characterization of Ni-doped HZSM-5 catalysts for selective trimerization of n-butene.* Fuel Processing Technology, 2009. **90**(7-8): p. 863-870.

[16] Yoon, J.W., S.H. Jhung, and J.-S. Chang, *Trimerization of Isobutene over Solid Acid Catalysts: Comparison between Cation-exchange Resin and Zeolite Catalysts.* Bulletin of the Korean Chemical Society, 2008. **29**(2): p. 339-341.

[17] Hauge, K., et al., *Oligomerization of isobutene over solid acid catalysts.* Catalysis Today, 2005. **100**(3-4): p. 463-466.

[18] Yoon, J.W., et al., *Trimerization of Isobutene over Solid Acid Catalysts under Wide Reaction Conditions.* Bulletin of the Korean Chemical Society, 2007. **28**(11): p. 2075-2078.

[19] Gee, J.C. and S.T. Williams, *Dimerization of linear olefins on Amberlyst® 15: Effects of chain length and double-bond position.* Journal of Catalysis, 2013. **303**: p. 1-8.

[20] Lee, J.S., et al., *Trimerization of isobutene over WOx/ZrO2 catalysts.* Applied Catalysis A: General, 2009. **366**(2): p. 299-303.

[21] Coelho, A., et al., *1-Butene oligomerization over ZSM-5 zeolite: Part 1 – Effect of reaction conditions.* Fuel, 2013. **111**: p. 449-460.

[22] Bekker, R. and N.M. Prinsloo, *Butene Oligomerization over Phosphoric Acid: Structural Characterization of Products.* Industrial & Engineering Chemistry Research, 2009. **48**(22): p. 10156-10162.

[23] Kim, Y.T., et al., *Low-temperature oligomerization of 1-butene with H-ferrierite.* Journal of Catalysis, 2015. **323**: p. 33-44.

[24] Lavrenov, A.V., et al., *Heterogeneous oligomerization of light alkenes: 80 years in oil refining.* Catalysis in Industry, 2016. **8**(4): p. 316-327.

[25] Antunes, B.M., et al., *Alkenes oligomerization with resin catalysts.* Fuel Processing Technology, 2015. **138**: p. 86-99.

[26] Jhung, S.H. and J.-S. Chang, *Trimerization of Isobutene Over Solid Acid Catalysts.* Catalysis Surveys from Asia, 2009. **13**(4): p. 229-236.

[27] Izumi, Y., *Acid catalysis of silica-included heteropolyacid in polar reaction media.* Applied Catalysis A: General, 1999. **181**(2): p. 277-282.

[28] Okuhara, T., N. Mizuno, and M. Misono, *Catalysis by heteropoly compounds—recent developments.* Applied Catalysis A: General, 2001. **222**(1-2): p. 63-77.

[29] Kamiya, Y., et al., *Catalytic Chemistry of Supported Heteropolyacids and Their Applications as Solid Acids to Industrial Processes.* Catalysis Surveys from Asia, 2008. **12**(2): p. 101-113.

[30] Kozhevnikov, I.V., et al., *Study of catalysts comprising heteropoly acid H3PW12O40 supported on MCM-41 molecular sieve and amorphous silica.* Journal of Molecular Catalysis A: Chemical, 1996. **114**(1-3): p. 287-298.

[31] Popa, A., V. Sasca, and J. Halasz, *Catalytic properties of molecular sieves MCM41 type doped with heteropolyacids for ethanol oxidation.* Applied Surface Science, 2008. **255**(5): p. 1830-1835.

[32] Kozhevnikov, I.V., *Heterogeneous acid catalysis by heteropoly acids: Approaches to catalyst deactivation.* Journal of Molecular Catalysis A: Chemical, 2009. **305**(1-2): p. 104-111.

[33] Wu, Y., et al., *Heterogenization of Heteropolyacids: A General Discussion on the Preparation of Supported Acid Catalysts.* Industrial & Engineering Chemistry Research, 1996. **35**(8): p. 2546-2560.

[34] Timofeeva, M.N., *Acid catalysis by heteropoly acids.* Applied Catalysis A: General, 2003. **256**(1-2): p. 19-35.

[35] Pizzio, L.R., C.V. Cáceres, and M.N. Blanco, *Acid catalysts prepared by impregnation of tungstophosphoric acid solutions on different supports.* Applied Catalysis A: General, 1998. **167**(2): p. 283-294.

[36] Yang, W., et al., *H3PW12O40 supported on Cs modified mesoporous silica: catalytic activity in n-butane isomerisation and in situ FTIR study.* Catalysis Today, 2002. **73**(1-2): p. 153-165.

[37] Barton, D.G., S.L. Soled, and E. Iglesia, *Solid acid catalysts based on supported tungsten oxides.* Topics In Catalysis, 1998. **6**(1-4): p. 87-99.

[38] Zhang, J., et al., *Preferential oligomerization of isobutene in mixtures of isobutene and 1-butene over 12-tungstosilicic acid supported on silica.* Applied Catalysis A: General, 2009. **353**(1): p. 68-73.

[39] Madhusudhanrao, P., et al., *Immobilization of molecular H3PW12O40 heteropolyacid catalyst in alumina-grafted silica-gel and mesostructured SBA-15 silica matrices.* Journal of Catalysis, 2005. **232**(1): p. 210-225.

[40] Kozhevnikov, I.V., S. Holmes, and M.R.H. Siddiqui, *Coking and regeneration of H3PW12O40/SiO2 catalysts.* Applied Catalysis A: General, 2001. **214**(1): p. 47-58.

[41] Blasco, T., et al., *Supported heteropolyacid (HPW) catalysts for the continuous alkylation of isobutane with 2-butene: The benefit of using MCM-41 with larger pore diameters.* Journal of Catalysis, 1998. **177**(2): p. 306-313.

[42] Corma, A., A. Martínez, and C. Martínez, *Acidic Cs+, NH4+, and K+Salts of 12-Tungstophosphoric Acid as Solid Catalysts for Isobutane/2-butene Alkylation.* Journal of Catalysis, 1996. **164**(2): p. 422-432.

[43] Méndez, F.J., et al., *Mesoporous catalysts based on Keggin-type heteropolyacids supported on MCM-41 and their application in thiophene hydrodesulfurization.* Fuel, 2013. **110**: p. 249-258.

[44] Verhoef, M.J., et al., *A study on the stability of MCM-41-supported heteropoly acids under liquid- and gas-phase esterification conditions.* Microporous and Mesoporous Materials, 1999. **27**(2-3): p. 365-371.

[45] Sushkevich, V.L., V.V. Ordomsky, and I.I. Ivanova, *Isoprene synthesis from formaldehyde and isobutene over Keggin-type heteropolyacids supported on silica.* Catalysis Science & Technology, 2016. **6**(16): p. 6354-6364.

[46] Zhang, J., et al., *Changes in Surface Acidity of Silica-Supported Dodecatungstosilicic Acid in Relation to the Loading Amount.* The Journal of Physical Chemistry C, 2011. **115**(30): p. 14762-14769.

[47] Ghanbari-Siahkali, A., et al., *The acidity and catalytic activity of heteropoly acid on MCM-41 investigated by MAS NMR, FTIR and catalytic tests.* Applied Catalysis A: General, 2000. **192**(1): p. 57-69.

[48] Sayari, A., *Catalysis by Crystalline Mesoporous Molecular Sieves.* Chemistry of Materials, 1996(8): p. 1840-1852.

[49] Wilson, K. and J.H. Clark, *Solid acids and their use as environmentally friendly catalysts in organic synthesis.* Pure and Applied Chemistry, 2000. **72**(7).

[50] Taguchi, A. and F. Schüth, *Ordered mesoporous materials in catalysis.* Microporous and Mesoporous Materials, 2005. **77**(1): p. 1-45.

[51] Kozhevnikov, I.V., et al., *New acid catalyst comprising heteropoly acid on a mesoporous molecular sieve MCM-41.* Catalysis Letters, 1994. **30**(1-4): p. 241-252.

[52] Newman, A.D., et al., *Structural studies of high dispersion H3PW12O40/SiO2 solid acid catalysts.* Phys Chem Chem Phys, 2006. **8**(24): p. 2893-902.

[53] Wenxing Kuang, A.R., Michel Fournier, Robert Hubaut, *Structure and reactivity of silica-supported 12-tungstophosphoric acid.* Applied Catalysis A: General, 2003. **250**(2): p. 221-229.

[54] Berry, F.J., et al., *Silica-supported silicotungstic acid: A study by X-ray photoelectron spectroscopy.* Materials Chemistry and Physics, 2009. **114**(2-3): p. 1000-1003.

[55] Olivier-Bourbigou, H., et al., *Comparison of the Acidity of Heteropolyacids Encapsulated in or Impregnated on SBA-15.* Oil & Gas Science and Technology – Revue d'IFP Energies nouvelles, 2016. **71**(2): p. 25.

[56] Sarazen, M.L., E. Doskocil, and E. Iglesia, *Catalysis on solid acids: Mechanism and catalyst descriptors in oligomerization reactions of light alkenes.* Journal of Catalysis, 2016. **344**: p. 553-569.

[57] Yoon, J.W., et al., *Oligomerization of isobutene over aluminum chloride-loaded USY zeolite catalysts.* Journal of Porous Materials, 2009. **16**(6): p. 631-634.

[58] Yoon, J.W., et al., *Oligomerization of isobutene over dealuminated Y zeolite catalysts.* Applied Catalysis A: General, 2008. **337**(1): p. 73-77.

[59] Yoon, J.W., et al., *Trimerization of isobutene over cation exchange resins: Effect of physical properties of the resins and reaction conditions.* Journal of Molecular Catalysis A: Chemical, 2006. **260**(1-2): p. 181-186.

[60] Alcántara, R., et al., *Trimerization of isobutene over Amberlyst-15 catalyst.* Reactive and Functional Polymers, 2000. **45**(1): p. 19-27.

[61] Mantilla, A., et al., *Oligomerization of isobutene on sulfated titania: Effect of reaction conditions on selectivity.* Catalysis Today, 2005. **107-108**: p. 707-712.

[62] Chen, G., et al., *Surface-appropriate lipophobicity—Application in isobutene oligomerization over Teflon-modified silica-supported 12-silicotungstic acid.* Applied Catalysis A: General, 2006. **310**: p. 16-23.

[63] Tzompantzi, F., et al., *IMPROVED SELECTIVITY TO C8-OLEFINS FOR ISOBUTENE OLIGOMERIZATION ON NIO-W_2O_3/Al_2O_3CATALYSTS.* Chemical Engineering Communications, 2009. **196**(10): p. 1198-1205.

[64] Bernauer, M., et al., *Proton proximity – New key parameter controlling adsorption, desorption and activity in propene oligomerization over H-ZSM-5 zeolites.* Journal of Catalysis, 2016. **344**: p. 157-172.

[65] Sarazen, M.L. and E. Iglesia, *Experimental and theoretical assessment of the mechanism of hydrogen transfer in alkane-alkene coupling on solid acids.* Journal of Catalysis, 2017. **354**: p. 287-298.

[66] Sarazen, M.L., E. Doskocil, and E. Iglesia, *Effects of Void Environment and Acid Strength on Alkene Oligomerization Selectivity.* ACS Catalysis, 2016. **6**(10): p. 7059-7070.

Chapter 6

CONCLUSIONS

Cracking units of refineries, delayed coking and fluid catalytic cracking unit, produce valuable products ranging from gasoline to diesel by processing heavier feedstocks. In these processes, gaseous products containing considerable amount of olefins are also produced. These gaseous unsaturated components are utilized in LPG fractions or petrochemical industry. Thus, a recent trend is to develop new technologies to convert these undervalued gaseous fractions to more valuable liquid products to be able to use them in gasoline, distillate, and diesel pools.

Alkylation and oligomerization are widely used technologies to produce liquid products from gaseous olefins. However, alkylation process uses olefins and paraffins as a feedstock and produces only gasoline range products over very strong acids HF or H_2SO_4. Oligomerization, on the other hand, is flexible process about both feedstocks (C_2-C_4 range olefins) and product distribution (gasoline, distillate and diesel). Various types of solid acids, such as solid phosphoric acid, zeolites, and cation exchange resins are used for the oligomerization process. However, they have some drawbacks, such as corrosion and disposal, high operating conditions, low thermal stability respectively. Keggin type heteropolyacids (HPAs) are new candidates offering strong acidity and tunable redox and acidic properties. However, because they have very low surface area, they are impregnated on high surface area supports. Among these supports, silica is the most widely used one to preserve the heteropolyacid structure because of the weakly interaction with Keggin anion. Thus, the acid properties and the consequent catalytic performances of HPAs on these supports can be varied simply by changing the corresponding HPA loading.

In the first part of this thesis study, a screening study on different HPAs (TSA, TPA and MPA) supported on different silica-based supports (SiO_2, SBA-15 and MCM-41) at various loading amounts was performed. Results of isobutene oligomerization at identical reaction conditions (393 K, 15 bar and WHSV: 46 h^{-1}) showed that the product selectivity can be varied by changing the heteropolyacid type, support type, and heteropolyacid loading. In order to

understand the relationships between the structural parameters of the catalysts and the catalytic performance in more detail, one family of catalysts were selected, TPA/MCM-41 for deeper analysis. TPA/MCM-41 catalysts illustrated that the selectivity towards distillate to gasoline ratio decreased with TPA loading at high conversion values.

In the second part, TPA was supported on MCM-41 support at varying loadings from 1 to 90 wt%.Then they were characterized by BET, XRD, FTIR, and NH_3-TPD analyses. XRD analyses showed the presence of interactions between TPA and MCM-41 supports, especially at lower loadings than 50 wt%, monolayers. These interactions were supported by IR analyses showing the band shifts from pristine TPA when TPA was supported on MCM-41. These band shifts were more significant at low loadings indicating that more interaction occurs. The effects of these interactions on acid properties of the catalysts were investigated by NH_3-TPD analyses. Data indicated that the strength of acid sites decreased at low loadings of TPA. Amount of acid sites, on the other hand, showed a volcano type trend such that the amount of acid sites increased up to monolayer coverage and then decreased. Consequences of these changes on the catalytic performance were investigated on oligomerization of isobutene. Results showed that high conversion values were provided even at a very high WHSV value of 46 h^{-1}. Trimer to dimer ratio decreased from 4 to 1.5 with increasing TPA loading from 1 wt%. Distillate to gasoline ratio, on the other hand, was found to be strongly correlated with the acid site density illustrating the significance of high surface area and high degree of dispersion capability of MCM-41. Results presented in this thesis offer broad potential for utilizing HPAs on high surface area mesoporous supports to have high catalytic performance that can be simply be tuned by the choice of HPA, its loading and the support type.

For a future work, relationship between catalyst structural parameters and oligomerization reaction performance may be studied for other type of olefins (1-butene, cis-2-butene, trans-2-butene and propylene) existed in LPG fractions. These will provide to design a catalyst producing desired product distributions under desired conversions from refinery LPG fractions.

Chapter A1

THE SCREENING STUDY - APPENDIX

A1.1 Pristine HPAs

The pristine HPAs were characterized in detail by NH_3-TPD, FTIR, and TGA analysis.

A1.1.1 Characterization of pristine HPAs

TGA was used to analyze the thermal stabilities of pristine HPAs. Figure A1.1 showed the results of the TGA measurements of three different pristine HPA excluding isothermal period at 373 K for 4 h to eliminate water content.

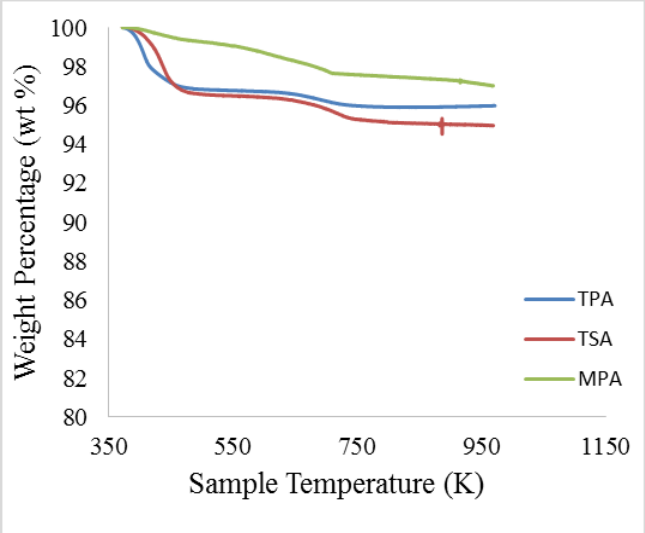

Figure A1.1. TGA analyses of different heteropolyacids.

According to the TGA results, TPA has the highest thermal stability, while MPA had the lowest one supported by literature [1]. The weight loss at approximately 450 K is still considered as water content in literature [2].

NH_3-TPD analyses of pristine HPAs, TPA, TSA, and MPA, were performed by the procedure identified in experimental method, in Chapter 3. Figure A1.2 showed the NH_3-TPD results of pristine HPAs.

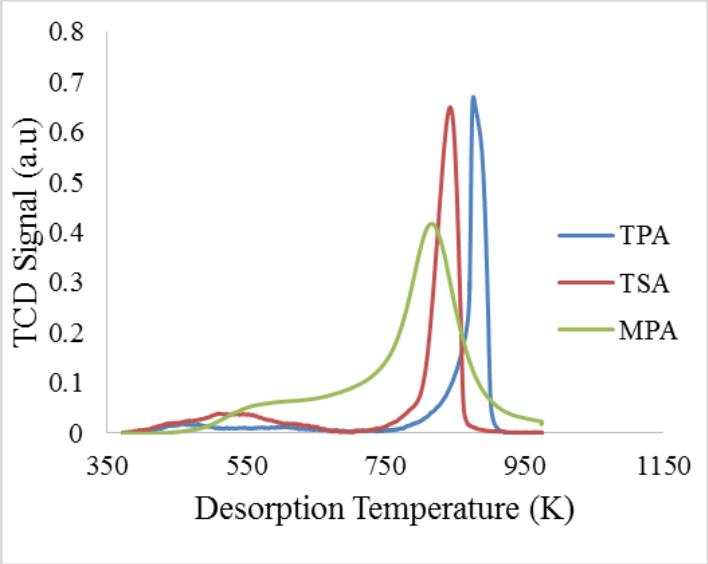

Figure A1.2. NH_3-TPD analyses of pristine heteropolyacids.

NH_3-TPD analyses of bulk heteropolyacids show a very sharp peak between 750 and 900 K region and very small broad peak between 450 and 650 K. These high temperature sharp peaks will be considered as decomposed acid sites of TPA in the following chapters after screening study section.

Fourier transform infrared (FT-IR) spectra of HPAs stated in Figure A1.3 show the features of TPA at 1081, 996,894 and 751 cm^{-1} corresponding the typical antisymmetrical stretching vibrations of $\upsilon_{as}(P–O_a)$, $\upsilon_{as}(W=O_d)$, $\upsilon_{as}(W–O_b–W)$, and $\upsilon_{as}(W–O_c–W)$ bands [3], for TSA antisymmetrical stretching vibrations of 979, 926, 879 and 782 cm^{-1} $\upsilon_{as}(W=O_d)$, $\upsilon_{as}(Si–O_a)$, $\upsilon_{as}(W–O_c–W)$, and $\upsilon_{as}(W–O_b–W)$[4] and for MPA stretching vibrations at 006, 995, 920-896, 800, 620 and 245-214 cm^{-1} assigned to $\upsilon_s(M=O_t)$, $\upsilon_{as}(M=O_t)$, $\upsilon_s(M–O_b–M)$, $\upsilon_s(M–O_c–M)$, and $\upsilon_s(M–O_a)$, respectively (as shown in Figure A1.3 in the fingerprint region from 700 to 1400 cm^{-1})[5].

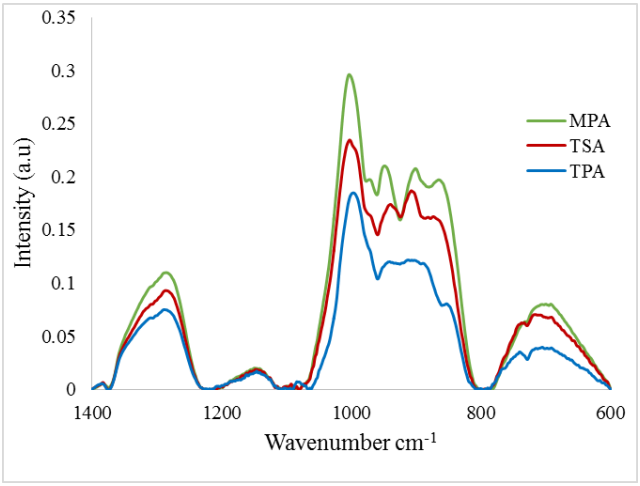

Figure A1.3. FTIR spectra of pristine heteropolyacids.

A1.2 Isobutene Oligomerization Performance of Pristine TPA

Oligomerization of isobutene was performed over unsupported TPA. All liquid products were analyzed by GC-Simdis analyzer with respect to their boiling point temperatures. Results, in Table A1.1, were reported as weight percentages at certain boiling point temperatures. Products were grouped as C_5-C_8, C_9-C_{12}, and C_{12+} selectivities. Additionally, gasoline and distillate selectivities were also reported. Catalytic performances were evaluated according to these selectivities and conversion values. Table A1.1 showed reaction results over pristine TPA.

Table A1.1. Isobutene oligomerization over pristine TPA

C_5-C_8 wt%	C_9-C_{12} wt%	C_{12+} wt%	Gasoline wt%	Distillate wt%	D/G	Conversion %
23.9	54.8	21.3	41.0	60.0	1.5	32

According to the results, conversion value was found to be very low compared with the corresponding supported catalyst results below. Oligomerization is a surface type reaction and unsupported heteropolyacid has very low surface area [1]. Thus, low conversion is expected result.

A1.2 Supported HPAs

A1.2.1 Supported TSA

TSA was supported on SiO_2, SBA-15, and MCM-41 at different loading amounts. TSA loading effect on catalytic properties and isobutene oligomerization reaction performance was investigated. Isobutene oligomerization reactions were performed at identical operating conditions, 393 K, 15 bar and WHSV:46 h^{-1}.

A1.2.1.1 Characterization of Supported TSA

TSA was supported on SiO_2 with various loadings. NH_3-TPD and FTIR spectroscopy analysis were performed.

SiO_2 Supported

Figure A1.4 showed the NH_3-TPD analysis of SiO_2-supported TSA catalysts. Acid strength and amount of acid sites were analyzed as defined methodology in Chapter 3.

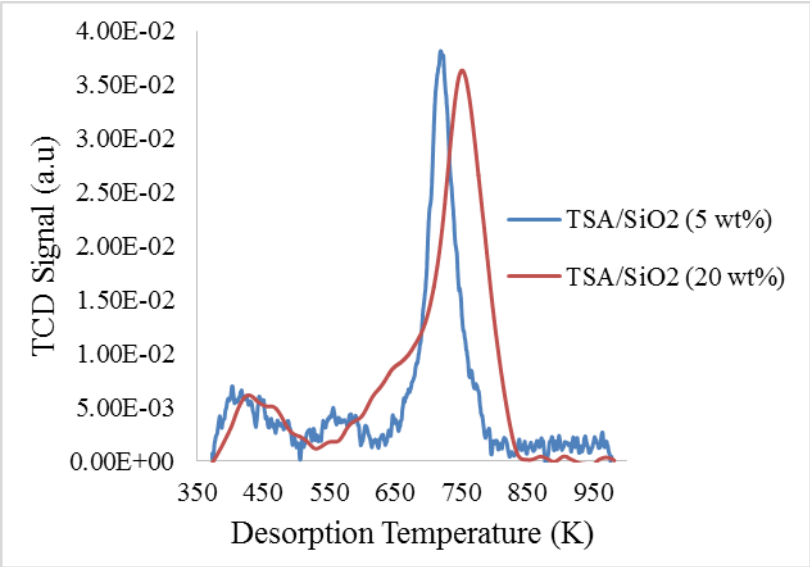

Figure A1.4. NH_3-TPD analyses of SiO_2 supported TSA.

Table A1.2 showed desorption peak positions and the amount of acid sites calculated from peaks areas under the curves with NH_3 calibration.

Table A1.2. NH_3-TPD analyses of SiO_2 supported TSA (TSA/SiO_2).

Catalyst	LT* K	MT** K	HT*** K	LT $mmolNH_3/g$	MT $mmolNH_3/g$	HT $mmolNH_3/g$
TSA/SiO_2 (5 wt%)	411.3	567.6	719.5	0.059	0.030	0.253
TSA/SiO_2 (20 wt%)	443.0	-	758.0	0.068	-	0.446

* Low Temperature Peak, ** Medium Temperature Peak, *** High Temperature Peak

According to the results, three separate peaks were observed at approximately 450, 600, and 800 K regions for supported HPAs that were different from pristine TSA suggesting the interaction between TSA and surface hydroxyl group of silica [6]. Studies reported that formation of $Si–OH^{2+}$ surface species lowered strength of acids with regard to the strong Brønsted acid sites of bulk HPA [6]. These newly formed peaks at lower temperature regions were called weaker acid sites compared with bulk HPA [6]. Zhang et al. reported three peaks 550, 660 and 750 K as weak, medium and strong bulk acid sites for TSA/SiO_2 [7]. In here, desorption peak temperatures were called as low temperature (LT), medium temperature (MT) and high temperature acid sites (HT). High temperature acid sites were not considered in the following sections after Chapter 4 screening studies, because temperature was higher than decomposition temperature of TPA.

FTIR analyses of SiO_2 supported TSA catalysts were given in Figure A1.5. Results showed that the fingerprint bands of heteropolyacid as 979, 926, 879, and 782 cm^{-1} with respect to $\upsilon_{as}(W=O_d)$, $\upsilon_{as}(Si–O_a)$, $\upsilon_{as}(W–O_c–W)$, and $\upsilon_{as}(W–O_b–W)$ were apparent. The results illustrated that when the TSA supported on SiO_2, there were band shifts changing with loading amount. These shifts supported the chemical interactions between the HPAs and the supports.

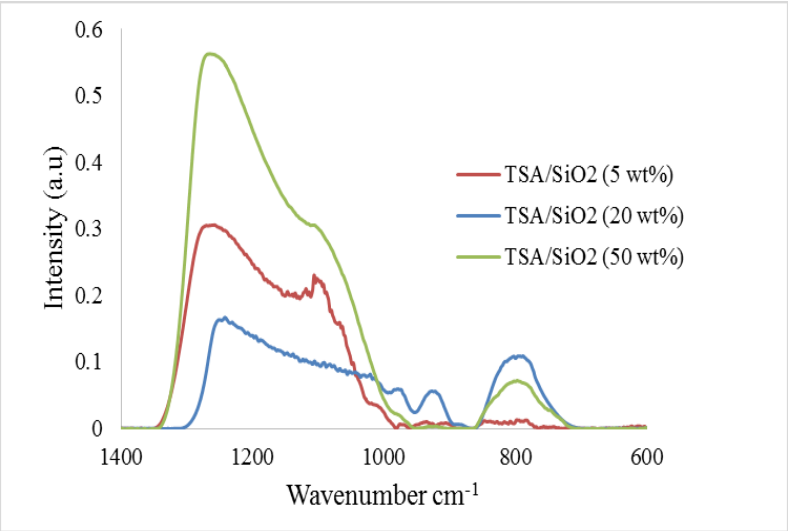

Figure A1.5. FTIR spectra of SiO_2 supported TSA.

SBA-15 Supported

TSA was supported on SBA-15 at various loadings. NH_3-TPD and FTIR spectroscopy analysis were performed to determine structural properties. BET analyses of catalysts were also conducted to determine the effect of HPA loading on the surface area and pore volume of SBA-15 support.

NH_3-TPD analyses of TSA supported SBA-15 were given in Figure A1.6.

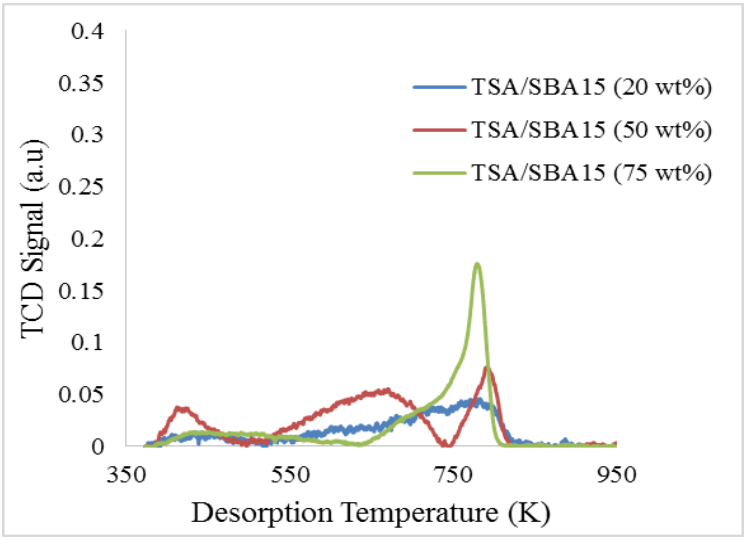

Figure A1.6. NH_3-TPD Analyses of SBA-15 Supported TSA.

Table A1.3 shows the peak position temperatures and amount of acid sites calculated from areas under curves according to three separate peaks. Results illustrated that amount of acid sites calculated from first peak area increased with HPA loading.

Table A1.3. NH_3-TPD analyses of SBA-15 supported TSA (TSA/SBA-15).

Catalyst	L.T K	M.T K	H.T K	L.T mmolNH_3 /g	M.T mmolNH_3 /g	H.T mmolNH_3 /g
TSA/SBA-15 (20 wt%)	453.2	631.5	736.2	0.047		0.346
TSA/SBA-15 (50 wt%)	425.1	644.1	791.4	0.113	0.380	0.152
TSA/SBA-15 (75 wt%)	485.8	718.5	783.5	0.272		1.050

FTIR analysis of supported TSA on SBA-15 with the loadings from 5% to 75 wt % were shown in Figure A1.7. Results showed that fingerprint bands of heteropolyacid as 979, 926, 879, and 782 cm^{-1} with respect to $\upsilon_{as}(W{=}O_d)$, $\upsilon_{as}(Si{-}O_a)$, $\upsilon_{as}(W{-}O_c{-}W)$, and $\upsilon_{as}(W{-}O_b{-}W)$ were still apparent.

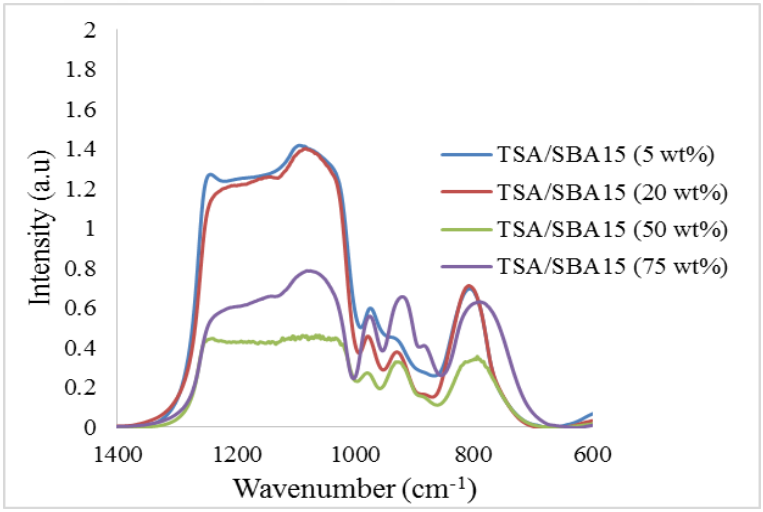

Figure A1.7. FTIR Spectra of SBA-15 Supported TSA.

Intensity values were not related to HPA loadings that may be because of the sample amount used in FTIR analyses. Band shifts represented the chemical interaction between support and heteropolyacid.

BET analyses of catalysis were also carried out. Results were shared in Table A1.4. Both BET surface area and pore volume decreased with heteropolyacid loading as expected.

Table A1.4. BET analyses of SBA-15 supported Tungstosilicic Acid (TSA/SBA-15).

Catalyst	BET Surface Area m^2/g	Pore Volume cm^3/g	Pore Size nm
TSA/SBA-15(20 wt%)	1022.4	0.84	3.31
TSA/SBA-15(50 wt%)	486.1	0.69	5.68
TSA/SBA-15(75 wt%)	144.1	0.15	4.28

MCM-41 Supported

Tungstosilicic acid was supported on MCM-41 at various loadings. NH_3-TPD and FTIR spectroscopy analysis were performed to determine catalyst properties. BET analysis of catalysts were also conducted.

NH_3-TPD analysis of MCM-41 supported tungstosilicic acid were performed. Results were given as per gram supported heteropolyacid in Figure A1.8 and Table A1.5.

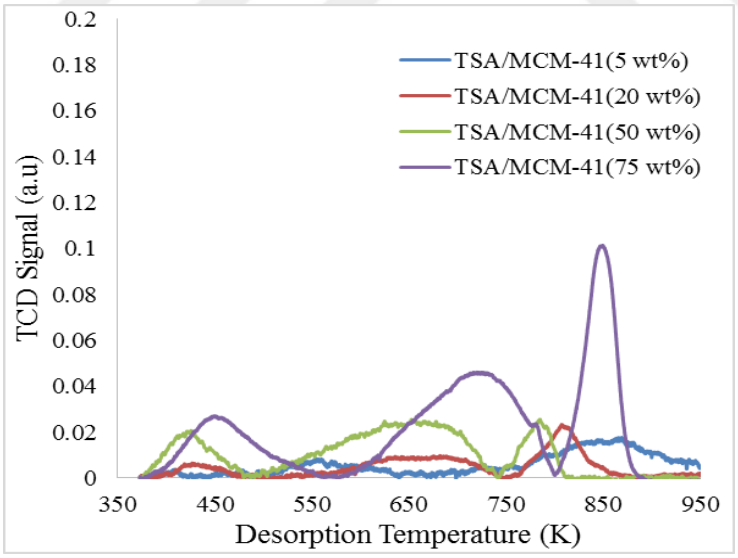

Figure A1.8. NH_3-TPD Analyses of MCM-41 Supported TSA.

Table A1.5. NH_3-TPD analyses of MCM-41 supported TSA (TSA/MCM-41).

Catalyst	L.T K	M.T K	H.T K	L.T mmolNH_3 /g	M.T mmolNH_3 /g	H.T mmolNH_3 /g
TSA/MCM-41(5 wt%)	405.2	566.2	854.2	0.018	0.077	0.303
TSA/MCM-41(20 wt%)	433.1	658.8	808.4	0.028	0.104	0.083
TSA/MCM-41(50 wt%)	424.9	642.2	783.2	0.132	0.409	0.104
TSA/MCM-41(75 wt%)	458.6	713.5	848.7	0.186	0.426	0.262

NH_3-TPD analyses showed that first peak temperature increased with increasing TSA ratio in catalyst with an exception of TSA/MCM-41(50 wt%). Amount of acid sites in first peak area increased with loading on the other hand.

FTIR analyses of supported heteropolyacid were done and shown in Figure A1.9. Fingerprint peaks as 979, 926, 879 and 782 cm^{-1} with respect to $\upsilon_{as}(W{=}O_d)$, $\upsilon_{as}(Si{-}O_a)$, $\upsilon_{as}(W{-}O_c{-}W)$ and $\upsilon_{as}(W{-}O_b{-}W)$ existed.

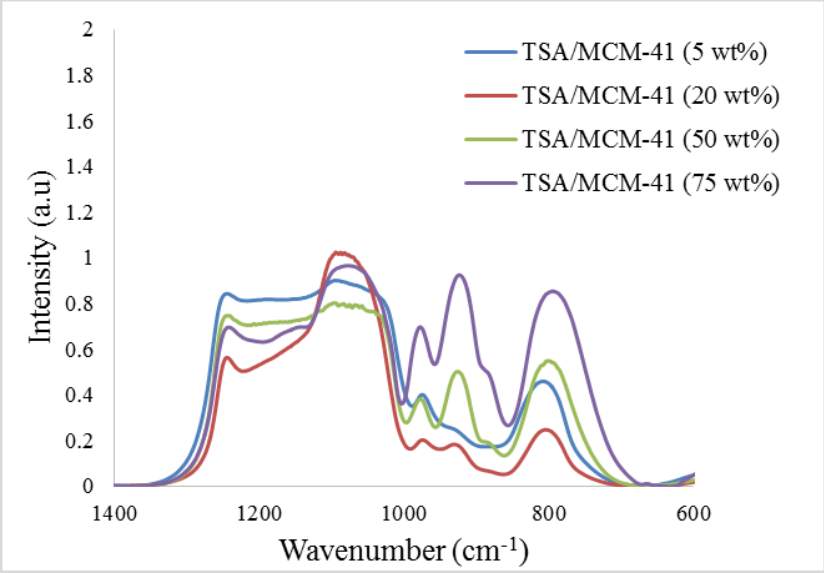

Figure A1.9. FTIR Spectra of MCM-41 Supported TSA.

BET analyses of MCM-41 supported TSA were resulted as expected such that BET surface area and pore volume decreased with heteropolyacid loading given in Table A1.6.

Table A1.6. BET analyses of MCM-41 supported TSA (TSA/MCM-41).

Catalyst	BET Surface Area m^2/g	Pore Volume cm^3/g	Pore Size nm
TSA/MCM-41(5 wt%)	838.4	0.69	3.33
TSA/MCM-41(20 wt%)	735.7	0.60	3.31
TSA/MCM-41(50wt%)	391.8	0.31	3.26
TSA/MCM-41(75 wt%)	139.8	0.10	3.10

A1.2.1.2 Isobutene Oligomerization Reaction Performance on Supported TSA

SiO_2 Supported

Reaction performances of varying loadings of TSA on SiO_2 catalysts were investigated. Reaction selectivities were evaluated according to three cut points with respect to C_5-C_8 (309-387K), C_9-C_{12} (387-458K) and C_{12+} hydrocarbons (>458 K). Additionally, gasoline and distillate cut points were evaluated at a temperature from 309 to 448 K and higher than 448 K respectively. Table A1.7 showed isobutene oligomerization performance over TSA/SiO_2 catalysts.

Table A1.7. Isobutene oligomerization over SiO_2 supported TSA (TSA/SiO_2).

Catalyst	C_5-C_8 wt%	C_9-C_{12} wt%	C_{12+} wt%	Gasoline wt%	Distillate wt%	D/G	Conversion
TSA/SiO_2 (5wt%)	19.0	51.5	29.5	38.2	61.8	1.6	75
TSA/SiO_2 (20 wt%)	13.5	50.5	36.0	32.4	67.6	2.1	73
TSA/SiO_2 (50 wt%)	15.7	35.7	48.5	36.7	63.3	1.7	74

Figure A1.10 showed the reaction selectivity related to C_5-C_8, C_9-C_{12} and C_{12+} from bottom to top part of columns respectively over TSA/SiO_2 catalysts. Gasoline and distillate selectivity were also shown as from bottom part to top respectively. Conversion values were shown with dots.

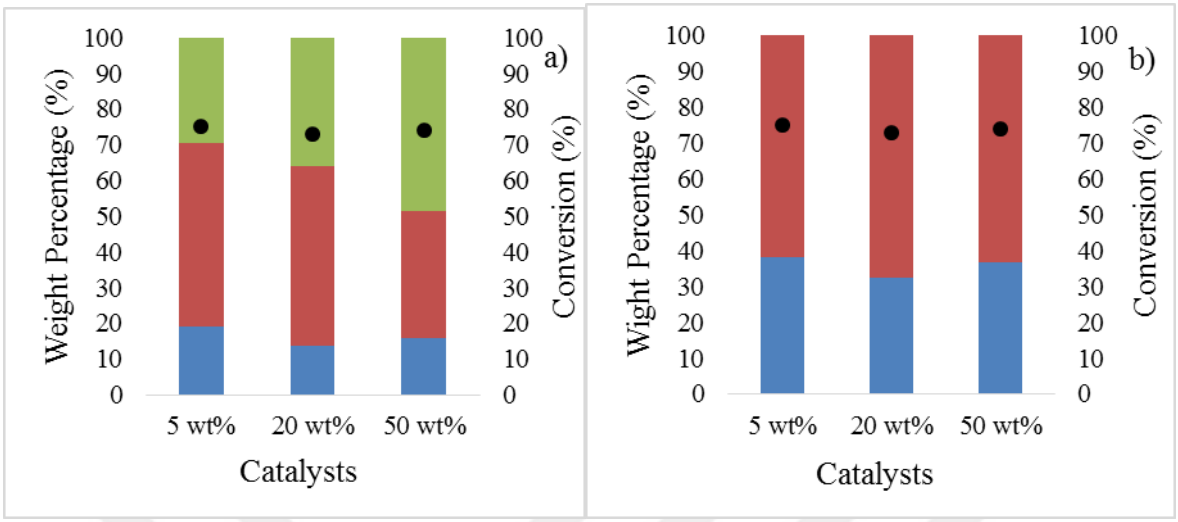

Figure A1.10. C_5-C_8, C_9-C_{12} and C_{12+} selectivity (a) and Gasoline, Distillate selectivity (b)

According to results, conversion values were similar and highest distillate/gasoline ratio was obtained over TSA/SiO_2 (20 wt%) catalyst. Lower distillate/gasoline ratios obtained over both TSA/SiO_2 (5 wt%) and TSA/SiO_2 (50 wt%). Results in Figure A1.10 also showed that while C_5-C_8 selectivity was highest, C_{12+} selectivity was the lowest on TSA/SiO_2 (5 wt%) catalyst among prepared catalysts. For TSA/SiO_2 (50 wt%), since the catalyst has lowest surface area, highest amount of acid sites and highest acid strength, cracking reactions may be triggered. Although C_{12+} selectivity was highest, a considerable amount of C_5-C_8 selectivity existed that may be because of cracking reactions. Figure A1.11 showed GC-Simdis curve of TSA/SiO_2 (5 wt%) and TSA/SiO_2 (50 wt%) to explain cracking reactions more clearly.

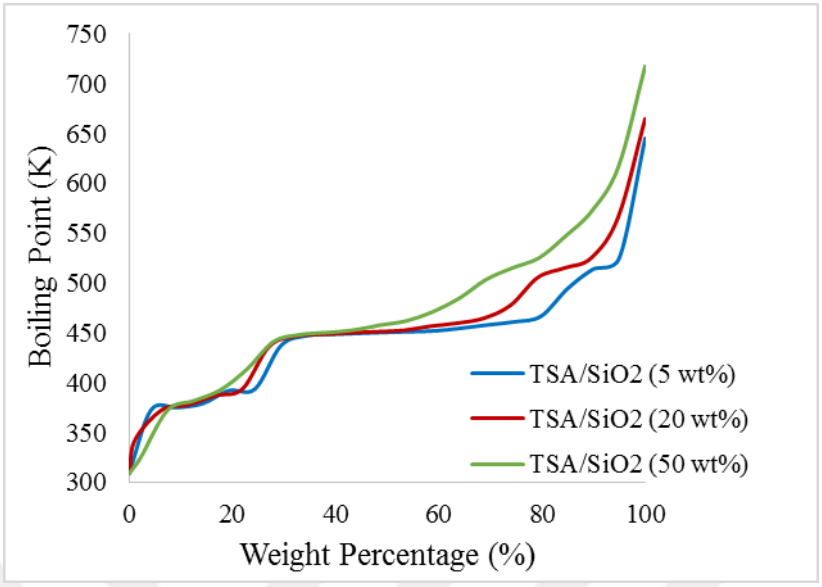

Figure A1.11. GC-Simdis Curve Analysis of TSA/SiO_2 Catalysts Reaction Products.

As can be seen from Figure 4A.7, more cracking reactions occurred with TSA/SiO_2 (50 wt%) catalyst. Staircase trend was expected when there were no cracking reactions. On the other hand, close to staircase trend was obtained by TSA/SiO_2 (5 wt%) catalyst that was corroborative trend for the discussion above.

SBA-15 Supported

Oligomerization of isobutene performance was also investigated by supported TSA on SBA-15 with different loading amount of TSA. Table A1.8 showed the reaction performances at identical operating conditions. Reaction selectivity was calculated with respect to three cut points which were stated above as C_5-C_8 (309-387 K), C_9-C_{12} (387-458 K) and C_{12+} (>458 K) hydrocarbons. Additionally, gasoline and distillate cut points were reported for a temperature from 309 to 448 K and higher than 448 K respectively.

Table A1.8. Isobutene oligomerization over SBA-15 supported TSA (TSA/SBA-15).

Catalyst	C_5-C_8 wt%	C_9-C_{12} wt%	C_{12+} wt%	Gasoline wt%	Distillate wt%	D/G	Conversion
TSA/SBA-15(5 wt%)	19.8	55.0	25.2	37.9	62.1	1.6	91
TSA/SBA-15(20 wt%)	16.9	41.7	41.4	40.2	59.8	1.5	94
TSA/SBA-15(50 wt%)	26.6	48.3	25.1	43.0	57.0	1.3	86
TSA/SBA-15(75 wt%)	24.3	45.3	31.0	48.5	51.5	1.1	88

Reaction selectivity related to C_5-C_8, C_9-C_{12}, and C_{12+} were shown in Figure A1.12 from bottom to top part of columns respectively. Gasoline and distillate selectivity were also shown from bottom part to top respectively. Conversion values were shown in secondary axis with dots.

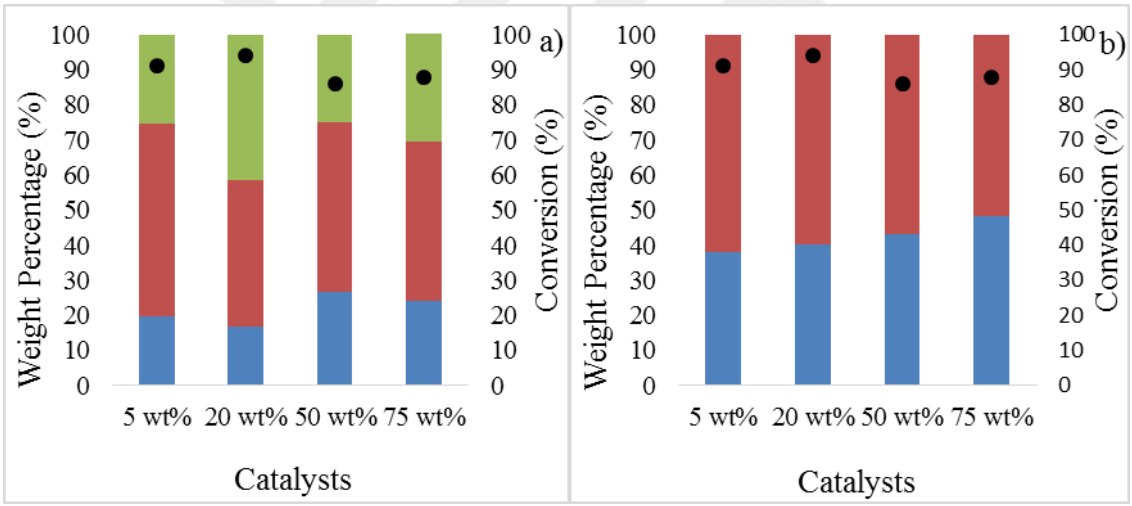

Figure A1.12. C_5-C_8, C_9-C_{12} and C_{12+} selectivity (a) and Gasoline, Distillate selectivity (b).

According to results, varying selectivities for each fraction (C_5-C_8, C_9-C_{12} and C_{12+}) were obtained at comparable conversion values. Firstly, distillate over gasoline ratio decreased with increasing TSA loading. Results were different from SiO_2 supported TSA, that was may be because of high surface area of SBA-15. Since SiO_2 has very low surface area compared with SBA-15, surface area and amount of acid sites per unit area may also have significance effect on reaction selectivity. NH_3-TPD results showed that amount of acid sites increased with TSA

loading. Distillate amount, on the other hand, decreased with heteropolyacid loading. When the amount of acid sites increased, more active sites were close to each other. Hydrocarbon chain may not become longer because of lowered surface area. Commenting on selectivities for cut points of C_5-C_8, C_9-C_{12} and C_{12+} may not elucidate trends obtained, so more cut points should be specified to explain trends accurately.

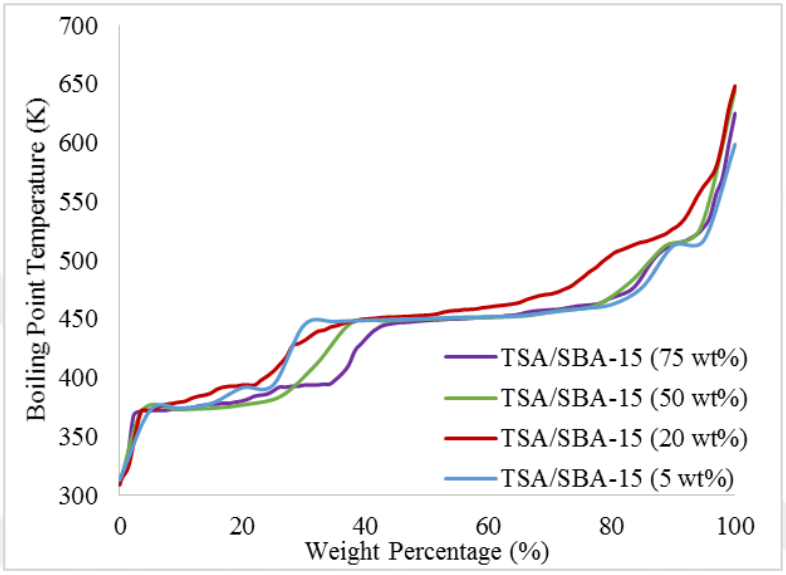

Figure A1.13. GC-Simdis Curve Analysis of TSA/SBA-15 Catalysts Reaction Products.

Figure A1.13 showed GC-Simdis curve of reaction products to observe craking products more clearly.

MCM-41 Supported

Isobutene oligomerization on MCM-41 supported tungstosilicic acid was investigated at identical reaction conditions. Selectivity was again calculated with identical method such that three cut points as C_5-C_8 (309-387K), C_9-C_{12} (387-458K) and C_{12+} (>458K). Additionally, gasoline and distillate cut points were taken as temperature between 309 and 448K and higher than 448K respectively.

Table A1.9. Isobutene oligomerization over MCM-41 supported TSA (TSA/MCM-41).

Catalyst	C_5-C_8 wt%	C_9-C_{12} wt%	C_{12+} wt%	Gasoline wt%	Distillate wt%	D/G	Conversion
TSA/MCM-41(5 wt%)	35.2	48.8	16.0	45.4	54.6	1.2	90
TSA/MCM-41(20 wt%)	27.6	50.0	22.5	47.1	52.9	1.1	82

Reaction selectivity related to C_5-C_8, C_9-C_{12} and C_{12+} were shown in Figure A1.14 from bottom to top part of columns respectively. Gasoline and distillate selectivity were also shown as from bottom to top respectively. Conversion values were shown in secondary axis with dots.

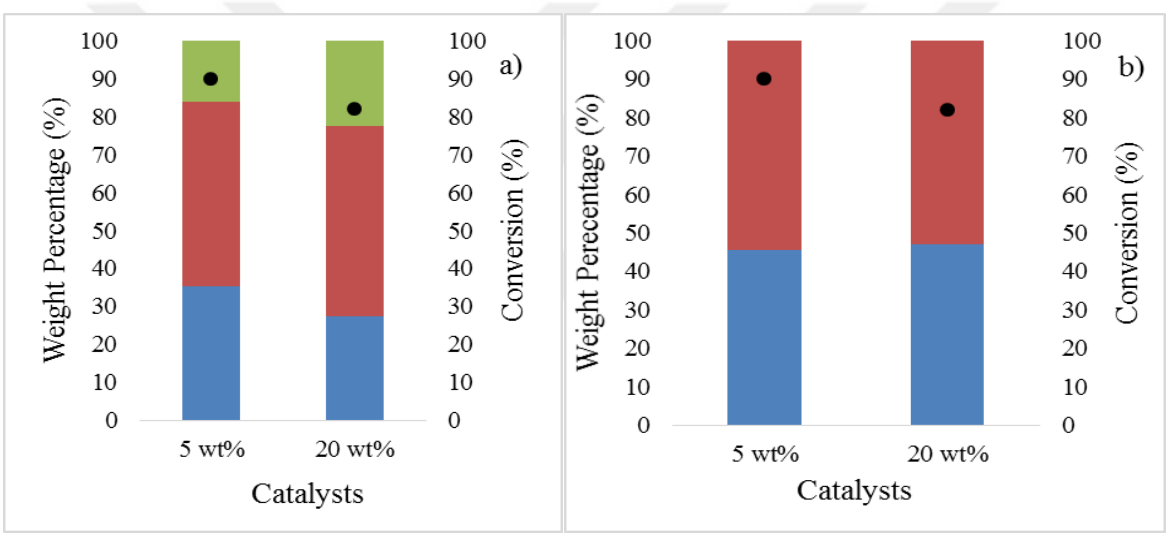

Figure A1.14. C_5-C_8, C_9-C_{12} and C_{12+} selectivity (a) and Gasoline, Distillate selectivity (b).

Data indicated that C_5-C_8 selectivity decreased with heteropolyacid loading, while C_{12+} increased.

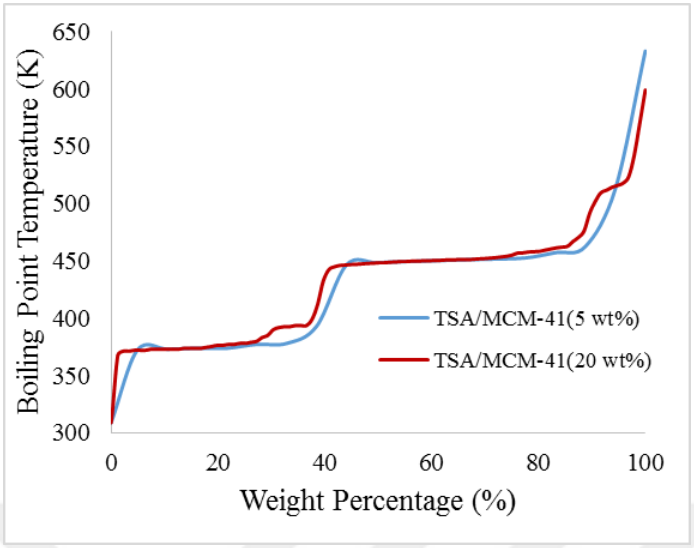

Figure A1.15. GC-Simdis curve analysis of TSA/MCM-41 catalysts reaction products.

GC-Simdis curves of reaction products also showed that low amount of C_5-C_8 range products were produced by TSA/MCM-41(20 wt%) catalyst.

A1.2.2 Supported TPA

A1.2.2.1 Characterization of Supported TPA

TPA was supported on SiO_2, SBA-15 and MCM-41 with varying loadings. Heteropolyacid loading effect on catalyst properties and reaction performance was investigated.

SiO_2 Supported

TPA was supported on SiO_2 at various loadings. NH_3-TPD and FTIR spectroscopy analysis were performed to determine catalyst properties.

NH_3-TPD analyses of SiO_2 supported tungstophosphoric acid were conducted. Peak positions and area under curves illustrated an alteration. Figure A1.16 showed NH_3-TPD results of SiO_2 supported TPA catalysts.

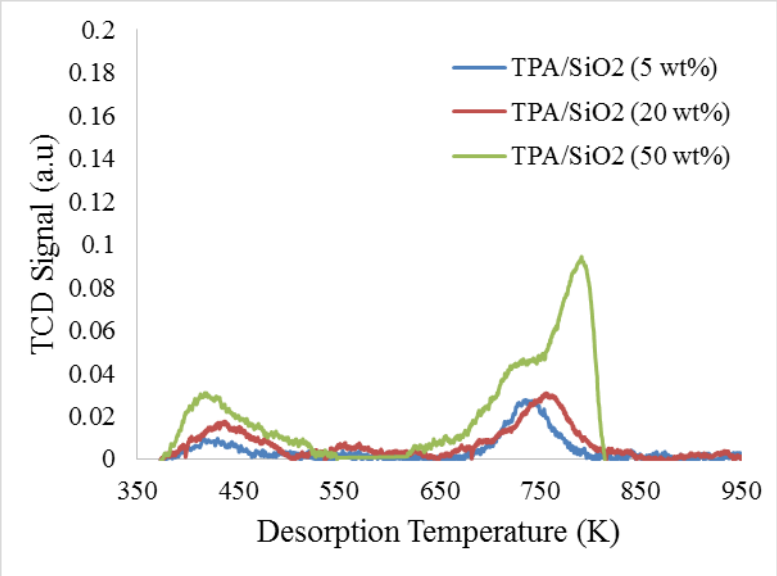

Figure A1.16. NH_3-TPD analyses of SiO_2 supported TPA.

Amount of acid sites calculated from first peak area changed with respect to heteropolyacid loading. As can be seen from Table A1.10 amount of acid sites increased with the loading amount of TPA on SiO_2 support.

Table A1.10. NH_3-TPD analyses of SiO_2 supported TPA (TPA/SiO_2).

Catalyst	L.T K	M.T K	H.T K	L.T mmolNH_3/g	M.T mmolNH_3/g	H.T mmolNH_3/g
TPA/SiO_2 (5 wt%)	429.9		738.3	0.074		0.203
TPA/SiO_2 (20 wt%)	437.6	568.8	756.1	0.147	0.065	0.256
TPA/SiO_2 (50 wt%)	434.3		789.8	0.332		0.864

FTIR analyses of SiO_2 supported TPA were given in Figure A1.17. Fingerprint bands of TPA as antisymmetrical stretching vibrations of $\upsilon_{as}(P–O_a)$, $\upsilon_{as}(W=O_d)$, $\upsilon_{as}(W–O_b–W)$, and $\upsilon_{as}(W–O_c–W)$ were apparent. Band shifts existed because of chemical interaction between heteropolyacid and host material.

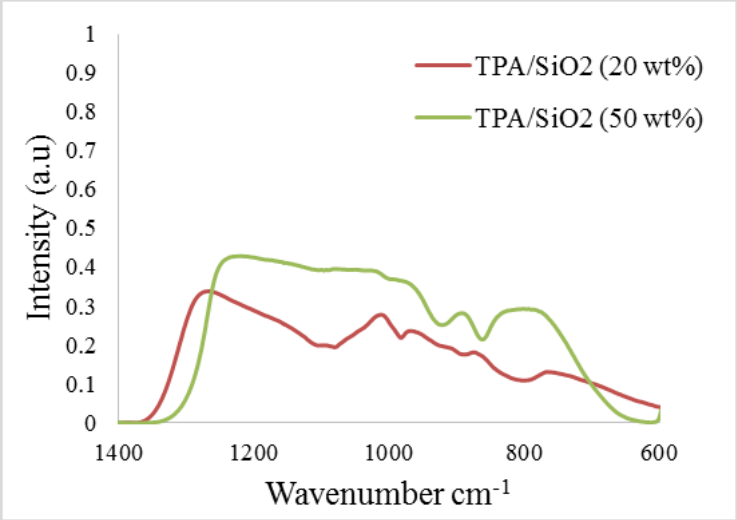

Figure A1.17. FTIR spectra of SiO_2 supported TPA.

SBA-15 Supported

TPA was supported on SBA-15 at various loadings. NH_3-TPD and FTIR spectroscopy analysis were performed to determine catalyst properties.

NH_3-TPD analyses of SBA-15 supported TPA were performed. Results were shown in Figure A1.18 and Table A1.11.

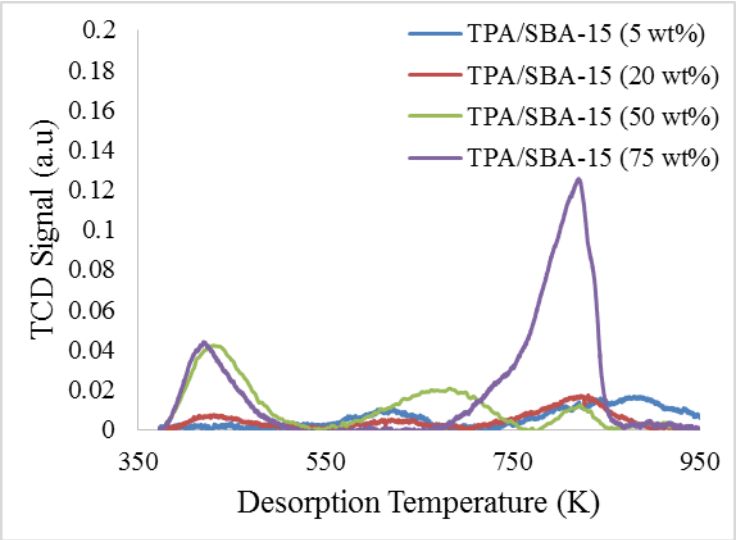

Figure A1.18. NH_3-TPD analyses of SBA-15 supported TPA.

Table A1.11. NH_3-TPD analyses of SBA-15 supported TPA (TPA/SBA-15).

Catalyst	L.T K	M.T K	H.T K	L.T mmolNH_3 /g	M.T mmolNH_3 /g	H.T mmolNH_3 /g
TPA/SBA-15(5 wt%)	421.3	618.8	885.2	0.016	0.102	0.276
TPA/SBA-15(20 wt%)	437.2	624.3	820	0.070	0.045	0.183
TPA/SBA-15(50 wt%)	433.9	670.3	819.7	0.386	0.301	0.061
TPA/SBA-15(75 wt%)	421.3	-	819.6	0.336	-	0.964

Data indicated that both peak temperatures and amount of acid sites changed with respect to TPA loading.

FTIR analyses of SBA-15 supported TPA showed the fingerprint bands of tungstophosphoric acid that are 1081, 996,894 and 751 cm^{-1} corresponding to typical antisymmetrical stretching vibrations of $\upsilon_{as}(P–O_a)$, $\upsilon_{as}(W=O_d)$, $\upsilon_{as}(W–O_b–W)$, and $\upsilon_{as}(W–O_c–W)$ bonds. Data shown in Figure A1.19 indicated that band shifts from their positon supported interactions between TPA and SBA-15.

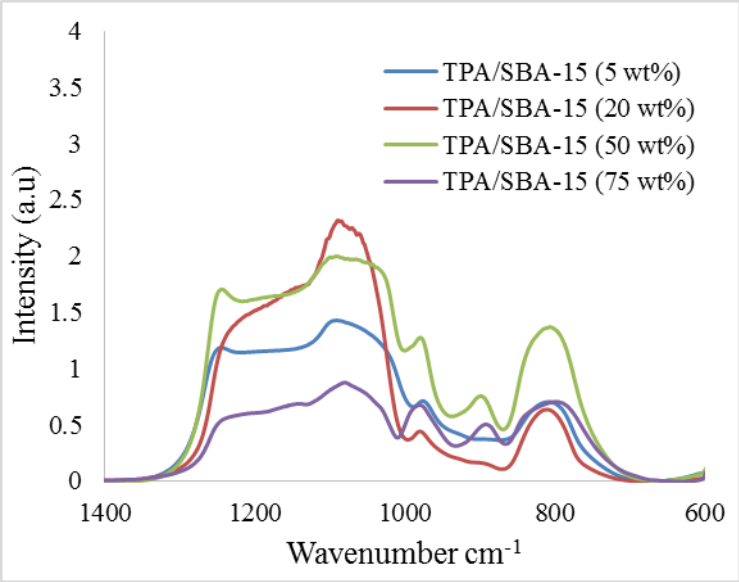

Figure A1.19. FTIR spectra of SBA-15 supported TPA.

MCM-41 Supported

TPA was supported on MCM41 at various loadings. FTIR spectroscopy and NH_3-TPD analysis were performed to determine catalyst properties.

NH_3-TPD analyses of MCM41 supported TPA catalysts were performed. Changes in peak positions and concentration of acid sites were provided in Figure A1.20.

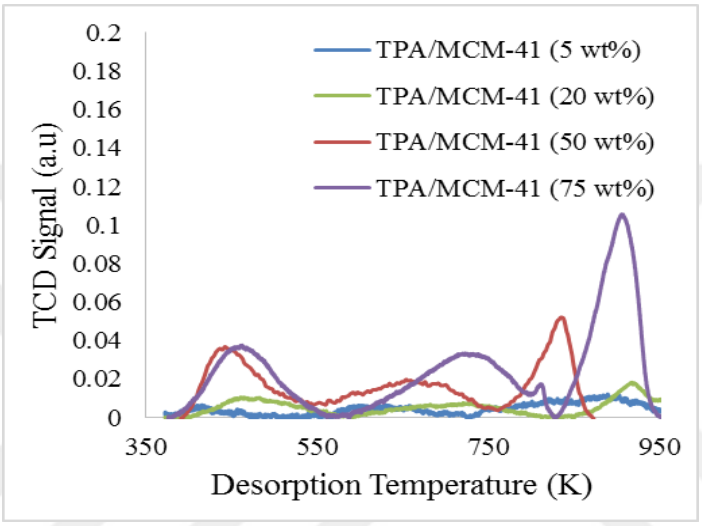

Figure A1.20. NH_3-TPD analyses of MCM-41 supported TPA.

NH_3-TPD results stated in Table A1.12 indicated that first peak temperature increased with TPA loading. On the other hand, amount of acid sites calculated from first peak area presented increasing trend up to 50 wt % loading and then decreased.

Table A1.12. NH_3-TPD analyses of SBA-15 supported TPA (TPA/MCM-41).

Catalyst	L.T K	M.T K	H.T K	L.T mmolNH_3 /g	M.T mmolNH_3 /g	H.T mmolNH_3 /g
TPA/MCM-41(5 wt%)	416.9	602.1	854.7	0.028	0.067	0.205
TPA/MCM-41(20 wt%)	417.2	703.7	918.6	0.077	0.068	0.053
TPA/MCM-41(50 wt%)	449.1	694.1	835.5	0.295	0.186	0.285
TPA/MCM-41(75 wt%)	462.4	727.4	906.9	0.242	0.320	0.419

FTIR analyses of MCM-41 supported TPA were stated in Figure A1.21. Fingerprint bands of TPA as 1081, 996,894 and 751 cm^{-1} corresponding to typical antisymmetrical stretching vibrations of $\upsilon_{as}(P–O_a)$, $\upsilon_{as}(W=O_d)$, $\upsilon_{as}(W–O_b–W)$, and $\upsilon_{as}(W–O_c–W)$ bonds were apparent. Band shifts indicating interaction between TPA and MCM-41 corresponding to TPA loading presented.

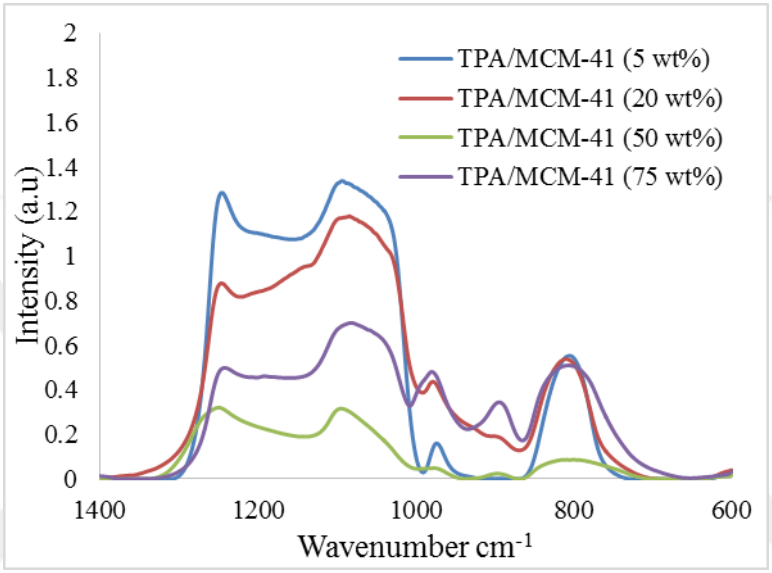

Figure A1.21. FTIR spectra of MCM-41 supported TPA.

BET analysis of MCM-41 supported TPA were tabulated in Table A1.13. Results presented that BET surface area and pore volume decreased with TPA loading.

Table A1.13. BET Analyses of MCM-41 Supported TPA.

Catalyst	BET Surface Area m^2/g	Pore Volume cm^3/g
TPA/MCM-41(5 wt%)	838.1	0.006
TPA/MCM-41(20 wt%)	689.7	0.029
TPA/MCM-41(50 wt%)	376.7	0.132
TPA/MCM-41(75 wt%)	97.1	0.772

A1.2.2.2 Isobutene Oligomerization Reaction Performance on Supported TPA

SiO_2 Supported

Reaction performances of SiO_2 supported TPA catalysts were investigated under identical operating conditions. Reaction selectivity was evaluated according to three cut points which were related to C_5-C_8 (309-387K), C_9-C_{12} (387-458K) and C_{12+} (>458K). Additionally, gasoline and distillate cut point were taken as temperature from 309 to 448 K and higher than 448 K respectively.

Table A1.14. Isobutene oligomerization over SiO_2 supported TPA (TPA/SiO_2).

Catalyst	C_5-C_8 wt%	C_9-C_{12} wt%	C_{12+} wt%	Gasoline wt%	Distillate wt%	D/G	Conversion
TPA/SiO_2 (5 wt%)	21.0	51.1	27.8	39.3	60.7	1.5	95
TPA/SiO_2 (20 wt%)	16.1	47.5	36.3	36.7	63.3	1.7	87
TPA/SiO_2 (50 wt%)	18.6	41.1	40.3	38.0	62.0	1.6	89

Figure A1.22 showed the reaction selectivity related to C_5-C_8, C_9-C_{12} and C_{12+} from bottom to top part of columns respectively. Gasoline and distillate selectivity were also shown as from bottom to top respectively. Conversion values were shown with dots.

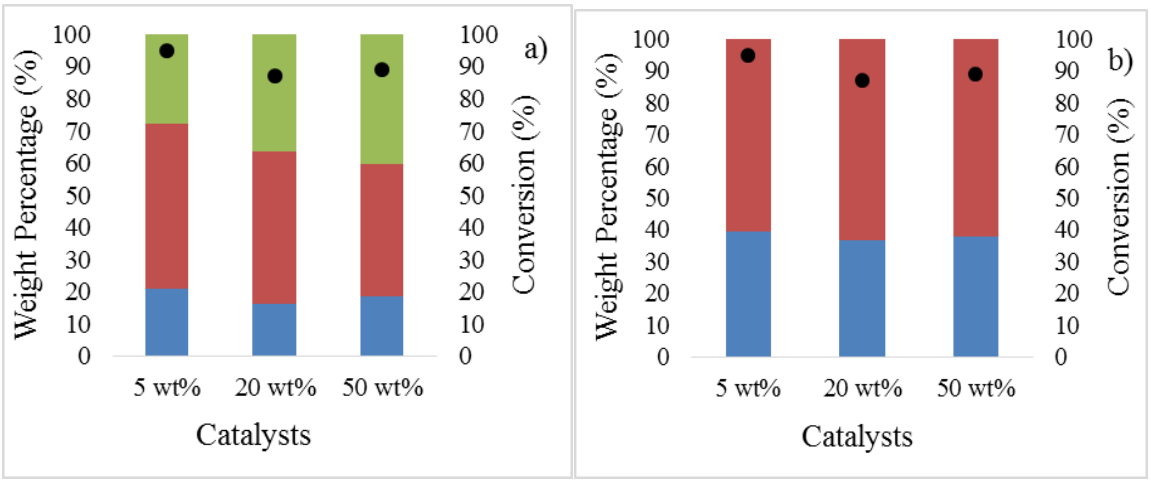

Figure A1.22. C_5-C_8, C_9-C_{12} and C_{12+} selectivity (a) and Gasoline, Distillate selectivity (b).

According to results, there were no apparent differences between distillate over gasoline ratio and conversion values. However, detailed data illustrated that C_{12+} selectivity increased with heteropolyacid loading clearly.

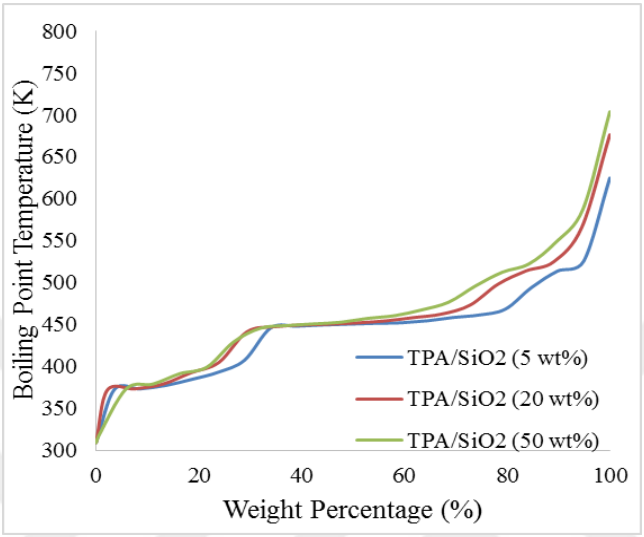

Figure A1.23. GC-Simdis curve analysis of TPA/SiO_2 catalysts reaction products.

Figure A1.23 represented cracking reactions over all catalysts. Cracking reactions increased with heteropolyacid loading that may be because of low surface area.

SBA-15 Supported

Reaction performances of SBA-15 supported TPA catalysts were investigated under identical operating conditions. Reaction selectivity was evaluated according to three cut points which were related to C_5-C_8 (309-387K), C_9-C_{12} (387-458K) and C_{12+} (>458K). Additionally, gasoline and distillate cut point were taken as temperature from 309 to 448 K and higher than 448 K respectively. Table A1.15 showed the isobutene oligomerization performances of SBA-15 supported TPA catalysts.

Table A1.15. Isobutene oligomerization over SBA-15 supported TPA (TPA/SBA-15).

Catalyst	C_5-C_8 wt%	C_9-C_{12} wt%	C_{12+} wt%	Gasoline wt%	Distillate wt%	D/G	Conversion
TPA/SBA-15(5 wt%)	31.6	53.8	14.5	45.6	54.4	1.2	81
TPA/SBA-15(20 wt%)	16.6	48.9	34.5	39.1	60.9	1.6	75
TPA/SBA-15(50 wt%)	38.3	43.9	17.8	47.8	52.2	1.1	85
TPA/SBA-15(75 wt%)	29.2	43.6	27.1	47.5	52.5	1.1	50

Figure A1.24 showed the reaction selectivity related to C_5-C_8, C_9-C_{12} and C_{12+} from bottom to top part of columns respectively. Gasoline and distillate selectivity were also shown as from bottom to top respectively. Conversion values were shown with dots.

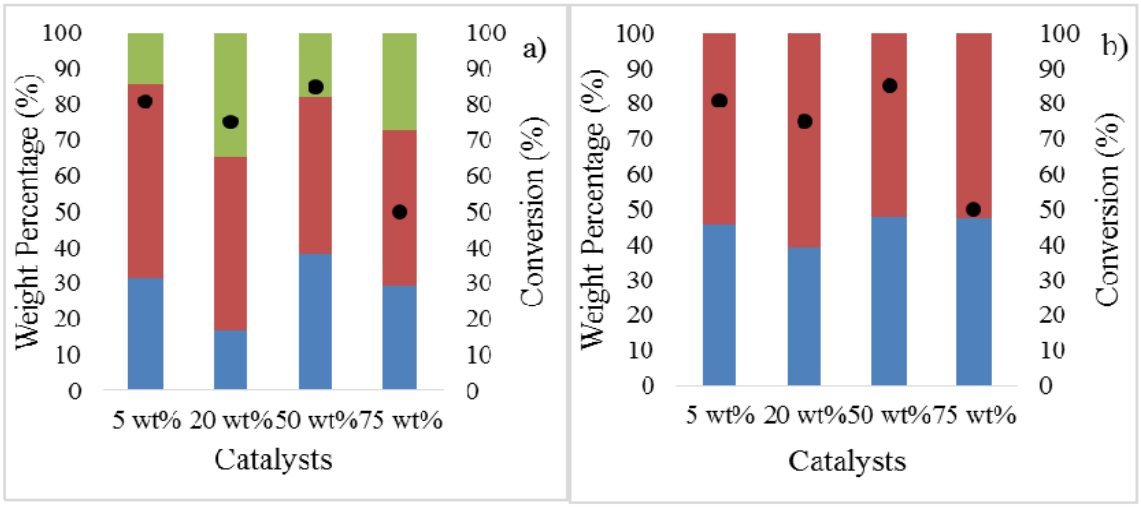

Figure A1.24. C_5-C_8, C_9-C_{12} and C_{12+} selectivity (a) and Gasoline, Distillate selectivity (b).

Results showed that TPA/SBA-15(20 wt%) catalyst was more selective towards distillate range products.

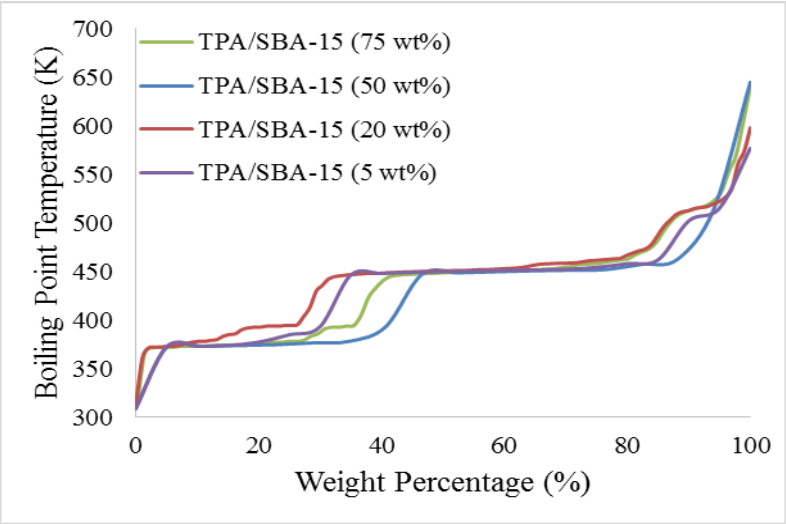

Figure A1.25. GC-Simdis curve analysis of TPA/SiO_2 catalysts reaction products.

MCM-41 Supported

Reaction performances of MCM-41 supported TPA catalysts were investigated under identical operating conditions. Reaction selectivity was evaluated according to three cut points which were related to C_5-C_8 (309-387K), C_9-C_{12} (387-458K) and C_{12+} (>458K). Additionally, gasoline and distillate cut point were taken as temperature from 309 to 448K and higher than 448 K respectively. Table A1.16 showed the isobutene oligomerization performances of MCM41 supported tungstophosphoric acids.

Table A1.16. Isobutene oligomerization over MCM-41 supported TPA.

Catalyst	C_5-C_8 wt%	C_9-C_{12} wt%	C_{12+} wt%	Gasoline wt%	Distillate wt%	D/G	Conversion
TPA/MCM-41(5 wt%)	21.9	53.0	25.2	38.0	62.0	1.6	95
TPA/MCM-41(20 wt%)	22.8	46.7	30.5	44.8	55.2	1.2	80
TPA/MCM-41(50 wt%)	36.4	46.9	16.7	50.7	49.3	1.0	89
TPA/MCM-41(75 wt%)	40.6	44.0	15.3	55.2	44.8	0.8	96

Figure A1.26 showed the reaction selectivity related to C_5-C_8, C_9-C_{12} and C_{12+} from bottom to top part of columns respectively. Gasoline and distillate selectivity were also shown as from bottom to top respectively. Conversion values were shown with dots.

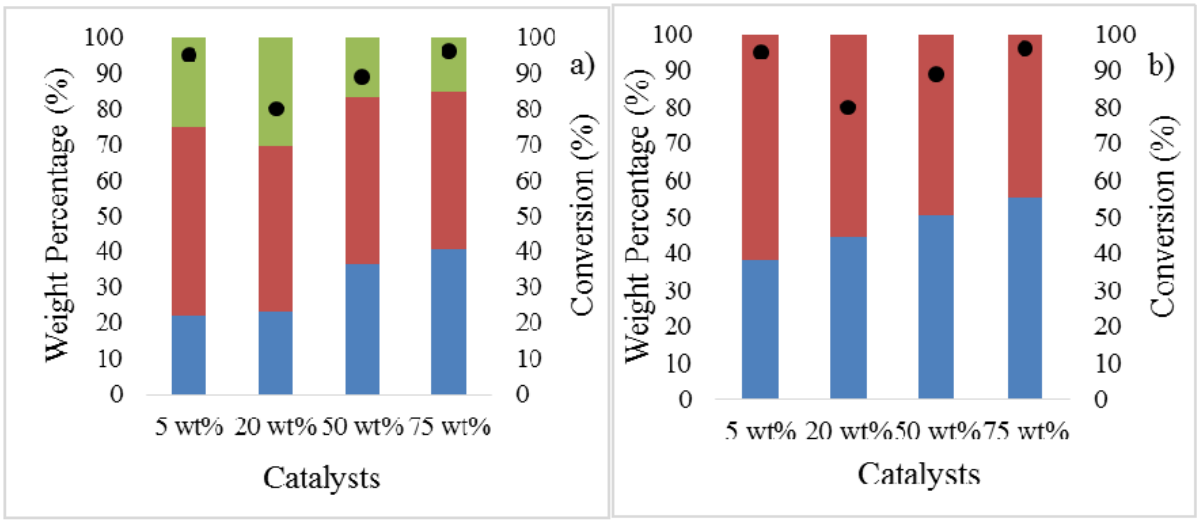

Figure A1.26. C_5-C_8, C_9-C_{12} and C_{12+} selectivity (a) and Gasoline, Distillate selectivity (b).

Data presented that distillate to gasoline ratio decreased with TPA loading. When the amount of acid sites increased, more active sites were close to each other. Hydrocarbon chain may not become longer because of low surface area. We infer that low amount of acid sites may provide more distillate fractions.

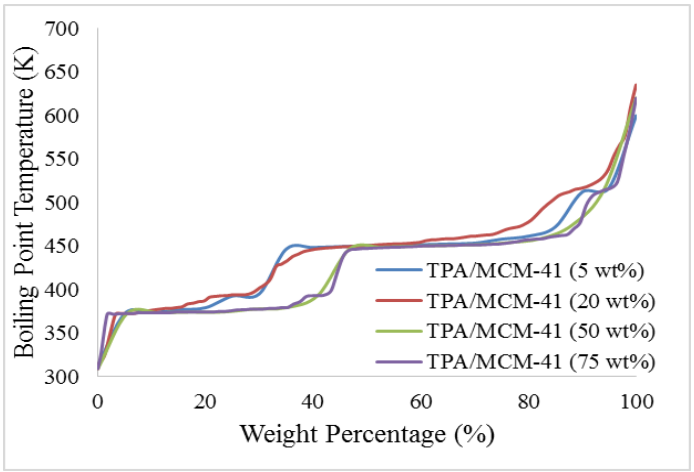

Figure A1.27. GC-Simdis curve analysis of TPA/MCM-41 catalysts reaction products.

A1.2.3 Supported MPA

A1.2.3.1 Characterization of Supported MPA

SiO_2 Supported

Molybdo phosphoric acid was supported on SiO_2, SBA-15 and MCM-41 with different loadings. Loading effect on catalyst properties and reaction performance was investigated.

NH_3-TPD analyses of SiO_2 supported molybdo phosphoric acid were performed. Results per gram of supported heteropolyacid were shared below.

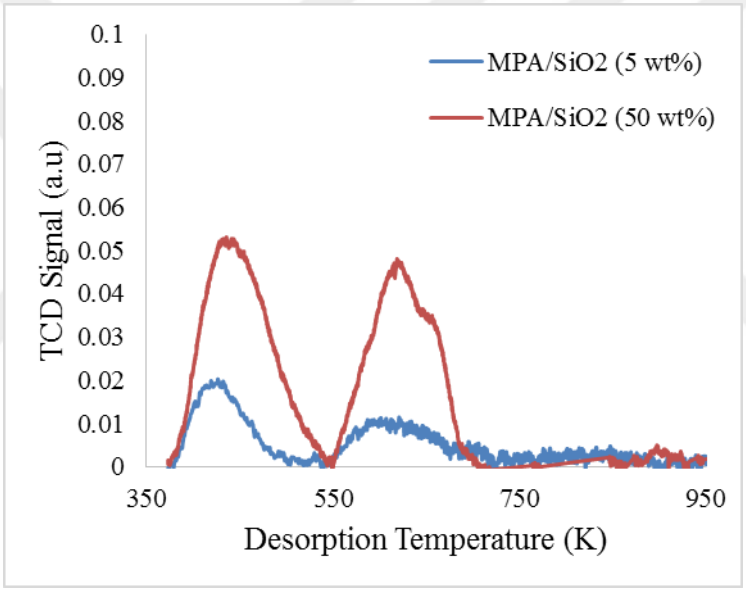

Figure A1.28. NH_3-TPD analyses of SiO_2 supported MPA.

Table A1.17. NH_3-TPD analyses of SiO_2 supported MPA (MPA/SiO_2)

Catalyst	L.T K	M.T K	L.T mmolNH_3/g	M.T mmolNH_3/g
MPA/SiO_2 (5 wt%)	427.2	614.2	0.171	0.137
MPA/SiO_2 (50 wt%)	446.6	621.3	0.542	0.477

NH_3-TPD analyses indicated two main peaks at around 400 K and 600K respectively. Amount of acid sites increased with MPA loading on SiO_2 surface.

FTIR analyses suggested that fingerprint bands of MPA as stretching vibrations of 1006, 995, 920-896, 800, 620 and 245-214 cm^{-1} as υ_s (M=O_t), υ_{as} (M=O_t), υ_s(M–O_b–M), υ_s(M–O_c–M) and υ_s(M–O_a) existed. Band shifts presented interactions between SiO_2 and MPA.

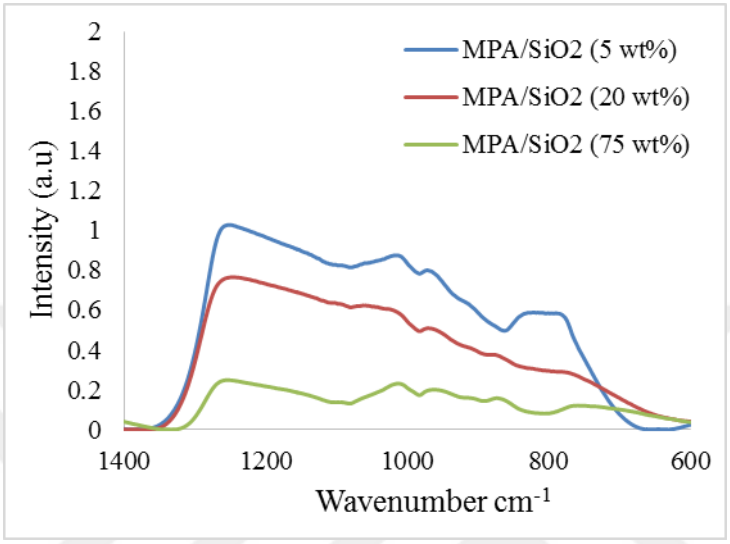

Figure A1.29. FTIR analyses of SiO_2 supported MPA.

SBA-15 Supported

NH_3-TPD analyses of SBA-15 supported molybdo phosphoric acid were stated in Figure A1.30 and Table A1.18.

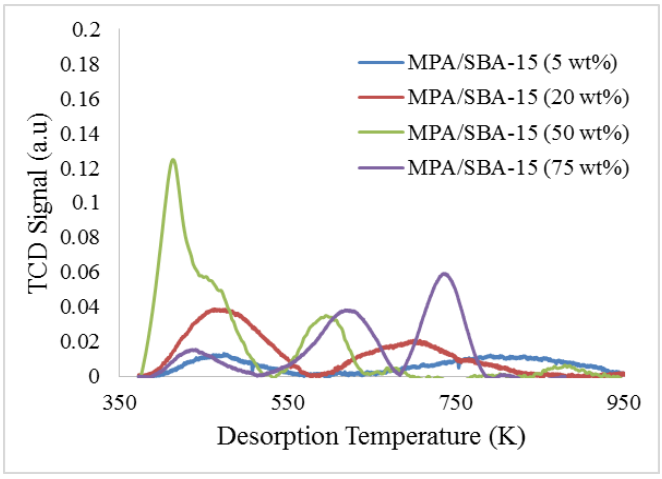

Figure A1.30. NH_3-TPD analyses of SBA-15 supported MPA.

Table A1.18. NH_3-TPD analyses of SBA-15 supported MPA.

Catalyst	L.T K	M.T K	H.T K	L.T mmolNH_3/g	M.T mmolNH_3/g	H.T mmolNH_3/g
MPA/SBA-15(5 wt%)	471.2		805.2	0.082		0.167
MPA/SBA-15(20 wt%)	474.9	698.1		0.303	0.204	
MPA/SBA-15(50 wt%)	413.0	594.5		1.068	0.244	

FTIR analyses of SBA-15 supported MPA were performed. Fingerprint peaks as stretching vibrations of 1006, 995, 920-896, 800, 620 and 245-214 cm^{-1} as υ_s (M=O_t), υ_{as} (M=O_t), υ_s(M–O_b–M), υ_s(M–O_c–M) and υ_s(M–O_a) existed.

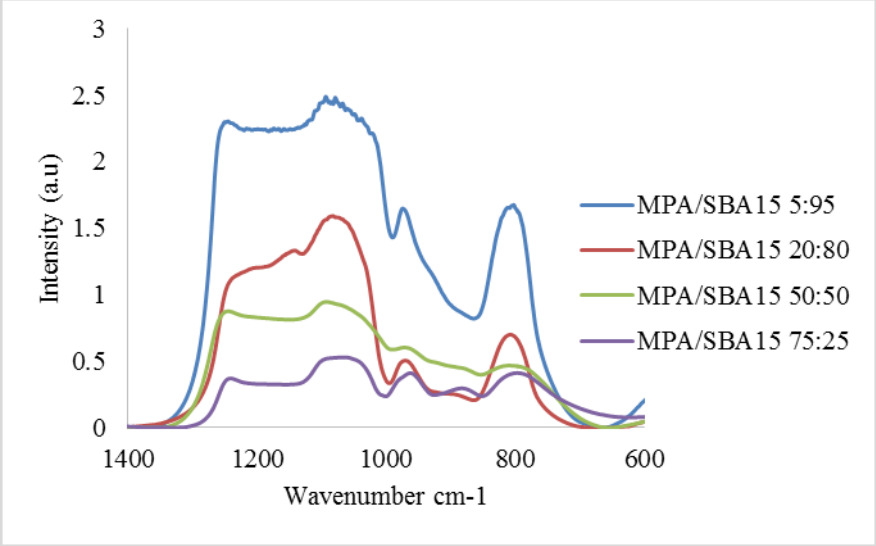

Figure A1.31. FTIR analyses of SBA-15 supported MPA.

MCM-41 Supported

NH_3-TPD analyses of MCM-41 supported molybdo phosphoric acid were stated in Figure A1.32 and Table A1.19.

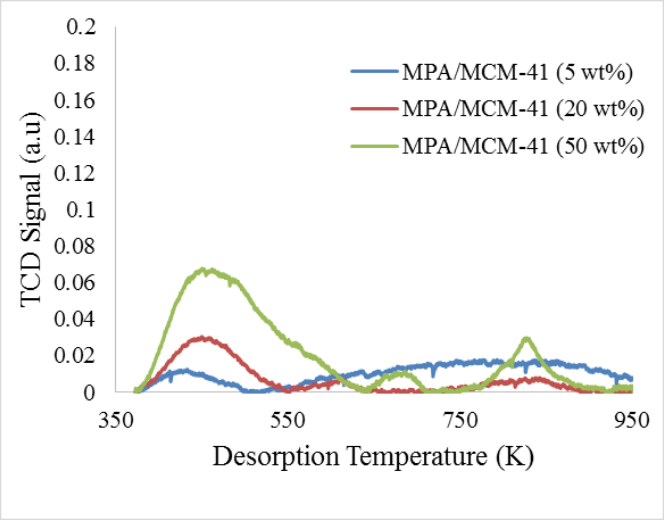

Figure A1.32. NH_3-TPD analyses of MCM-41 supported MPA.

Table A1.19. NH_3-TPD analyses of MCM-41 supported MPA.

Catalyst	L.T K	M.T K	H.T K	L.T $mmolNH_3/g$	M.T $mmolNH_3/g$	H.T $mmolNH_3/g$
MPA/MCM-41(5 wt%)	431.3		780.6	0.122		0.652
MPA/MCM-41(20 wt%)	454.8	604.2	819.8	0.335	0.039	0.071
MPA/MCM-41(50 wt%)	456.6	681	829.3	1.141	0.058	0.217

FTIR analyses of MCM-41 supported MPA were performed. Fingerprint peaks as stretching vibrations of 1006, 995, 920-896, 800, 620 and 245-214 cm^{-1} as υ_s ($M=O_t$), υ_{as} ($M=O_t$), υ_s($M–O_b–M$), υ_s($M–O_c–M$) and υ_s($M–O_a$) existed.

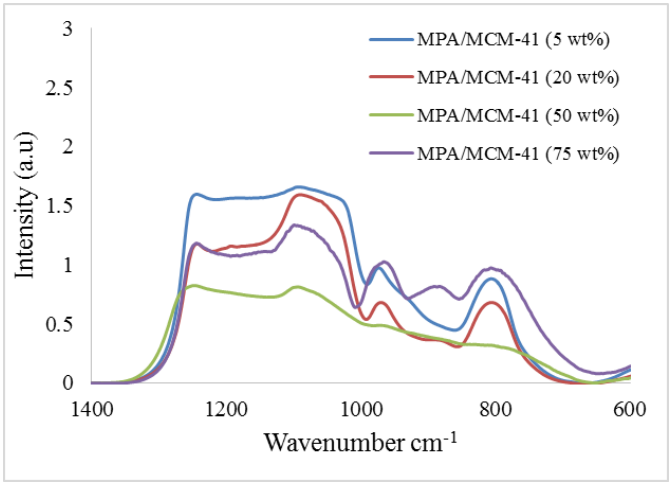

Figure A1.33. FTIR analyses of MCM-41 supported MPA.

A1.2.3.2 Isobutene Oligomerization Reaction Performance on Supported MPA

SiO_2 Supported

Isobutene oligomerization over SiO_2 supported MPA catalysts was performed at identical reaction conditions. Reaction selectivity was evaluated according to three cut points which were related to C_5-C_8 (309-387K), C_9-C_{12} (387-458K) and C_{12+} (>458K). Additionally, gasoline and distillate cut point were taken as temperature from 309 to 448 K and higher than 448 K respectively.

Table A1.20. Isobutene oligomerization over SiO_2 Supported MPA (MPA/SiO_2).

Catalyst	C_5-C_8 wt%	C_9-C_{12} wt%	C_{12+} wt%	Gasoline wt%	Distillate wt%	D/G	Conversion
MPA/SiO_2 (5 wt%)	35.2	50.8	14.0	48.7	51.3	1.1	83
MPA/SiO_2 (20 wt%)	32.5	48.2	19.3	46.0	54.0	1.2	77
MPA/SiO_2 (50 wt%)	30.2	51.5	18.4	45.7	54.3	1.2	79

Figure A1.34 showed the reaction selectivity related to C_5-C_8, C_9-C_{12} and C_{12+} from bottom to top part of columns respectively. Gasoline and distillate selectivity were also shown as from bottom to top respectively. Conversion values were shown with dots.

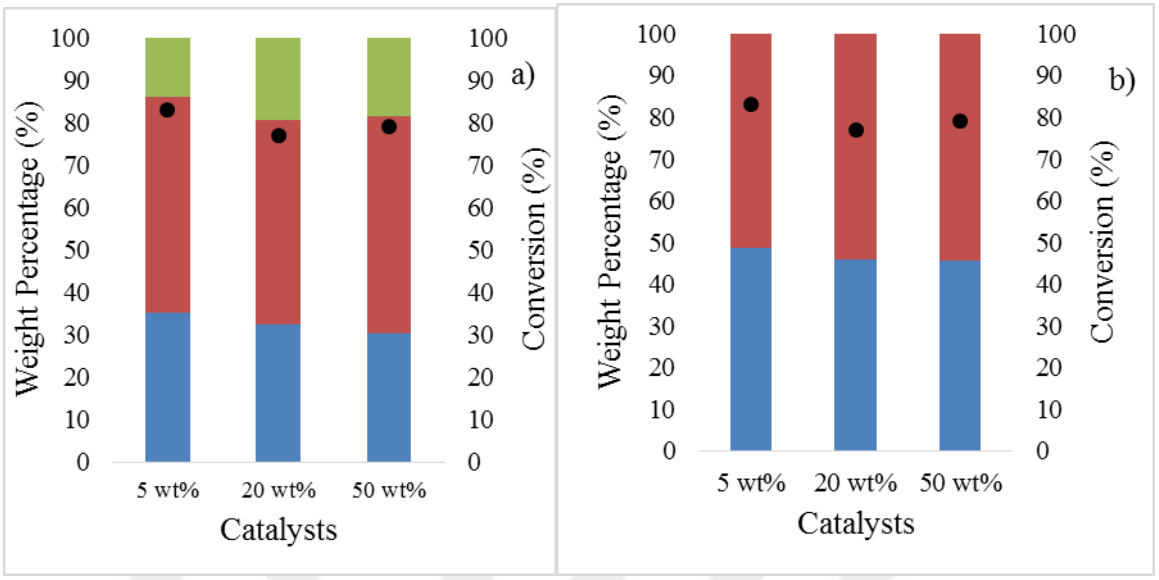

Figure A1.34. C_5-C_8, C_9-C_{12} and C_{12+} selectivity (a) and Gasoline, Distillate selectivity (b).

According to results, conversion values were similar. However, changes over selectivities according to determined cut points existed. Higher MPA loading were seem to be produce more distillate and C_{12+} range products.

SBA-15 Supported

Oligomerization of isobutene was investigated over SBA-15 supported molybdate phosphoric acid with different MPA loadings at identical reaction conditions. Reaction selectivity was evaluated according to three cut points which were related to C_5-C_8 (309-387 K), C_9-C_{12} (387-458 K) and C_{12+} (>458 K). Additionally, gasoline and distillate cut point were taken as temperature from 309 to 448K and higher than 448K respectively.

Table A1.21. Isobutene oligomerization over SBA-15 Supported MPA.

Catalyst	C_5-C_8 wt%	C_9-C_{12} wt%	C_{12+} wt%	Gasoline wt%	Distillate wt%	D/G	Conversion
MPA/SBA-15(5 wt%)	56.0	31.1	12.9	64.5	35.5	0.6	88
MPA/SBA-15(20 wt%)	40.4	46.9	12.6	50.7	49.3	1.0	85
MPA/SBA-15(50 wt%)	36.8	46.6	16.6	49.9	50.1	1.0	89

Figure 4A.40 showed the reaction selectivity related to C_5-C_8, C_9-C_{12} and C_{12+} from bottom to top part of columns respectively. Gasoline and distillate selectivity were also shown as from bottom to top respectively. Conversion values were shown in secondary axis with dots.

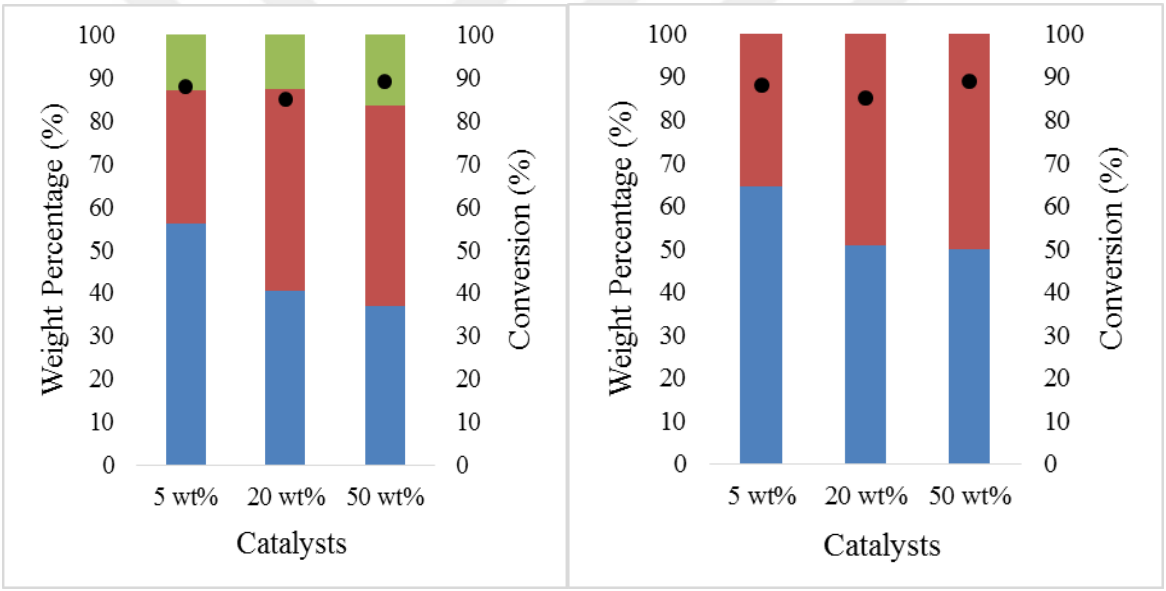

Figure A1.35. C_5-C_8, C_9-C_{12} and C_{12+} selectivity (a) and Gasoline, Distillate selectivity (b).

According to results, conversion values were similar at identical reaction conditions. Low distillate to gasoline ratio was obtained over MPA/SBA-15(5 wt%) catalyst.

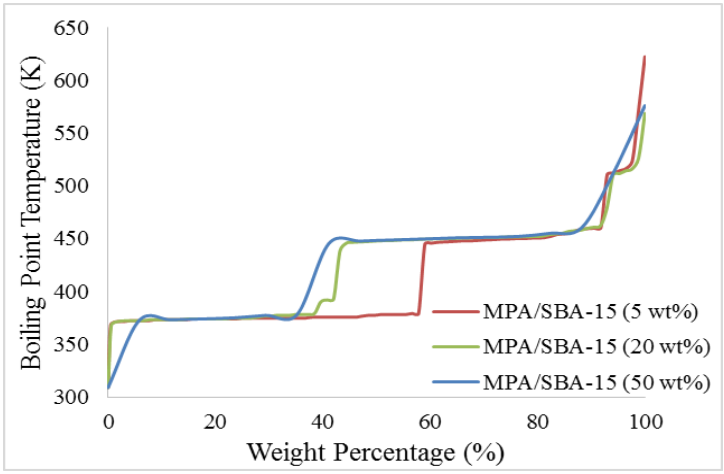

Figure A1.36. GC-Simdis curve analysis of MPA/SBA-15 catalysts reaction products.

MCM-41 Supported

Oligomerization of isobutene was investigated over MCM-41 supported MPA with different MPA loadings at identical reaction conditions. Reaction selectivity was evaluated according to three cut points which were related to C_5-C_8 (309-387 K), C_9-C_{12} (387-458 K) and C_{12+} (>458 K). Additionally, gasoline and distillate cut point were taken as temperature from 309 to 448K and higher than 448K respectively.

Table A1.22. Isobutene oligomerization over MCM-41 Supported MPA.

Catalyst	C_5-C_8 wt%	C_9-C_{12} wt%	C_{12+} wt%	Gasoline wt%	Distillate wt%	D/G	Conversion
MPA/MCM-41(5 wt%)	23	51	25	45	55	1.25	89
MPA/MCM-41(50 wt%)	45	44	12	54	46	0.85	80

Figure A1.37 showed the reaction selectivity related to C_5-C_8, C_9-C_{12} and C_{12+} from bottom to top part of columns respectively. Gasoline and distillate selectivity were also shown as from bottom to top respectively. Conversion values were shown in secondary axis with dots.

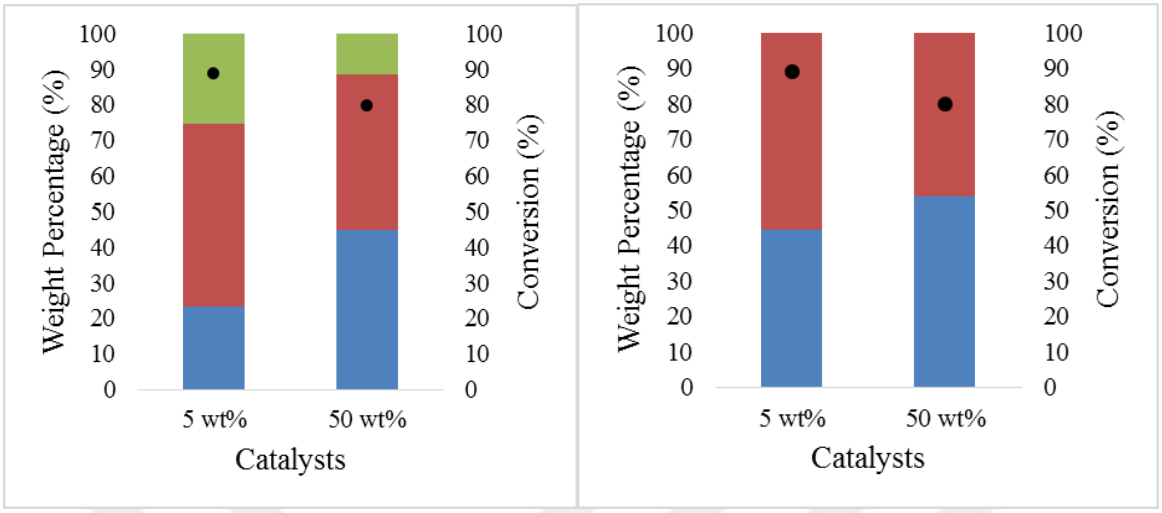

Figure A1.37. C_5-C_8, C_9-C_{12} and C_{12+} selectivity (a) and Gasoline, Distillate selectivity (b).

According to reaction results, high distillate to gasoline ratio was obtained over MPA/MCM-41 (5 wt%) catalysts under similar conversion values with MPA/MCM-41 (50 wt%).

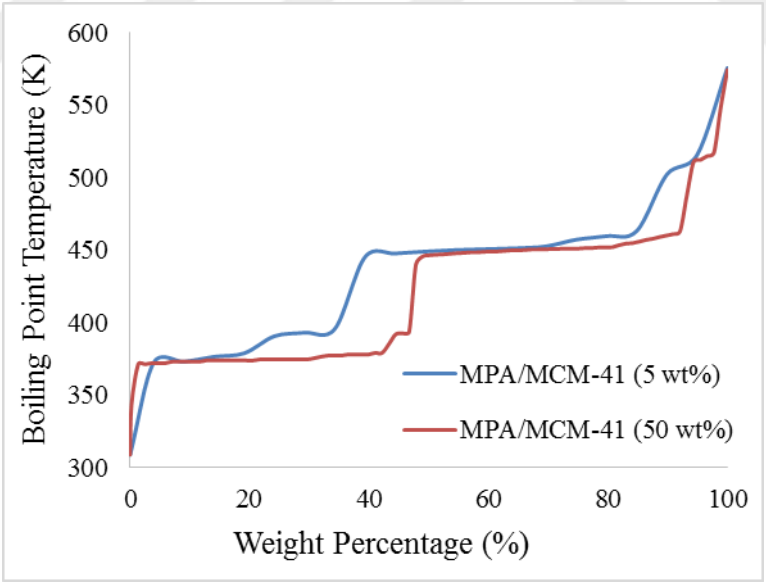

Figure A1.38. GC-Simdis curve analysis of MPA/MCM-41 catalysts reaction products.

References

[1] Zhang, J., et al., *Preferential oligomerization of isobutene in mixtures of isobutene and 1-butene over 12-tungstosilicic acid supported on silica.* Applied Catalysis A: General, 2009. **353**(1): p. 68-73.

[2] Kozhevnikov, I.V., *Heterogeneous acid catalysis by heteropoly acids: Approaches to catalyst deactivation.* Journal of Molecular Catalysis A: Chemical, 2009. **305**(1-2): p. 104-111.

[3] Wenxing Kuang, A.R., Michel Fournier, Robert Hubaut, *Structure and reactivity of silica-supported 12-tungstophosphoric acid.* Applied Catalysis A: General, 2003. **250**(2): p. 221-229.

[4] Zhang, J., et al., *Changes in Surface Acidity of Silica-Supported Dodecatungstosilicic Acid in Relation to the Loading Amount.* The Journal of Physical Chemistry C, 2011. **115**(30): p. 14762-14769.

[5] J.G. Hernández-Cortez, E.L.-S., Ma. Manríquez, J.A. Toledo, M.A. Cortes-Jacome *Acid and base properties of molybdophosphoric acid supported on zirconia: Characterized by IR spectroscopy, TPD and catalytic activity.* Fuel, 2012. **100**: p. 144-151.

[6] Sushkevich, V.L., V.V. Ordomsky, and I.I. Ivanova, *Isoprene synthesis from formaldehyde and isobutene over Keggin-type heteropolyacids supported on silica.* Catalysis Science & Technology, 2016. **6**(16): p. 6354-6364.

[7] Yang, W., et al., *H3PW12O40 supported on Cs modified mesoporous silica: catalytic activity in n-butane isomerisation and in situ FTIR study.* Catalysis Today, 2002. **73**(1-2): p. 153-165.

Chapter A2

ISOBUTENE OLIGOMERIZATION ON MCM-41 SUPPORTED TUNGSTOPHOSPHORIC APPENDIX

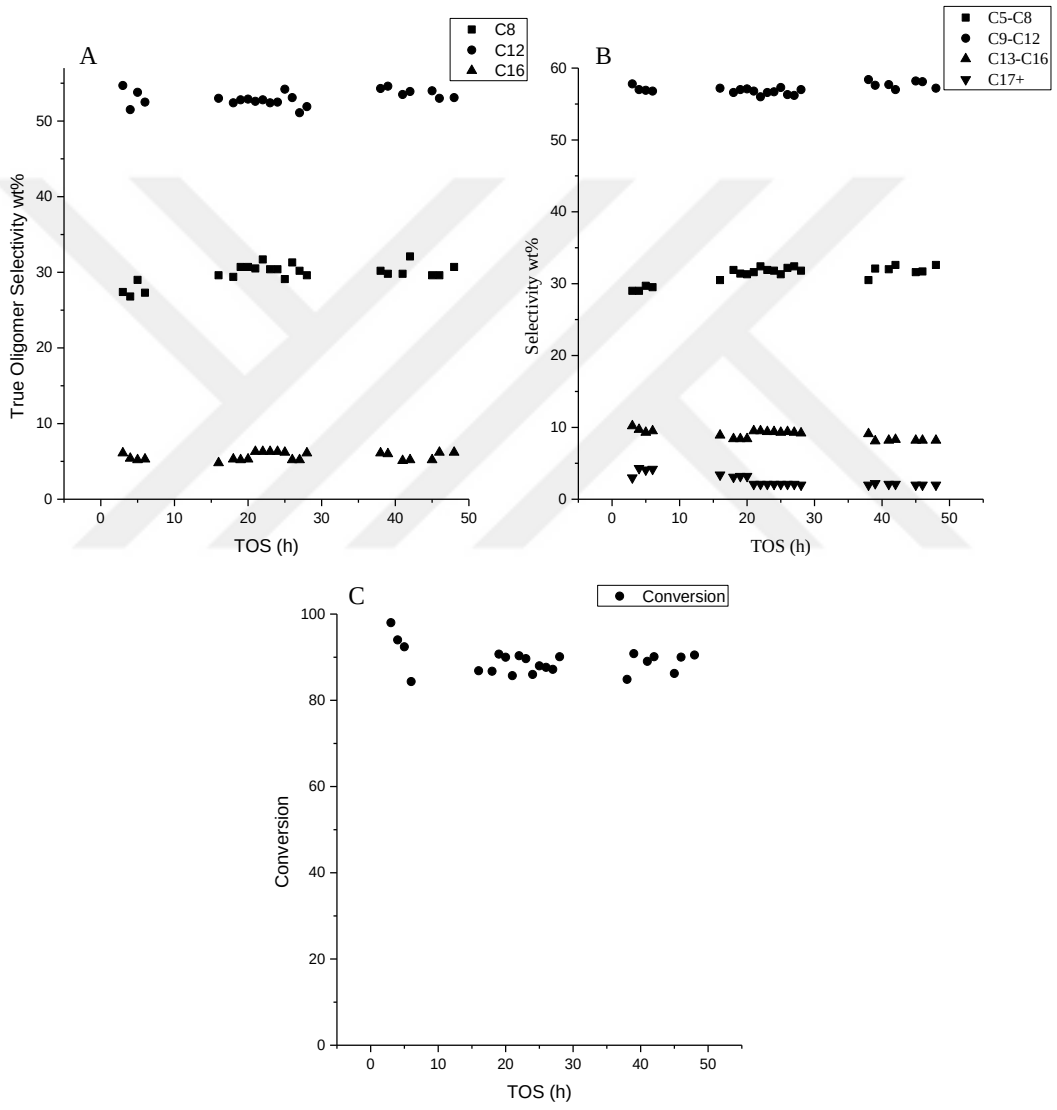

Figure A2.1. Long term run of TPA/MCM-41(90 wt%) catalyst: A) True oligomer selectivity; B) Overall oligomer selectivity and C) variation of conversion with time on stream

Data includes standard errors less than 1 % (standard error values: C_8:0.27; C_{12}:0.19; C_{16}:0.11; C_5-C_8:0.23; C_9-C_{12}:0.13; C_{13}-C_{16}:0.13; C_{17+}:0.16 and conversion: 0.63).

Equation E1.

$$Thickness\ (nm) = \frac{Pore\ Volume_{MCM-41} - Pore\ Volume_{Supported\ Catalyst}}{BET\ Surface\ Area_{Supported\ Catalyst}} \times 10^3$$

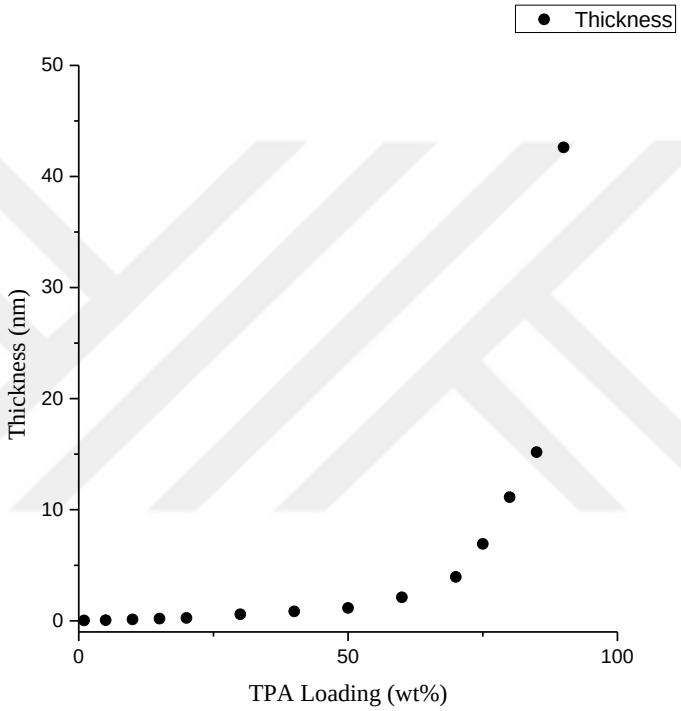

Figure A2.2. Layer thickness corresponding to TPA loading

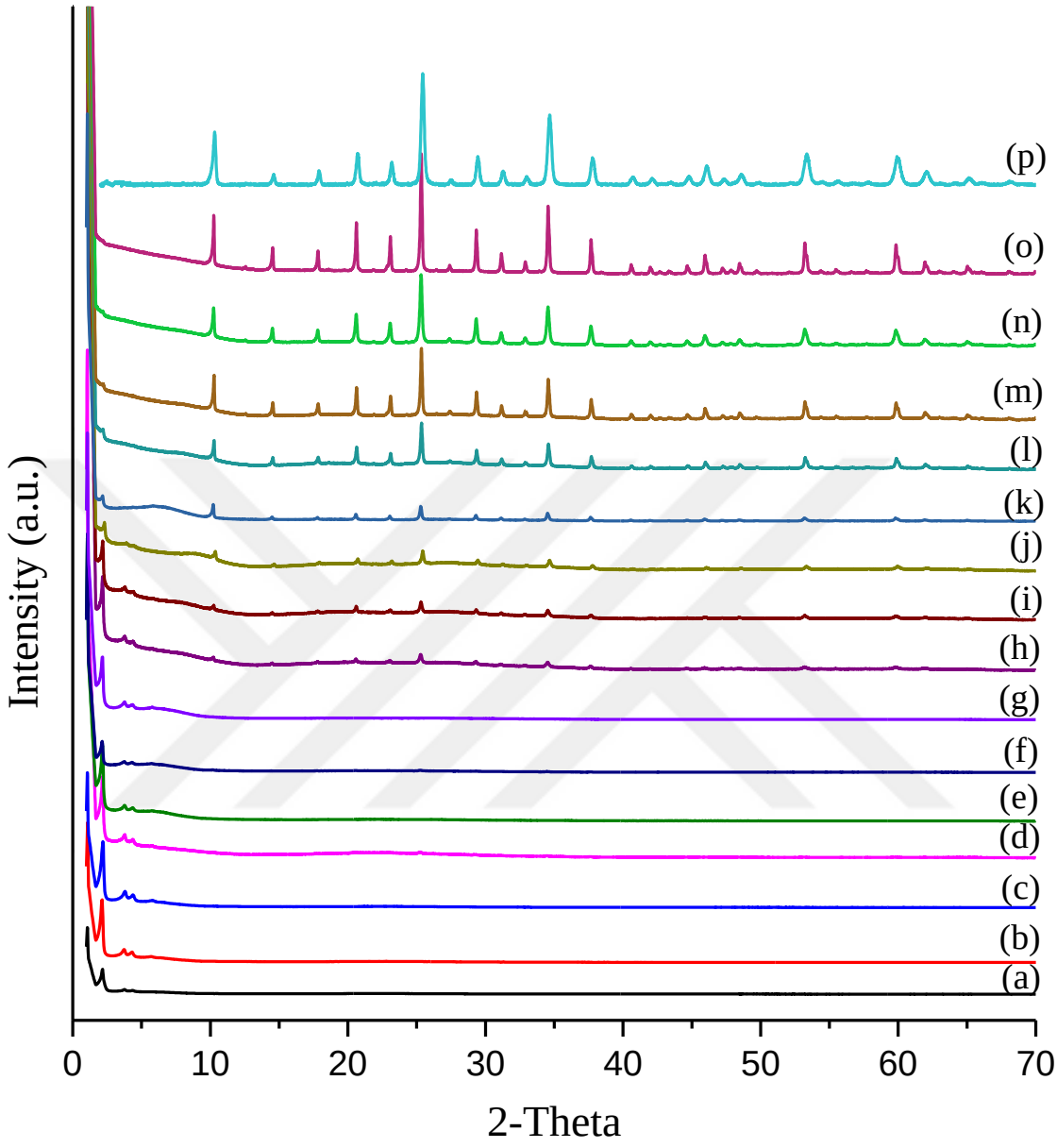

Figure A2.3. Complete data of XRD: (a) pure MCM-41, (b) 1 wt%; (c) 5 wt%; (d) 10 wt%; (e) 15 wt%; (f) 20 wt%; (g) 30 wt%; (h) 40 wt%; (i) 50 wt%; (j) 60 wt%; (k) 70 wt%; (l) 75 wt%; (m) 80 wt%; (n) 85 wt%; (o) 90 wt% of TPA/MCM-41 catalysts and (p) pure TPA

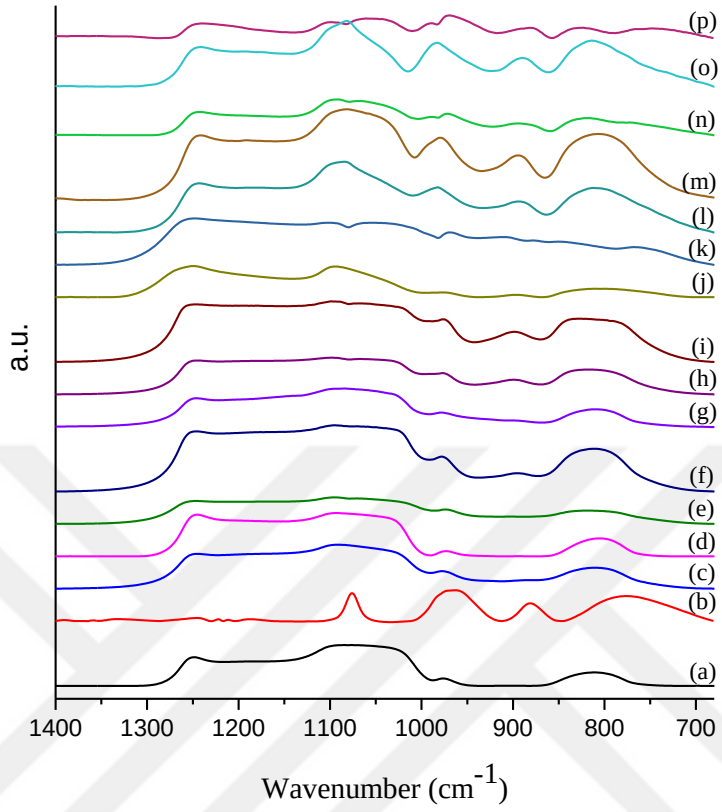

Figure A2.4. IR Spectra of TPA/MCM-41 catalysts without substraction of MCM-41 sprectrum: (a) pure MCM-41, (b) pure TPA, (c) 1 wt%; (d) 5 wt%; (e) 10 wt%; (f) 15 wt%; (g) 20 wt%; (h) 30 wt%; (i) 40 wt%; (j) 50 wt%; (k) 60 wt%; (l) 70 wt%; (m) 75 wt%; (n) 80 wt%; (o) 85 wt%; (p) 90 wt% of TPA/MCM-41 catalysts

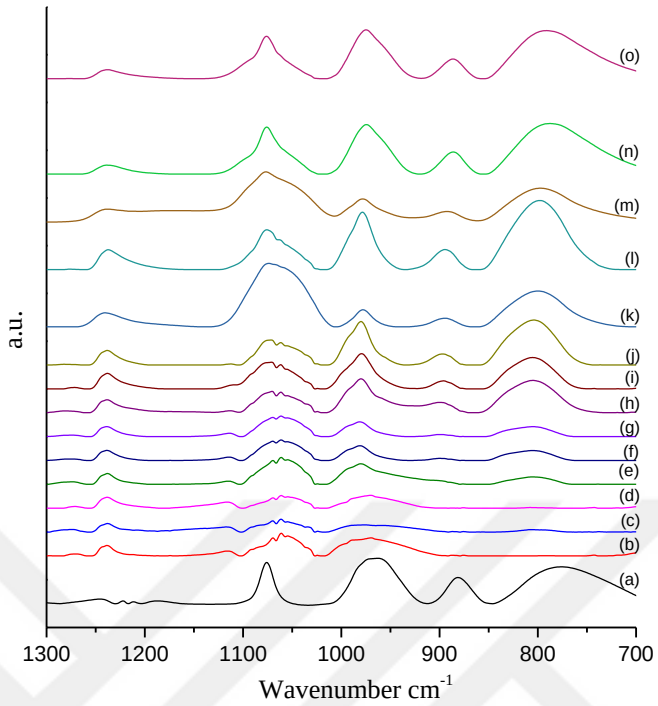

Figure A2.5. Difference IR spectra of TPA/MCM-41 catalysts obtained by subtracting the spectrum of MCM-41 from that of the corresponding sample: (a) pure TPA, (b) 1 wt%; (c) 5 wt%; (d) 10 wt%; (e) 15 wt%; (f) 20 wt%; (g) 30 wt%; (h) 40 wt%; (i) 50 wt%; (j) 60 wt%; (k) 70 wt%; (l) 75 wt%; (m) 80 wt%; (n) 85 wt%; (o) 90 wt% of TPA/MCM-41 catalysts

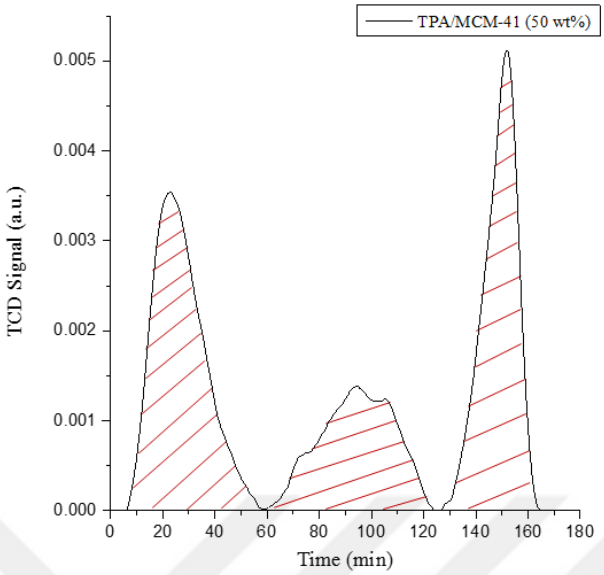

Figure A2.6. Representative NH_3-TPD Data. Amount of acid sites were calculated by area under curves corresponding to calibration of TCD signal by time.

Table A2.1. Low and medium strength acid sites peak positions of prepared TPA/MCM-41 catalysts by NH_3-TPD analysis.

TPA Loading, wt%	Low Temperature Desorption Peak, K	Medium Temperature Desorption Peak, K	Number of Acid Sites Determined from L.T Desorption Peak, $mmolH^+/g$	Number of Acid Sites Determined from M.T Desorption Peak, $mmolH^+/g$
1	453	655	0.010	0.043
5	417	602	0.050	0.025
10	439	673	0.060	0.052
15	454	668	0.070	0.067
20	471	704	0.065	0.056
30	442	698	0.165	0.233
40	441	701	0.144	0.267
50	449	694	0.256	0.281
60	453	694	0.158	0.335
70	454	698	0.181	0.441
75	462	727	0.204	0.259
80	451	691	0.196	0.212
85	458	686	0.196	0.126
90	460	673	0.112	0.108
100	461	602	0.054	0.027

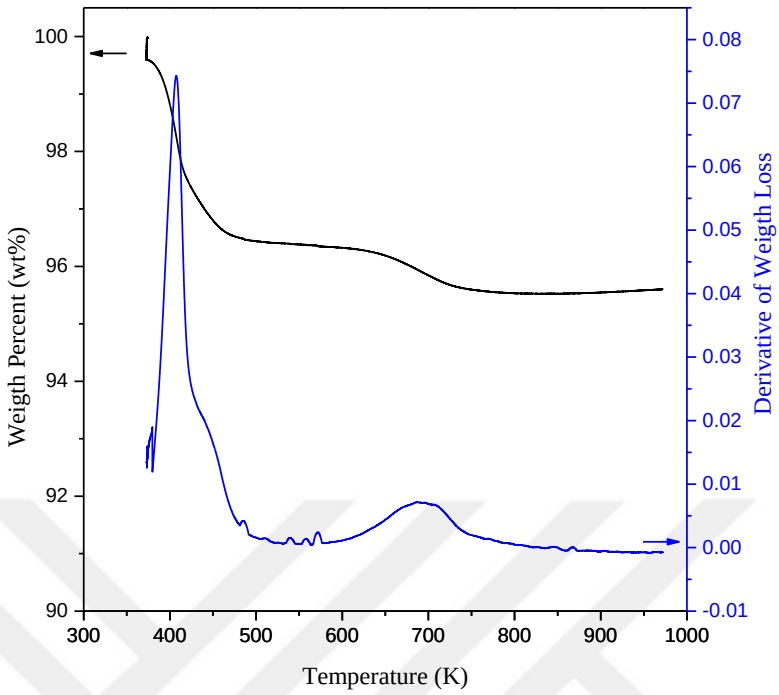

Figure A2.7. TGA results of pristine TPA.

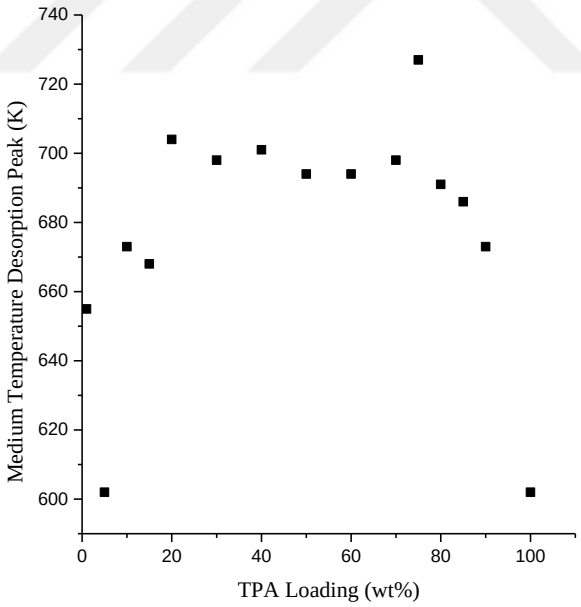

Figure A2.8. Variation of the medium desorption peak temperature with TPA loading

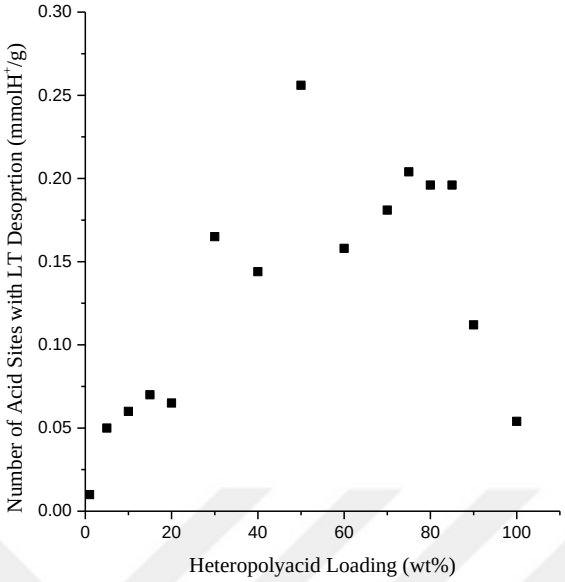

Figure A2.9. Variation of the number of acid sites by low temperature desorption with TPA loading

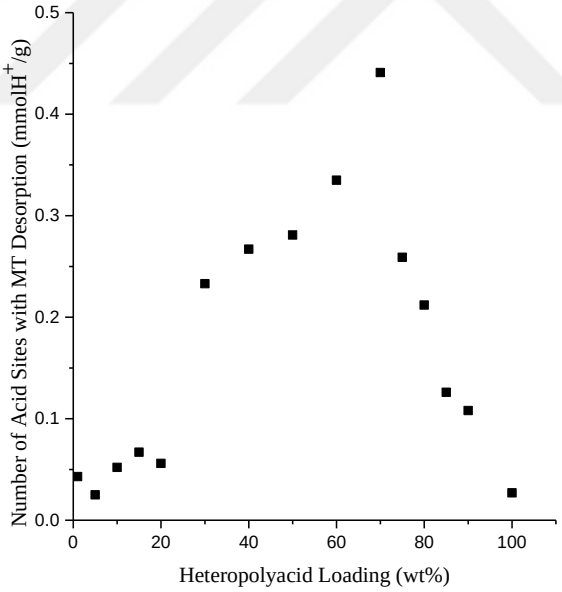

Figure A2.10. Variation of the number of acid sites by medium temperature desorption with TPA loading

Table A2.2. Oligomerization product distribution over TPA/MCM-41 catalysts corresponding to TPA loading under identical reaction conditions (393 K, 15 bar, WHSV: 46 h^{-1})

Loading	Dimer		Trimer				Tetramer		Pentamer	Conversion
	C_5-C_7	C_8	C_9-C_{11}			C_{12}	C_{13}-C_{15}	C_{16}	C_{17+}	
1	2	15	4	7	4	51	8	4	4	75
5	5	15	5	5	5	45	10	5	5	94
10	3	16	4	6	9	42	8	5	7	83
15	2	20	5	2	6	42	10	5	6	72
20	2	18	5	7	9	38	11	4	5	78
30	4	23	5	5	9	31	11	5	7	69
40	4	26	5	4	9	34	9	3	6	81
50	5	30	6	0	6	35	0	6	12	81
60	3	29	3	5	6	39	8	3	4	85
70	2	32	3	4	5	42	5	4	3	54
75	3	36	3	4	4	39	5	3	3	84
80	3	31	2	3	3	45	6	4	3	50
85	1	30	2	2	4	50	4	4	3	88
90	3	34	3	4	3	42	5	3	3	83
100	4	21	3	3	3	49	7	5	5	31